Fall 2011

Cerebral spasticity modeled as disorded equilibrium point control

Darnell Simon
New Jersey Institute of Technology

Copyright Warning & Restrictions

The copyright law of the United States (Title 17, United States Code) governs the making of photocopies or other reproductions of copyrighted material.

Under certain conditions specified in the law, libraries and archives are authorized to furnish a photocopy or other reproduction. One of these specified conditions is that the photocopy or reproduction is not to be "used for any purpose other than private study, scholarship, or research." If a, user makes a request for, or later uses, a photocopy or reproduction for purposes in excess of "fair use" that user may be liable for copyright infringement,

This institution reserves the right to refuse to accept a copying order if, in its judgment, fulfillment of the order would involve violation of copyright law.

Please Note: The author retains the copyright while the New Jersey Institute of Technology reserves the right to distribute this thesis or dissertation

Printing note: If you do not wish to print this page, then select "Pages from: first page # to: last page #" on the print dialog screen

ABSTRACT

CEREBRAL SPASTICITY MODELED AS DISORDED EQUILIBRIUM POINT CONTROL

by
Darnell Simon

Spasticity is a highly complex phenomenon, which has not been defined in precise and quantifiable terms. Although the muscle stretch reflex is thought to play an important role in spasticity generation, the pathophysiologic basis of spasticity is not completely understood. A valid measure of spasticity is one that is chosen within the context of a theory describing the physiological mechanisms underlying the control of posture and movement in healthy individuals and possible impairments of these mechanisms leading to motor disorders. This research's goal was to determine the role of stretch reflex threshold in the regulation of impaired motor control through the exploration of the following research questions:

1. Can experimental measures be produced leading to the development of a model of spasticity that can be interpreted within the framework of a general theory of motor control?
2. Can the underlying motor control framework provide unique parameters capable of describing both normal and altered/abnormal movement?
3. Can the model be robust enough to explain active as well as passive movement?

The research method outlined in this dissertation takes the novel approach of incorporating the equilibrium point hypothesis into a trajectory-based analysis of pendulum knee motion. The Equilibrium Point Hypothesis (EPH) of motor control theorizes that the central nervous system (CNS) provides a virtual trajectory of joint motion, representing space and time. A forward dynamic model has been developed that can reproduce kinematic data through the using optimized model parameters. The

incorporation of the equilibrium point hypothesis in forward model was not only recognition that examination of the entire trajectory of the limb, rather than just the first amplitude of swing, was necessary, but also, that movement can be characterized by the simple extraction of three parameters: a relative damping coefficient, relative stiffness coefficient and mathematical function which can act as an approximation CNS the virtual trajectory described in the EPH.

This research produced a model of passive motion with the ability to produce parameter values that not only differentiate subjects with spasticity from subjects with no clinical signs of spasticity but that can separate subjects based on severity of spastic condition. Research which began as an endeavor to model the passive motion of the pendulum knee test, led to the development of a unifying model of motor control that is robust enough to describe both active and passive movements.

CEREBRAL SPASTICITY MODELED AS DISORDED EQUILIBRIUM POINT CONTROL

by
Darnell Simon

A Dissertation
Submitted to the Faculty of
New Jersey Institute of Technology
in Partial Fulfillment of the Requirements for the Degree of
Doctor of Philosophy in Biomedical Engineering

Department of Biomedical Engineering

January 2012

APPROVAL PAGE

CEREBRAL SPASTICITY MODELED AS DISORDED EQUILIBRIUM POINT CONTROL
Darnell Simon

Dr. Richard A. Foulds, Dissertation Advisor Date
Associate Professor of Biomedical Engineering, NJIT

Dr. William Van Buskirk, Committee Member Date
Distinguished Professor and Chair of Biomedical Engineering, NJIT

Dr. Sergei Adamovich, Committee Member Date
Associate Professor of Biomedical Engineering, NJIT

Dr. Michael L. Rosenberg, Committee Member Date
Director of Neuro-ophthalmology at the New Jersey Neuroscience Institute, JFK Medical Center

---

Dr. Alma Merians, Committee Member Date
Professor and Chair of Rehabilitation and Movement Science, UMDNJ-SHRP

BIOGRAPHICAL SKETCH

Author: Darnell Simon

Degree: Doctor of Philosophy

Date: January 2012

Undergraduate and Graduate Education:

- Doctor of Philosophy in Biomedical Engineering,
  New Jersey Institute of Technology, Newark, NJ, 2012

- Master of Science in Mechanical Engineering,
  New Jersey Institute of Technology, Newark, NJ, 2009

- Bachelor of Science in Engineering Science,
  New Jersey Institute of Technology, Newark, NJ, 2001

Major: Biomedical Engineering

Presentations and Publications:

Simon, D., Androwis G. and Foulds, R.A. (2011). Equilibrium Point Model of Spastic Knee Joint. *Proceedings from NEBEC 2011: The IEEE 37th Annual Northeast Bioengineering Conference.*

Simon, D., Foulds, R.A. (2004). Developing a Quantitative Measure of Muscle Spasticity. *Proceedings from NEBEC 2004: The IEEE 30th Annual Northeast Bioengineering Conference.*

R.A. Foulds, J. Fee, D. Simon. (2004). Descending Neural Drive and its Contribution to Spasticity-Related Contracture. *International BioMedical Engineering Society (BMES) National Conference.* Philadelphia, PA. 2004.

Simon, D. (2003). Biomedical Engineering: Millennium Pathways. *Engineering Technologies and Computer Sciences Division Seminar*, Essex County College, Newark, NJ.

To **Sharon**, my best friend and love of my life, who dared to dream a dream bigger than both of our imaginations. Thank you for being my rock, my harbor during the rough seas, and the ying to my yang.

To **Shannon**, the greatest advice I ever heard was," never be the smartest person in the room and never think that you are". Every day you remind me that the truly smartest people not only don't think they are, but are the ones who passionately seek to be even smarter. Always seek the largest room of smart people possible.

To **Dad**, for showing me that our greatest asset as people of color is our ability to "make do what whatever we got". It's a lesson that I have NEVER forgotten! Thanks, son of Bishopville, S.C.

To, **Mom**, for all the trips to the Newark Public Library, Newark Museum and Essex County College when I was young. Thanks for never allowing the doubts of others to compromise you and dad's vision of what was possible for me.

To **Felecia**, though we have never had a conversation, my hope is that one day, my chosen profession will produce the means for us one day say to each other "What's Up".

To **Aunt Ruth**. Who knew all those years of adding up discount savings receipts from Bamberger's would lead to this?

ACKNOWLEDGMENT

I would like to express my deepest appreciation to Dr. Richard Foulds who not only served as my research supervisor, providing valuable and countless resources, insight, and intuition, but also constantly gave me support, encouragement, and reassurance. I will always be grateful for that fortuitous fall evening when I found myself in a lecture hall with Dr. Foulds. In the beginning it was just Dr. Foulds, myself and a bird. Thank you for always reminding reinforcing what the analogy of the bird represents and for helping me to take flight. Thanks are given to Dr. Sergei Adamovich, for actively sharing his expertise on motor control theory and research insights. Particular thanks to Dr. William Van Buskirk, Dr Alma Merians and Dr. Michael Rosenberg for their patience, enthusiasm and insights.

I would like to thank Dr. Gail Smith, CUNY AGEP Principal Investigator and Ms, Lorraine Towns for their tireless motivation, support and encouragement. This work was funded by the Nation Science Foundation Alliances for Graduate Education and the Professoriate Fellowship and the New Jersey Commission on Higher Education Minority Academic Career Fellowship.

Special thanks to Ms. Zara Williams and Dr. Angelo Perna of the Ronald E. McNair Postbaccalaureate Achievement program for their support and guidance. I am better scholar, researcher and leader because of your influence.

I like to thank my fellow graduate students and extend a personal thanks to Drs Anne Marie Petrock, Bruno Mantilla, Aysegul Ergin, Diane Donnelly and Jason Steffener – May this era never be forgotten. Thanks to Drs Karen Hare and Vetria Byrd and future Dr. Brooke Odel for actively sharing in my journey.

TABLE OF CONTENTS

TABLE OF CONTENTS
(Continued)

Chapter **Page**

TABLE OF CONTENTS
(Continued)

Chapter **Page**

LIST OF TABLES

LIST OF FIGURES

LIST OF FIGURES
(Continued)

LIST OF FIGURES
(Continued)

CHAPTER 1

INTRODUCTION

1.1 Objective

The objective of this dissertation is to present a novel model and identification methodology to describe the motion dynamics of knee joints affected and unaffected by spasticity utilizing multiple pendulum tests. The development of new modalities of treatment of spasticity necessitates a better understanding of the neural contributions to the clinically observed features of spasticity. This level of understanding begins with our ability to conceptualize the role that the central nervous system plays in altering stretch reflex threshold activation in cerebral lesion disorders. Our initial attempt to determine the role of stretch reflex threshold regulation in impaired motor control begins with defining foundational research questions:

1. Can we create experimental measures to develop a model of spasticity that can be interpreted within the framework of a general theory of motor control?
2. Can the underlying motor control framework provide unique parameters capable of describing both normal and altered/abnormal movement?
3. Can the model be robust enough to explain active as well as passive movement?

It is the belief of this research that the increased resistance during passive motion that characterizes spasticity, as well as many other aspects of disordered motor control that accompany cerebral lesion disorders can be explained by an equilibrium point model as impairment in the ability to regulate muscle force in all parts of the physiological range.

1.2 Background Information

1.2.1 Cerebral Palsy

Cerebral palsy (CP) is a disorder of movement and posture that results from a static injury to the brain before, during or shortly after childbirth. As the most common form of childhood physical disability, conceptually cerebral palsy describes a variety of motor disorders that arise from "developmental deficits or non progressive lesions of the immature brain" (Cheney, 1997). Variability in clinical expressions of CP results from dependence on the magnitude, extent, and location of the insult that causes permanent damage to the brain, brainstem, or spinal cord (Koman, 2004). The clinical hallmark of cerebral palsy is abnormal motor control ranging from subtle motor impairment to involvement of the whole body. In developed countries children are affected by cerebral palsy at rate of 2.0 to 2.5 incidences per 1000 live births (Graham, 2003). Spasticity, which is commonly seen in children with cerebral palsy, may interfere with functional performance and ease of caregiving which ultimately has a negative impact on the health-related quality of life of the CP child.

1.2.2 Spasticity

Spasticity is a sensorimotor phenomenon related to the integration of the nervous system motor responses to sensory input (Ivanhoe, 2004). It is a condition which results from excess motor neuron excitation, leading to involuntary muscle contraction in response to increased velocity of movement. The most commonly accepted definition of spasticity is the one offered by Lance describing spasticity as 'a motor disorder characterized by a velocity-dependent increase in tonic stretch reflexes (muscle tone) with exaggerated

tendon jerks, resulting from hyper excitability of the stretch reflexes, as one component of the upper motor neuron syndrome (Lance, 1980).

Often forgotten in the various descriptions of spasticity is that it represents only one of the positive symptoms of the upper motor neuron (UMN) syndrome. Upper motor neurons are neurons that originate in the higher regions of the brain, such as the motor cortex, and synapse on the lower motor neurons to convey descending commands for movement (Kandel, 2000). Upper motor neurons include supraspinal inhibitory and excitatory fibers, which descend to the spinal cord, exerting a balanced control on spinal reflex activity (Sheean, 2002). Upper motor neuron (UMN) syndrome is a series of symptoms that result from lesions to the descending motor pathways anywhere along this trajectory. UMN syndrome has two classical distinctions in terms of its signs or symptoms. The negative symptoms, which include weakness or paralysis, unusual fatigability, and lack of dexterity are commonly referred to as paresis. The positive features of UMN syndrome are characterized by muscle overactivity, either excessive muscle contraction or some sort of inappropriate muscle activity (Sheean, 2002). Although only one of the positive features of UMN syndrome, 'spasticity' is commonly used as a generic term for some of the other positive features of UMN syndrome such as hyperactive tendon reflexes, clonus and flexor spasms.

Lance's characterization of spasticity has led the clinical view of spasticity as a form of hypertonia due to a velocity-dependent increase in tonic stretch reflexes, which results from abnormal spinal processing of proprioceptive input. Hypertonia associated with spasticity can have one or both of the following features: 1) resistance to externally imposed movement increases with increasing speed of stretch and varies with the

direction of joint movement, and/or 2) resistance to externally imposed movement rises rapidly above a threshold speed or joint angle (Sanger, 2003). This resistance is in both stretch and lengthening, clinically described as a ‘spastic catch’ (Barnes, 2001). As a result, the muscle tends to remain in a shortened position for prolonged periods of time yielding changes in soft tissue, which yields restricted attempted movements. Excessive and uncontrolled spasticity limits functional recovery, causes pain and is associated with contractures.

1.2.3 Pathophysiology of Spasticity

The pathologic basis of spasticity is a complex subject that is not completely understood by clinicians due to the classification of spasticity as being one of many features of the upper motor neuron syndrome, as well as the lack of a very good animal model (Sheean, 2001). Lesions to the cortical motor system in cerebral palsy are a common cause of the upper motor neuron syndrome (UMN) in childhood. Injury to upper motor neurons decreases cortical input to the reticulospinal and corticospinal tracts, which in turn affects motor control, decreases the number of effective motor units, and produces abnormal muscle control and weakness (Koman et al., 2004). Simultaneously, the loss of descending inhibitory input through the reticulospinal tract and other systems increases the excitability of gamma and alpha neurons, producing spasticity.

It is generally understood that the stretch reflex arc, which normally causes a muscle to contract in order to resist the force that is stretching it, is the most basic neural circuit contributing to spasticity. It contains contractile muscle fibers and sensory and motor neurons. Alpha motor neurons and the muscles that it innervates comprise the final common pathway in the expression of motor function. There are numerous excitatory and

inhibitory modulatory synaptic influences on this pathway. For normal movement to occur, the brain must be able to selectively turn this reflex off, usually via inhibitory signals relayed to the spinal cord via the corticospinal tract (McClelland et al., 2007). However, damage to this circuit results in disinhibition of the stretch reflex; over time, this reduces the triggering threshold until excessive and complete muscle contraction can occur even at rest, making the limb virtually immovable (McClelland et al., 2007).

Some specific causes of spasticity that have been proposed (a) alpha motor neuron hyperexcitability resulting from an imbalance in excitatory vs. inhibitory alpha motor neurons (Figure 1.1), and (b) gamma motor neuron hyperactivity manifesting as increased sensitivity of muscle spindle to stretch (Satkunam, 2003). Additional causes involve damage to descending tracts that control interneurons responsible for (a) mediating presynaptic inhibition of the Ia terminals on the alpha motor neuron, (b) mediating type II afferents, and (c) reciprocal Ia inhibition (McClelland et al., 2007). Outcomes of this damage include increased afferent stimulus to the alpha motor neuron as a result of stretch, decreased inhibition from type II afferents, and loss of normal inhibition of antagonist muscle during muscle stretch. Although each of the proposed individual causes contributes to the clinical picture observed in spasticity, a single unilateral hypothesis to explain the mechanisms of spasticity has yet to emerge.

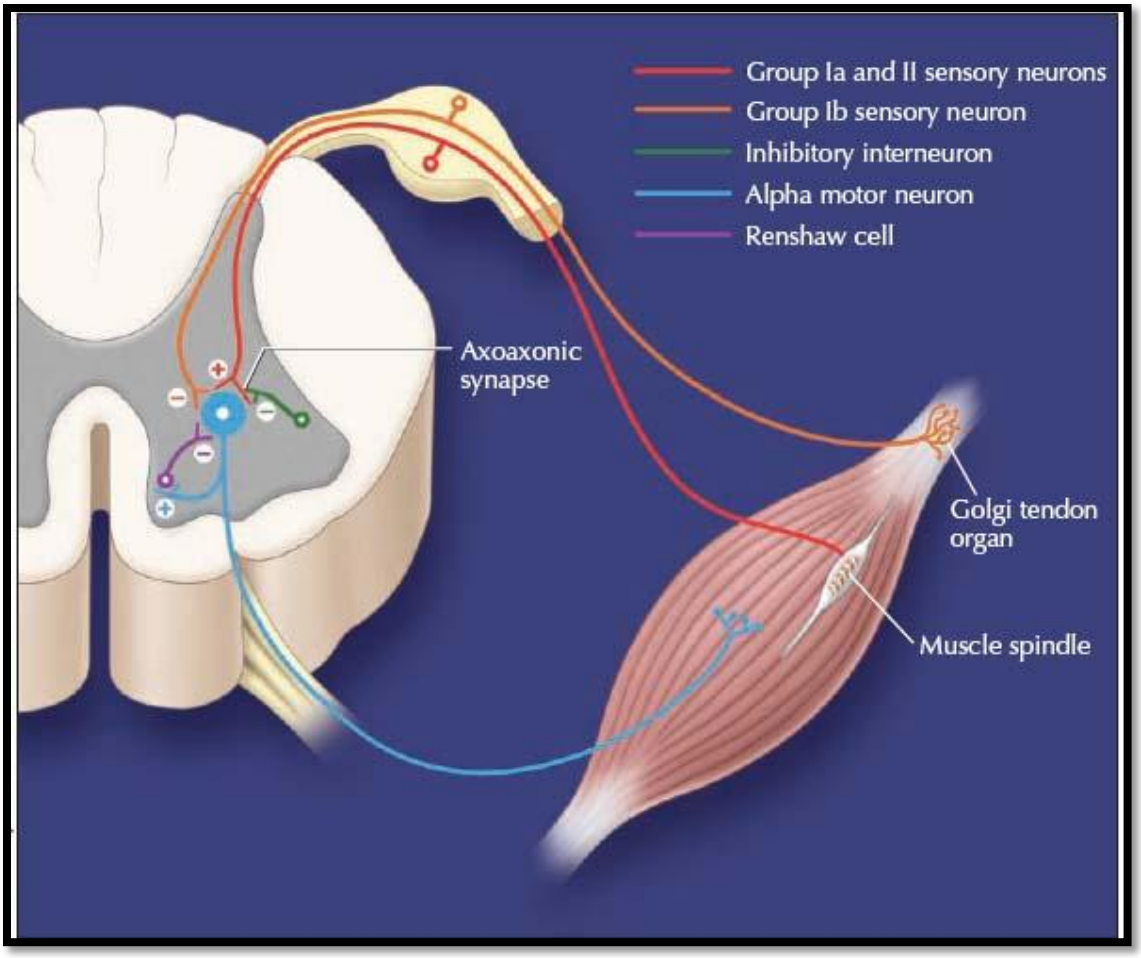

Figure 1.1 Spinal mechanisms of suppression of hyperactivity in final common pathway. Source (Satkunam, 2003)

1.3 Barriers to Meaningful Spasticity Measurement

Spasticity is generally defined as velocity-dependent increased resistance during passive movement of peripheral joints owing to increased involuntary muscle activity (Good, 2002). It is difficult for clinicians, however to correlate this definition of spasticity with the symptoms that they observe in patients. The clinically observed components of spasticity include increased resistance to passive movement, increased phasic-stretch reflexes, clonus, and flexor or extensor spasms (Good, 2002). These observations are

borne out of the inevitable consequence of clinicians viewing the whole UMN syndrome and regarding all the positive features of the syndrome as spasticity. Spasticity is seen in neurological conditions affecting the UMN anywhere from the cerebral cortex to the spinal cord. Depending on the location of the neurological lesion, spasticity may accompany hemiparesis, paraparesis, or tetraparesis (Good, 2002).

Spasticity, impaired mechanisms of movement production, muscle stiffness, and contracture all contribute to a net imbalance of forces affecting joint position statically and limb movement dynamically. Since observed spasticity is not a single pathophysiological entity, but a collection of motor program disturbances (Grimm, 1983), other components of UMN syndrome must be considered besides the enhanced stretch reflexes. Because spasticity can be associated with so many clinical conditions, has different components, and may vary in severity among individual patients, it is difficult to define in a comprehensive fashion.

The apparent mismatch between the reflex hyperexcitability definition of spasticity offered by Lance and the clinical observation of symptoms by physicians is rooted in a lack of differentiation between the neural and rheologic components of muscle tone. Spastic muscle hypertonia is normally attributed to hyperexcitability of stretch reflexes. As shown in Figure 1.2, increased resistance to passive movement, may also result from alterations in the passive mechanical characteristics of muscle, the most common being muscle contracture (O'Dwyer, 1996). Changes in the rheologic properties of muscle, tendons, and joints can be caused by pathologic states that alter the normal control of limb position and movement. These rheologic changes can, in turn, exacerbate these pathologies (Mayer, 1997).

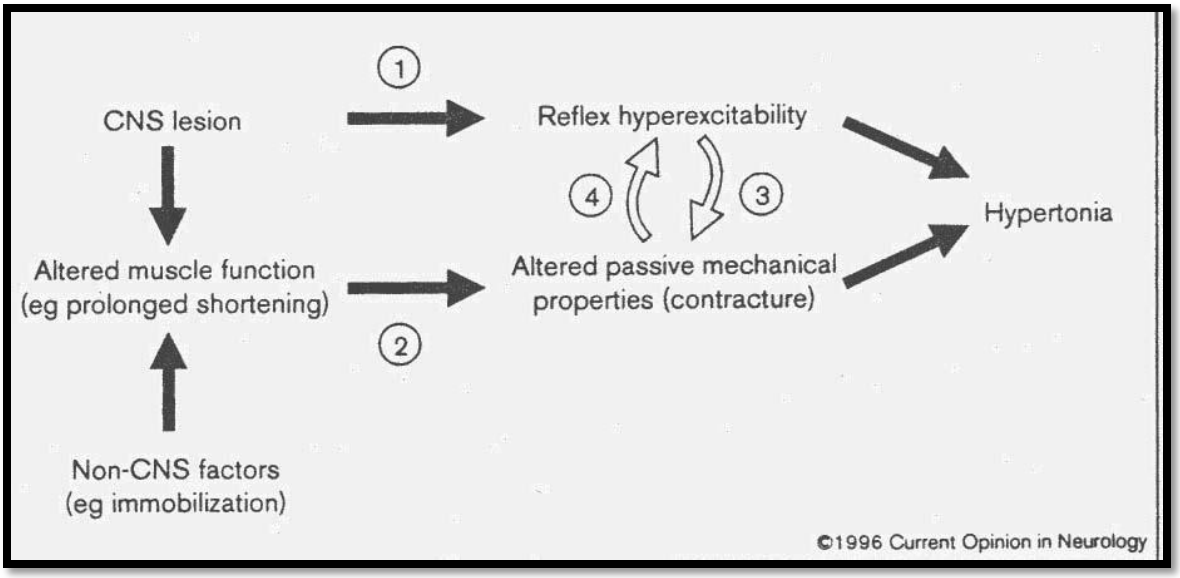

Figure 1.2 Two possible mechanism of hypertonia following an UMN lesion.
Source (Johnson, 2002)

The major challenge in spasticity treatment is the development of measurement techniques that are broadly consistent with the clinical definition and perception of the impairment, yet at the same time sensitive enough to separate the neural from the rheologic components of muscle tone. Lance's (1980) characterization of spasticity as "velocity dependent increase in tonic stretch reflex activity" establishes a paradigm that hyper-excited stretch reflexes are responsible for the increased resistance to passive movement and, with this in mind; different techniques to quantify spasticity in UMN syndrome patients have been developed. These techniques of spasticity measurement are grounded in the rationale that sustained overactivity in some way limits limb performance. Implicit in spasticity measurement is the concept that there exists a direct relationship between the velocity of stretch and the degree of hypertonia measured in a limb.

However, Burne et al. (2005) showed that spastic subjects exhibited a smaller range of reflex modulation, in comparison to non-spastic subjects, while also displaying decreased maximal contraction levels (weakness) and significant increases of resting contraction levels. The significance of this research is that it shows that even when limbs are at rest there exists increased tone in spastic limbs. As a consequence of this raised background contraction, when perturbations with amplitudes and frequencies comparable to those used clinically were imposed on the resting limb, the stretch reflex and the passive joint resistance were increased in the spastic subjects. The existence of increased tone in spasticity has generated a shift in the definition of spasticity from a velocity dependent increased in tone, to an increase that is both velocity and position dependent. This naturally poses a conundrum in spasticity research because Burne's results give us the opportunity to examine whether spasticity is a velocity–dependent phenomenon spasticity or disorder of resting limbs?

1.4 Outcome Measures of Spasticity

Lance's (1980) velocity dependent definition of spasticity forms the foundation of the majority of the techniques developed to quantify spasticity. The significance of these measurements, however, lies in the ability to match the biomechanical aspects measured to the clinical observations of spasticity. Traditionally clinicians describe spasticity as "a disorder of spinal proprioceptive reflexes manifested as profound changes in reflexes to muscle stretch with a strong velocity-dependent component, emergence of pathological reflexes and uncontrolled spasms, an increase in muscle tone, and impairment of voluntary motor function" (Latash, 1998). This reliance on descriptive features of spasticity in terms of signs and symptoms instead of underlying mechanisms, highlight

some of the areas of mismatch between clinical and biomechanical measure of spasticity. While there are many approaches to measurement, outcome measures of spasticity can be broadly grouped into 1 of 3 categories: Clinical scales, biomechanical measures, and physiological measurements.

1.4.1 Clinical Scales

In this category, outcome measures are assessed through passive movement, applied by the clinician, or researcher. Examples of passive activity quantification include clinically measuring the increases of distensibility and elasticity of connective tissue in the spastic patients, measuring muscle tone, and assessing passive range of motion (ROM) (Elovic, 2004). Scales are the most common approach to the routine measurement of levels of spasticity. In the clinical setting, the most commonly used assessment of spasticity is the Ashworth scale. The Ashworth test is based upon the assessment of resistance to passive stretch by the clinician who applies the movement (Johnson, 2002). The scale was first developed in 1964 as a tool to assess the effectiveness of a drug to treat spasticity associated with multiple sclerosis (Good, 2002).

The Ashworth scale is an ordinal scale that assesses muscle tone from 0 (no increase in tone) to 4 (affected part rigid in flexion and extension). A score of 1 is assigned to a slight increase in tone noted at the end of the ROM while a score of 4 is assigned when a limb is rigid (Elovic, 2004). In an attempt to strengthen the scale as an assessment tool, Bohannon and Smith created and published the modified Ashworth scale (MAS), which contains an additional level of measurement (1+) and contains a revised definition at the lower end of the Ashworth scale (Figure 1.3). Although the MAS is very subjective and divides the description of spasticity into rather broad categories of

Score	Ashworth Scale[12]	Modified Ashworth Scale[13]
0	No increase in tone	No increase in muscle tone
1	Slight increase in tone giving a catch when the limb was moved in flexion or extension	Slight increase in muscle tone, manifested by a catch and release or by minimal resistance at the end of the range of motion when the affected part(s) is moved in flexion or extension
1+		Slight increase in muscle tone, manifested by a catch, followed by minimal resistance throughout the remainder (less than half) of the range of movement (ROM)
2	More marked increase in tone but limb easily flexed	More marked increase in muscle tone through most of the ROM, but affected part(s) easily moved
3	Considerable increase in tone, passive movement difficult	Considerable increase in muscle tone, passive movement difficult
4	Limb rigid in flexion or extension	Affected part(s) rigid in flexion or extension

Figure 1.3 Ashworth and Modified Ashworth Scales.
Source (Pandyan et al., 1999)

increased tone, it has become the "gold standard" for semi-quantitative clinical assessment of spasticity (Good, 2002). Bohannon and Smith reported that there was good interrater reliability in its use in the assessment of elbow flexor spasticity secondary to intracranial pathology (Bohannon and Smith, 1987). However, the MAS reliability for use in lower extremities after traumatic brain injury has been questioned. Allison et al. stated that the MAS was only "minimally adequate" for plantar flexor tone for TBI patients, based on intrarater and interrater reliability (Allison et al., 1996). Blackburn et al. found questionable interrater reliability when looking at similar parameters in attempting to assess lower extremity spasticity in stroke patients (Blackburn, 2002).

Intrinsic limitations exist in the assessment of spasticity using the Ashworth or MAS scales. In performing the test the clinician is required to extend the joint rapidly, usually the elbow or the knee, and make a subjective judgment of the level of resistance to motion (Johnson, 2002). That makes the test very dependent on the examiner, which makes the results difficult to duplicate between raters. Also, the resistance to and range of

passive movement can result from changes in the level of voluntary and reflex activity in the alpha motor neuron of agonist and antagonist motor groups or from changes in the viscoelastic properties of soft tissues and joints (Pandyan, 1999). Using either the Ashworth or MAS, it is not possible to distinguish between these two components of resistance. The significance in this lack of differentiation is that different causes of increase resistance to movement may require different treatment paradigms. The Ashworth scale does not measure low tone and has doubtful reliability. Studies have either used correlation coefficients rather than reliability coefficients (Bohannon and Smith, 1987) or have reported unacceptable coefficients of reliability such as 0.397 (Allison et al., 1996) and 0.20-0.62 (Haas et al., 1996).

With the modified Ashworth scale there are limitations in the statistical interpretation of the data. The distinguishing feature of the MAS is the introduction of an additional level of measurement (1+). The scale represents a grading of the assessment of spasticity and there is no clear evidence that the 1+ score represents a greater level of spasticity, other than the presence of the catch (Pandyan, 1999). It can be concluded that if 1 and 1+ are not hierarchical, then the scale can no longer be regarded as ordinal, but it becomes categorical (Johnson, 2002). In addition, there is no unique definition of zero on this scale, or on the original Ashworth Scale, making it difficult to ascertain whether the distances between 1 and 1+, and between 1+ and 2, are equal. Without a certainty in the quantifiable differences between resistance grades, there exists a lack of statistical relevance to the MAS data, making it impossible to use data analysis techniques such as parametric analysis.

The Tardieu Scale is another measure of spasticity that addresses resistance to stretch. First published in 1954, the Tardieu scale addresses the effects of velocity in the assessment of muscle tone. The outcomes that the Tardieu scale quantifies include (a) intensity of the resistance of muscle to stretch, (b) the angle at which the catch is first appreciated, and (c) the differences noted when a muscle is stretch at different velocities (Elovic, 2004). It is believed that moving the limb at different velocities, since the stretch reflex responds differentially to velocity, can more easily assess the response of the muscle to stretch. The ability to objectify the velocity dependent nature of spasticity distinguishes the Tardieu scale from the Ashworth scales.

Gracies et al. (2000) examined the reliability of the Tardieu as a measure of spasticity and its ability to demonstrate intervention efficacy. Their worked observed that the angle where the clonus was first observed was increased due the prolonged stretch of the muscle due the Lycra splints utilized. The original Tardieu scale has been modified by Boyd & Graham in order to assess specified muscles in the lower limb by standardizing conditions for limb placement and alignment. Boyd defines the angle, 'R1' as the angle at which a "catch" or resistance is felt by the examiner in the muscle while moving the limb through its full range of movement at the fast velocity stretch, V3 (Boyd, 1999). The fast velocity stretch is defined in the Tardieu scale as a speed "as fast as possible, faster than the rate of the natural drop of the limb segment under gravity." It is theorized that the overactive stretch reflex in spastic muscles, which is velocity dependent, is represented by the 'catch' felt following the fast velocity stretch (Wallen, 2004). Angle 'R2' is defined as the passive range of movement following a slow velocity stretch, V1. A slow velocity stretch is characterized as movement as slow as possible,

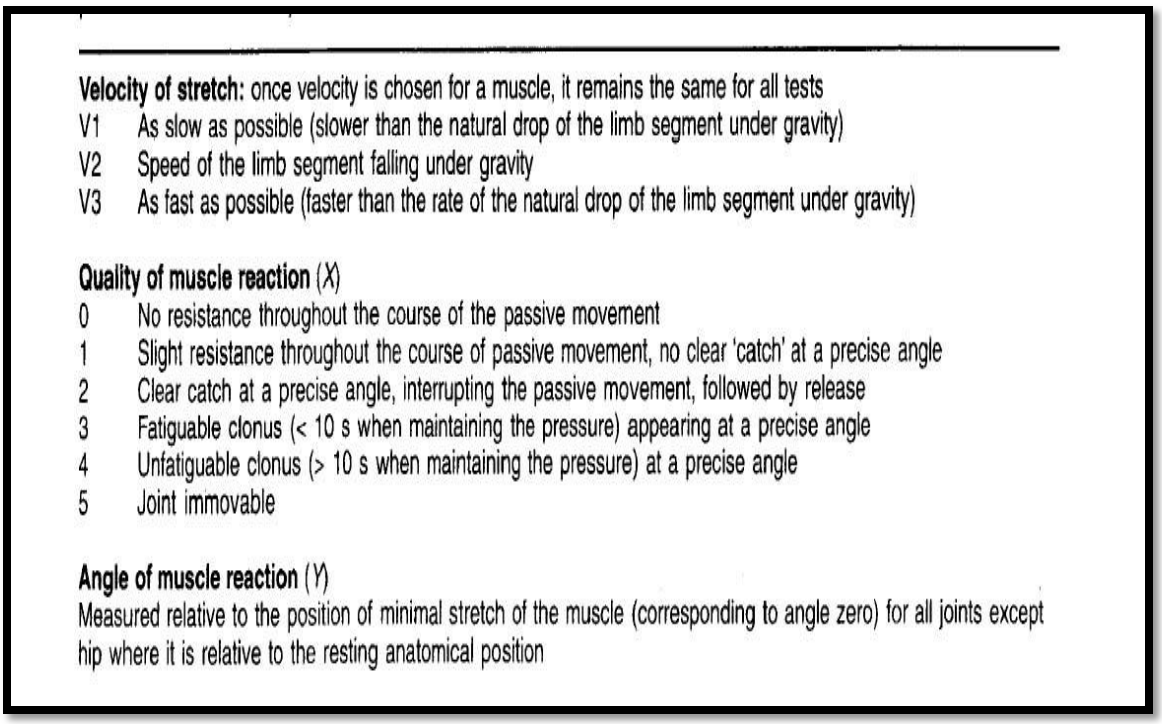

Velocity of stretch: once velocity is chosen for a muscle, it remains the same for all tests

V1 As slow as possible (slower than the natural drop of the limb segment under gravity)
V2 Speed of the limb segment falling under gravity
V3 As fast as possible (faster than the rate of the natural drop of the limb segment under gravity)

Quality of muscle reaction (*X*)

0 No resistance throughout the course of the passive movement
1 Slight resistance throughout the course of passive movement, no clear 'catch' at a precise angle
2 Clear catch at a precise angle, interrupting the passive movement, followed by release
3 Fatiguable clonus (< 10 s when maintaining the pressure) appearing at a precise angle
4 Unfatiguable clonus (> 10 s when maintaining the pressure) at a precise angle
5 Joint immovable

Angle of muscle reaction (*Y*)

Measured relative to the position of minimal stretch of the muscle (corresponding to angle zero) for all joints except hip where it is relative to the resting anatomical position

Figure 1.4 Tardieu scale.
Source (Boyd and Graham, 1999)

theoretically slower than the speed of a limb falling freely only under the influence of gravity. The importance of angle, 'R2' is that this range of movement represents the muscle stretch resistance that is solely due to the rheologic properties of the muscle. The difference between the catch angle, R1 and full passive range of motion of the joint, R2, reflects the potential range of motion available if spasticity could be eliminated (Wallen, 2004). A large difference between the two measures characterizes a large reflexive component of spasticity, whereas a small difference between R2 and R1 means that there is predominantly fixed contractures present (Boyd et al., 1998).

The principal shortcoming of the Tardieu and modified Tardieu scales is their reliance on the same level of examiner subjectivity of the Ashworth scales. The determination on when a 'catch' is felt is highly dependent on the experience of the

clinician. Additionally, the subjectivity of the Tardieu scale extends to the velocity characterizations, V1 and V3. Lack of a standardized protocol to facilitate exactness in movement velocity allows for the limb movement velocities to be dependent on the 'skill' of the clinician. In comparison to the Ashworth scales the modified Tardieu scale provides move quantifiable variables but the same level of subjectivity with the variables, thus further reducing both intrarater and interrater reliability.

1.4.2 Neurophysiological Evaluations

Neurophysiological techniques utilize the paradigm that hyper-excited stretch reflexes are responsible for the increased resistance to passive movement. These techniques seek to provide better information about the state of the reflex pathways. Electromyography (EMG) is considered to be the most direct technique of spasticity measurement during passive stretch because the presence of stretch-evoked muscle activity is the only way of distinguishing a neural component of stretch (Boyd, 2001). In general raw EMG signals are usually averaged and rectified for analysis. EMG measurement can be utilized to trace the onset and duration of muscle contraction in response to many self-induced and initiated movements. Technology has allowed researchers to apply repeatable inputs, perturbations, and well defined stretches to tendons and muscles during daily activities to better understand stretch reflex and joint mechanics (Elovic, 2004). The characterization of spasticity as being caused by abnormal processing of proprioceptive input along reflex pathways has led to numerous attempts to quantify spasticity through the analysis of abnormalities in reflex pathways. These abnormalities include altered presynaptic inhibition, excitability in the Ia afferent pathway and increased alpha motor neuron excitability (Johnson, 2001). There have several types of EMG patterns that have been

used to describe the level of spasticity in a patient. These patterns include inefficient muscle activation with abnormal EMG-force relationships, disturbances of spatial selection of muscles, and alterations in the time-course of EMG activation in agonist and antagonist muscles (Good, 2002). The most common neurophysiological measures of spasticity are tendon jerks, H-reflex studies and F-wave studies.

1.4.2.1 Tendon Jerk Method. Tendon jerk methods are designed utilizing the principle that muscle contractions can be elicited as a result of percussions of a tendon. A tendon jerk is elicited by a rapid, small stretch of a muscle. It is believed that the response to this stretch primarily involves the monosynaptic pathway, although it has also been suggested that this action could be influenced by oligosynaptic pathways (Rothwell, 1994). The theory of tendon jerk response quantification is that tendon jerks are more readily elicited in people with spasticity – i.e., they can be elicited with smaller levels of stimuli than normal yielding a response that has higher amplitude and more dispersed. The amplitude of tendon jerk response could therefore be used as quantifiable measure of spasticity. The tendon reflexes that are normally measured in the clinical setting are not quantified scrupulously due to the variability that exists in the tapping protocol. Variability exists in the force exerted by the tap and the position on which the tendon is hit. Experimental approaches to address these two limitations have included systems, such as an automated hammer to measure the force in addition to ensuring the same tap position is maintained (Fryer, 1972). This technique has been furthered improved by the use of motor controlled tendon tap that provide increase precision in position, direction, and force of application.

Parameters that can be quantified from tendon jerk techniques include the muscle contraction force in response to tendon stretch, contraction and relaxation times, as well as muscle EMG recordings (Good, 2002). Additionally, a comparison can be made between the amplitude of the EMG response to tendon stimulation and the amplitude of the M-wave obtained in response to supramaximal motor-nerve stimulation, as an indication of the number of motor units activated by the stretch reflex (Dimitrijevic, 1995). In comparison to mechanical stretching methods, tendon jerk methods are able to measure the neural component of muscle response directly. Thus tendon jerk methods avoid the issue of distinguishing between neurogenic and mechanical factors of stretch response. Despite this apparent advantage, the method of tendon jerks fails to determine whether the increase in the tendon jerk response is related to increase gain, decrease threshold or a combination of both factors (Johnson, 2001).

1.4.2.2 Hoffman Reflex. The Hoffman or H-reflex is a long latency reflex that is obtained by stimulating a peripheral nerve, eliciting a spinal monosynaptic reflex, and recording the resultant reflex compound muscle-action potential from a target distal muscle using an EMG electrode (Good, 2002). The muscle response, which results from stimulation from conduction via the Ia afferent pathways, is independent of the muscle spindle activity (Johnson, 2001). The H-reflex measurement concept is based on the assumption that in spastic patients, a larger percentage of the lower motor neuron pool can be activated in reflex response through the stimulation of peripheral nerves (Good, 2002). The H-reflex reflects the summation of excitatory and inhibitory influences on motor neurons. An increase in H-reflexes is typically associated with relative excitability

or depolarization of the motor neuron pool, and a decrease in H-reflexes reflects inhibition or hyperpolarization of the pool (Leonard, 1998).

H-reflex measurements typically suffer from variability due to stimulus intensity, the resting posture of the limb, the ability of a subject to relax, or the neck and vestibular reflexes (Johnson, 2001). As a result of this variability, the H-reflex is generally compared with a maximum muscle response obtained by direct supramaximal stimulation of the same nerve recording over the same distal target muscle (Good, 2002). This maximum response, known as the M wave or M response represents the total pool of motor neurons that can be excited by stimulation in contrast to the H-reflex response, which represents just the motor neurons that can be excited by antidromic stimulation mediated through Ia fibers (Elovic, 2004). The H/M ratio is obtained by dividing the amplitudes the H-reflex & M responses respectively. The function of the H/M ratio as a measurement of spasticity lies in the role that the excitability of Ia fibers plays in the spastic response. It has been reported that the H/M is higher in spastic patients with hyperactive tendon jerks (Little, 1993).

Higashi et al. (2001) compared the excitability of the motorneuron pools of both the spastic and unimpaired sides of hemiplegic patients by using a method of comparing H-reflexes and M responses. This technique of analysis determines the ratio of the developmental slope of the H-reflexes (Hslp) to the slope of the M response (Mslp). The Hslp is defined as the ratio of the increase number of recruited motorneurons to the increase in intensity of the electric stimulation of Ia afferents to evoke H-reflexes (Higashi, 2001). The Mslp however is defined as the ratio of the increased alpha motor nerves recruited in the nerve trunk at the site of the stimulus to the increase in stimulus

intensity applied to Ia afferent nerves. The results of the research showed that the motor neuron pool excitability of the spastic side, assessed via Hslp/Mslp was appreciably higher than that of the unimpaired side of the hemiplegic patients (Higashi, 2001).

1.4.2.3 F-Waves. The F-wave response is another electrophysiological measure used to provide an outcome assessment of spasticity by measuring alpha motor neuron excitability. The F-wave is formed due to antidromic stimulation of motor neurons and has been observed as being elevated in spasticity and hyperexcitability of the motorneuron pool (Elovic, 2004). Although the signal produced by F-wave acquisition is less influenced by resting posture and the ability of subjects to relax, intrarater variability still exist in terms of latency and amplitude making it necessary for repeated test (Johnson, 2001).

The major shortcoming of all neurophysiological measures continues to be the inability to correlate these measures with the present clinical techniques used. In addition, the equipment required to analyze electrophysiological data makes the techniques impractical for measuring spasticity in a clinical environment. While quantifiable and objective, the value of neurophysiological measures in predicting a high-level functional outcome is still limited (Elovic, 2004).

1.4.3 Biomechanical Measures

The velocity dependent characterization of spasticity in the literature has led to the development of many different biomechanical approaches in an attempt to describe spasticity in more quantifiable measures. Methods range from the relatively simple, to more sophisticated approaches that measure torque-angle relationships during passive and active movements (Good, 2002).

1.4.3.1 Sinusoidal Waveforms and Powered Systems. In attempting to identify the most useful quantitative measure of spasticity, many researchers cite the torque versus angle relationship at a joint to be the most applicable because it closely epitomizes the definition of spasticity as well shows correlation with the gold standard of the MAS (Elovic, 2004). This has lead to research into other forms of biomechanical measures of spasticity that involve the recordings of muscle torque and angular stiffness. This technology utilizes sinusoidal analysis and Nyquist plots to characterize stiffness and viscosity in response to force applied across spastic joints (Good, 2002). In the sinusoidal waveform method, the amplitude is generally fixed and the frequency of oscillation is varied. Movement occurs about a determine position, usually referring to the joint in a neutral position. It is argued that a sinusoidal movement, in addition to being reproducible and controllable, is similar to many functional movements such as walking (Becher, 1998). The major disadvantage of this method however lies in its predictability. Hunter and Kearney (1982) argue that predictability in assessment allows for the occurrence of voluntary, pre-programmed modulation of muscular contractions instead of eliciting involuntary responses.

Walsh (1996) developed an alternative approach to the measurement of spasticity involving the use of a powered system in which an electric motor is used to provide oscillation at the wrist. This technique utilize two approaches – a displacement can be applied and the resulting muscle stiffness measured, or the force can be applied and the natural frequency or resonance can be measured (Johnson, 2002). In Walsh's experiment the patient held a simple handle attached to an electric motor. The motor produced flexion and extension of the joint and the apparatus also measures EMG. Using this

system Walsh showed that the ability to measure different amplitude and natural frequency of oscillation depends on the joint stiffness. Additional he demonstrated that after the application of a number of cycles of movement, the resistance to motion would be reduce and larger amplitude of oscillation could be sustained (Johnson, 2001).

Corry et al. (1997) used the technique to study the use of botulinum (Botox) toxin in patients with cerebral palsy to measure the change in natural frequency before and after the injection. In a 14 year old patient the experimenters recorded the resonant frequency at the wrist. Before administration of Botox, the natural frequency of the wrist was high, indicating a very stiff joint. After the injection, the natural frequency decreased which was indicative of a reduction in stiffness. Although promising, the technology required in this type of analysis is not practical for the clinical setting and has thus been relegated to the laboratory research setting.

1.4.3.2 Pendulum Knee Test. The pendulum test is a biomechanical method of evaluating muscle tone by using gravity to provoke muscle stretch reflexes during passive swinging of the lower limb (Fowler, 200). First introduced by Wartenberg (1951), the method involves lifting the limb under investigation against gravity to full extension and when relaxed, releasing it, causing it to fall and swing freely as shown in Figure 1.5. Test subjects are instructed to relax and not to intervene when the limb is released. The emphasis is on the limb being relaxed in order to achieve the aim of measuring the muscle’s response to passive stretch.

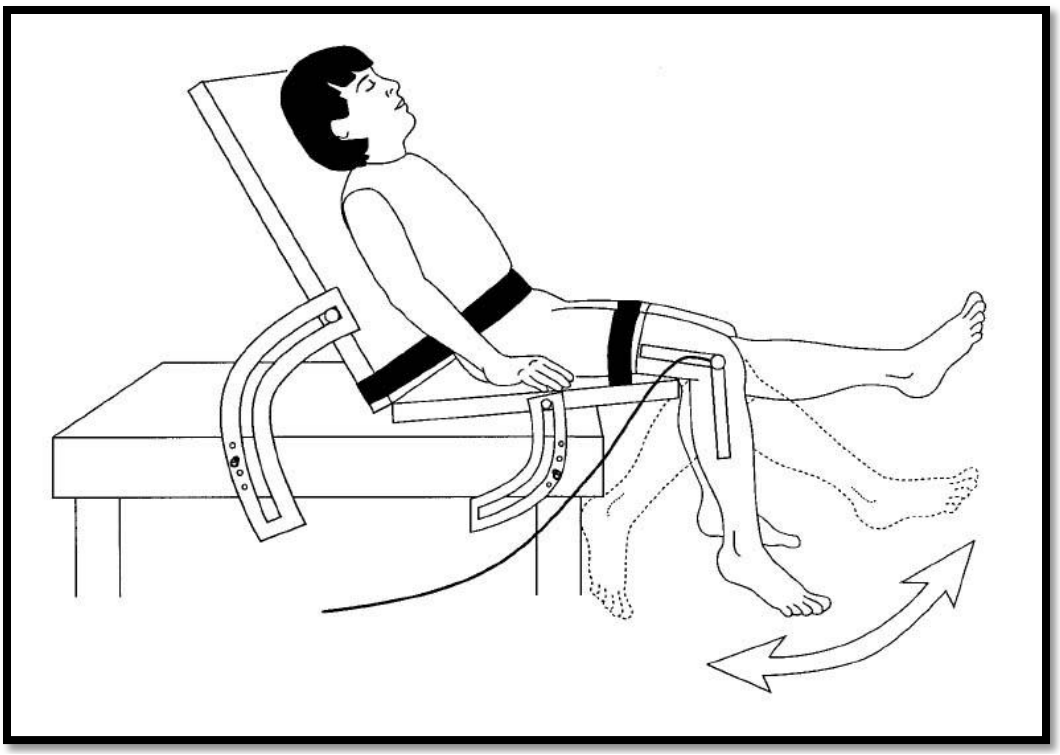

Figure 1.5 Positioning of subject in pendulum test.
Source (Fowler, 2000)

The test requires angular joint movement to be measured over time until the limb comes to rest. From the resulting angle-time plot, parameters defining characteristics of the swings can be calculated. In a normal healthy subject the leg will swing about six times, but in the presence of spasticity the number of swings is reduced in accordance with the velocity dependence (Johnson, 2002).

In unaffected individuals, the observed pattern of the swinging limb, typically quantified using an electrogoniometer, has been described as smooth, regular, and like that of a damped pendulum (Fowler, 2000). The limb movements appear to oscillate about the gravitational resting position (Fee and Foulds, 2004). In contrast, the spastic limb has a characteristic trajectory that appears to ratchet toward the gravitational orientation as shown in Figure 1.6. Wartenberg (1951) described spastic limb motion as

having decreased number of oscillations and an irregular characteristic motion. Simons and Mense (1998) observed that the overreactive reflex stretch responses of spastic muscles reduce the number and smoothness of oscillations of an affected limb and may interrupt the first swing before it can complete its initial downward phase. The spastic limb moves initially moves in flexion due to the torque exerted on the knee joint by gravity. This motion is accompanied by muscle activity producing movements which oppose movement in the gravitational direction (Fee and Foulds, 2004). This characteristic pattern of movement in the spastic limb of initial gravitational falling with arrest in gravitational motion has been characterized in the literature describing spasticity in stroke, cerebral palsy and multiple sclerosis (Vodovnik et al., 1984; He, 1998; Lin and Rymer, 1991).

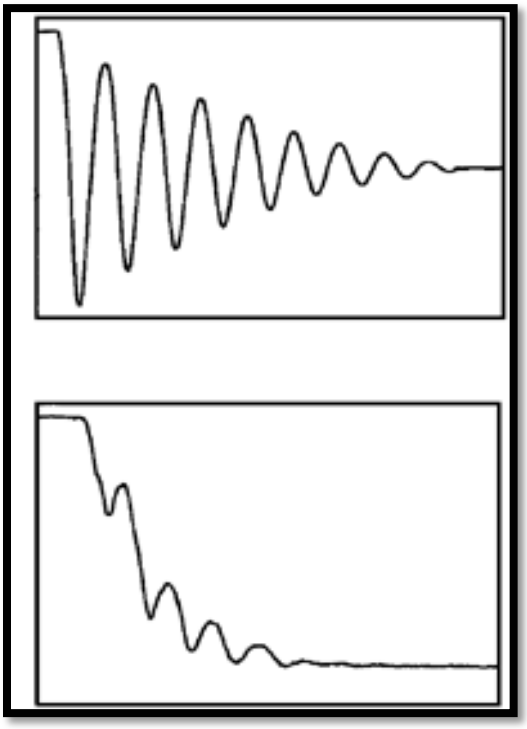

Figure 1.6 Trajectory of normal subject and subject with spasticity.
Source (Krause et al., 2004)

1.5 Trajectory Analysis of Pendulum Knee Data

Wartenberg's initial characterizations of limb motion from the pendulum test were mainly descriptive in nature, focusing the number of oscillations as a primary descriptor of spastic trajectory. Bajd & Vodovnik (1984) who attached a goniometer to the knee and recorded the movements at the joint after release further examined the test technique. They developed the Relaxation Index, based on the postulation that when the extended spastic limb is dropped, it behaves like a linear damped pendulum (Bajd & Vodovnik, 1984). The Relaxation Index, R2 (Figure 1.7) measures the angular excursion of the pendulum swing of the dropped limb as a fraction of the initial angle made by the suspended limb with the vertical (Kaeser, 1998). If the leg overshoots the vertical, R2 is greater than 1. If the swing is interrupted before the limb reaches the vertical, R2 is less than 1, indicating spasticity.

Leslie et al. (1992) investigated the use of the Relaxation Index and its relationship to the original Ashworth scale. They found a good correlation and showed that the pendulum test appeared to be a more sensitive measure than the Ashworth scale. Fowler et al.. (2000) used the same test with cerebral palsy patients. They looked at a range of outcome measures of spasticity, including the modified Ashworth score performed at the knee, in 30 subjects with cerebral palsy and compared them with 10 controls. Their conclusions were that the modified Ashworth Score, EMG measurements, and the number of oscillations, differed significantly between test subjects and controls (Johnson, 2002). They also found that the first swing excursion was the best predictor of spasticity and that the number and duration of swings differentiated between patients and

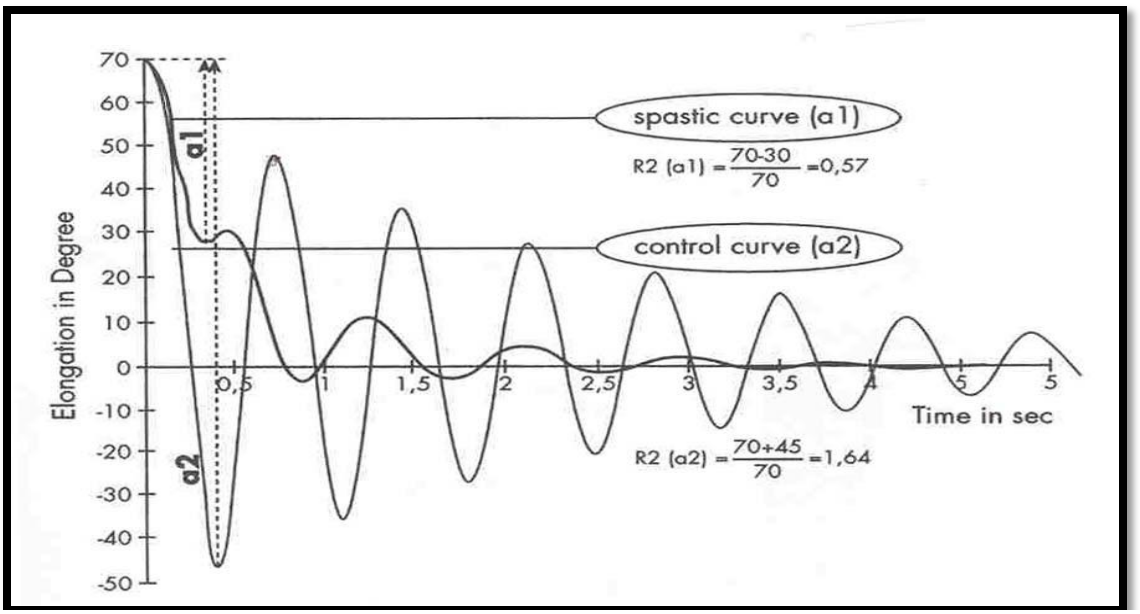

Figure 1.7 Calculation of index R2, from the pendulum data of a spastic and normal leg. Source (Good, 2002)

controls, but not between the patient groups. However, the Relaxation Index was considered not a good measure of spasticity (Johnson, 2002). The importance if this entire body of research is that it began to introduce the concept that the trajectories, originally described by Wartenberg, can be used to differentiate between non spastic and spastic individuals. Further, the work of Leslie and Fowler illustrates that the Relaxation Index may provide a measure that can correspond with clinical measures of spasticity such as the MAS.

In moving from a descriptive to more quantitative analysis of pendulum knee trajectory, there was still a need to understand to what degree the trajectory was based on the passive mechanical properties of muscle versus active inappropriate muscle activity? This quandary moved spasticity research in the direction of analyzing EMG activity occurring during the pendulum knee test. Measuring the timing of EMG activity relative to the measured increase in torque during passive muscle stretch provides an estimate of

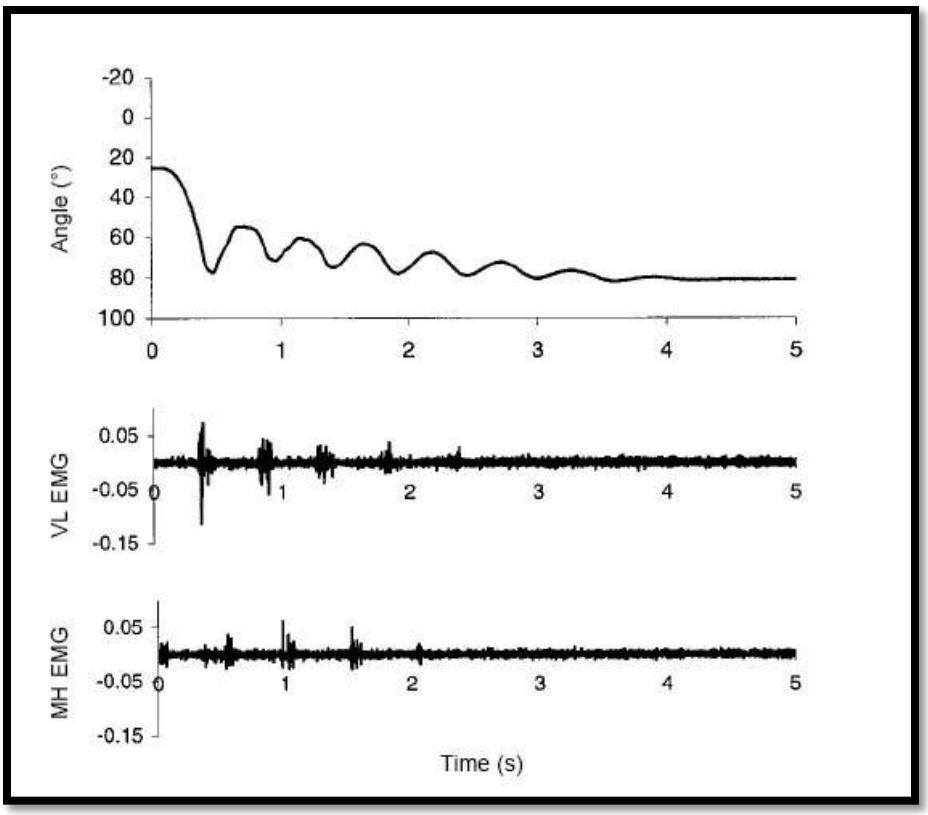

Figure 1.8 Subject with CP and severe spasticity measured on the Ashworth Scale. Source (Fowler, 2000)

stretch reflex threshold (Powers et al., 1989) or angular threshold (Allison and Abraham, 2001). The pendulum trajectories of subjects without spasticity show EMG recordings indicating a lack of active muscle contraction during swing, in contrast to the observations in spastic limbs (Fee and Foulds, 2004).

Vodovnik et al. (1984) observed quadriceps muscle activity after initial release of the spastic limb which produced a "dent in the damped sinusoid". In their analysis of the limb trajectory, the more spastic the limb, more 'dents' in the trajectory. The burst of EMG activity indicates a contractile force of the quadriceps which tends to extend the leg during the falling phase (Vodovnik et al., 1984). Fowler (2000) observed EMG bursts (Figure 1.8) in both the quadriceps and hamstrings in cerebral palsy subjects with

spasticity, in response to stretch due to limb the oscillations of the pendulum test. These EMG bursts produce a reversal in direction of leg motion in the opposite direction of gravity. Other authors have also shown that in spastic trajectory during the pendulum knee test there are EMG burst occurring in both extensor and flexors during the phase of the movement in which they are stretched (Lin and Rymer, 1991; He, 1998; Fee and Foulds, 2004). The EMG burst corresponds to the stretch reflex which introduces additional torque, causing the limb trajectory to deviate from a pendular appearance (Fee and Foulds 2004).

In order to reproduce the additional torque necessary to produce the spastic limb trajectories by mathematical modeling, Vodovnik et al. (1984) utilized a step function to approximate the force of the quadriceps. Fee and Foulds (2004) created an active element neuromuscular model of spasticity that utilizes two-step torques to each of the passive extensor and flexor plants of the model. Rather than relying on the timing of EMG like the model used by Vodovnik et al., the model proposed by Fee and Foulds implements an optimization algorithm to specify the timing and amplitude of torques that can be introduced to improve the performance of the best fitting passive model (Fee and Foulds, 2004).

With the beginnings of a neural contribution to spasticity being investigated, Fee and Samworth (1995) investigated the degree to which the differences in the neural contribution to spasticity can be captured in response to neurological interventions. They developed a model of spasticity of three triplets two of which had spasticity. Each child went through 15 min of vertical up and down acceleration on a specially constructed platform. They demonstrated that leg swings of the two siblings with spasticity appeared

considerably more pendular and look more in appearance like the swing of the non-spastic sibling. The reduction in spastic muscle firing evidenced through EMG recordings served as confirmation of this result. Fee and Miller (2004) show the elimination of spasticity by general anesthesia. Under anesthesia, results of a pendulum leg drop test are significantly different from those seen in limbs with spasticity. They demonstrated that for all of the spastic subjects, the removal of spasticity by general anesthesia produced a nearly normal leg drop as shown in Figures 1.9 and 1.10.

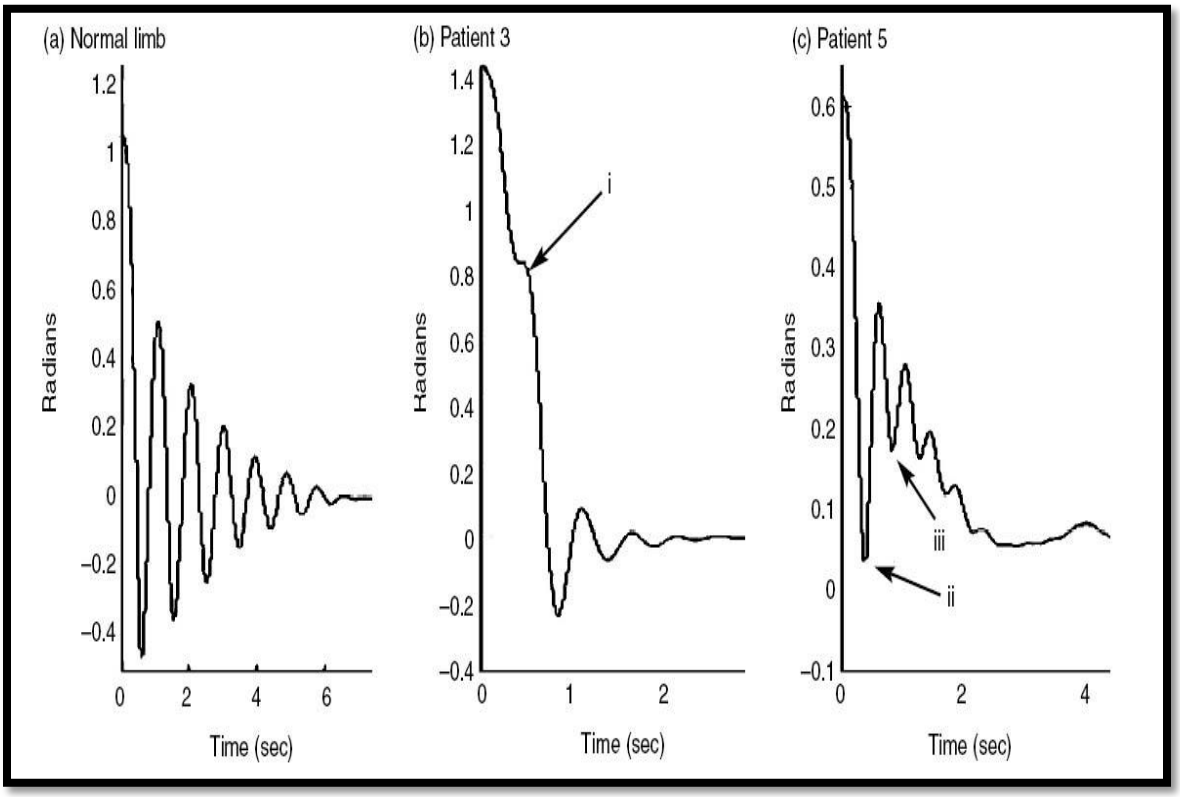

Figure 1.9 Leg drop pendulum test position tracing from (a) patient without disabilities and tracings from two patients with spasticity, (b) patient 3 (c) and patient 5.
Source (Fee and Miller, 2004)

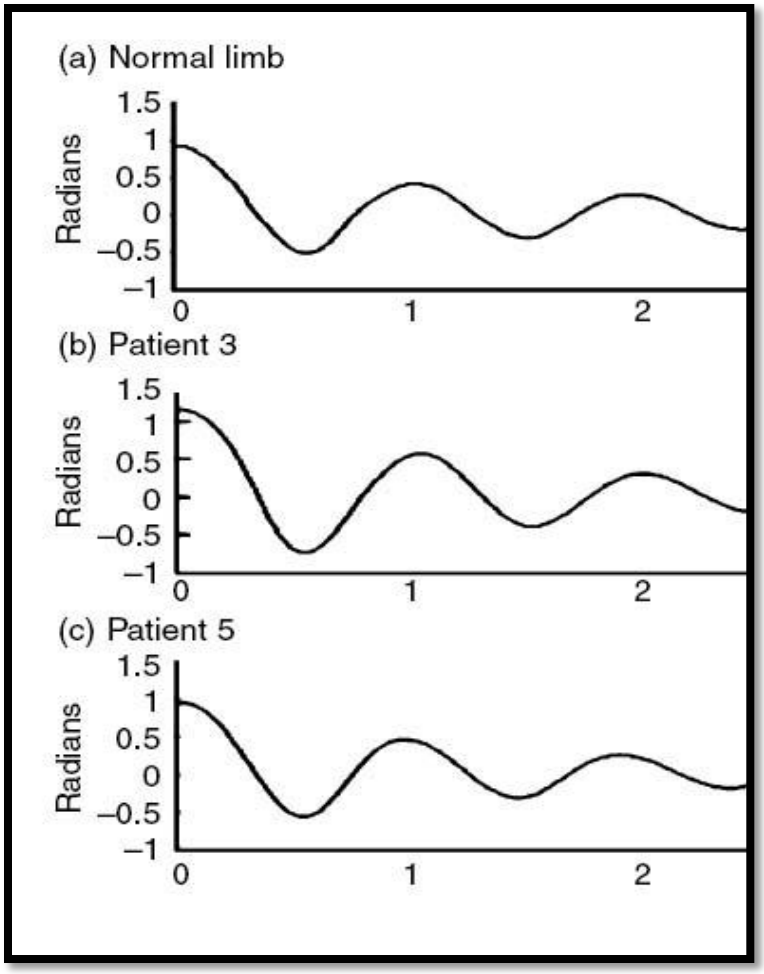

Figure 1.10 Pendulum Test under general anesthetic for same subjects in Figure 1.9. Source (Fee and Miller, 2004)

Fee's work in vertical accelerations and general anesthesia in conjunction with previous modeling of spastic limb trajectory with the addition of burst of torque (Vodovnik et al., 1984; Fee and Foulds, 2004) confirms that the cause of the characteristic trajectory in pendulum knee test is active muscle behavior under neural control.

1.6 Research Direction

In the literature it has been shown that the pendulum knee drop test can be used to extract measures of spasticity. Quantification of the spastic trajectory can be utilized to provide a measure of spasticity. The fact that this limb trajectory is influenced by neurally controlled muscle activation that can be perturbed and that a different limb trajectory results from this perturbation, suggest that there is a need for a model of spastic limb motion which goes beyond just describing the appearance of the pendulum knee drop trajectory. It also indicates that it may be possible to construct a forward dynamic model that is guided by features which typically characterize spasticity. Rather than research which seeks separate explanations for spasticity, weakness, co-contraction, and other outcomes of disordered motor control, the effort of this research is focused ultimately expanding the definition of spasticity to by taking into account the negative impact spasticity has on the achievement of motor control.

It is this research's belief that the equilibrium point hypothesis of motor control which theorizes that muscle force and active movements develop as a result of shifts in the equilibrium state of the motor system, structures the basis of understanding the nature of reflex and motor deficits such as spasticity (Levin, 2000). This remainder dissertation will focus on the development of a forward dynamic model incorporating the concept of the equilibrium point hypothesis. The scope of the proposed study focuses on two features which typically characterize spasticity, an increase in passive stiffness of muscle and the hyperactive behavior of the stretch reflexes. Passive joint stiffness, which is to be quantified in this research, refers to the resistance to movement or force that occurs even when motor neurons are quiescent and their myofibers are not actively contracting.

Research assessing the change in passive joint stiffness after neurological interventions such as general anesthesia (Krabak et al., 2001; Fee 2004), after the use of intrathecal baclofen (Remy-Neris et al., 2003; Francisco et al., 2005) and vertical accelerations (Fee and Samworth 1995; Kuczynski and Slonka 1999; Fee and Foulds 2004) support the intended goals of this research to:

- Apply the Equilibrium Point Hypothesis to characterize the ability of a lower limb to follow a virtual trajectory of joint motion.
- Assesses the model's robustness in characterizing the differences in motion between non-spastic and spastic subjects.
- Investigate the ability to define passive stiffness of the knee joint in terms its neutral body position

Understanding the neuromuscular influences on muscle tone (flexibility) will assist in the development of new rehabilitative techniques in cerebral palsy. This not only provides the clinician with a better understanding of the pathophysiology of spasticity but permits a better understanding of the clinical tools that are utilized to measure these abnormalities and better comprehension of the therapeutic and pharmacologic interventions that can modulate this abnormal tone.

CHAPTER 2

CNS MODELING OF STRETCH REFLEX THRESHOLD REGULATION

The complex nature of spasticity, as demonstrated in the previous chapter, demonstrates that the search for viable treatment methods for spasticity is rooted in the clinicians search to understand what exactly is disordered. This research illustrates that the understanding of spasticity is be rooted in our ability to conceptualize the role that the central nervous system plays in altering stretch reflex threshold activation.

Neuromuscular control is typically viewed from a top-down perspective. Commands are generated at the highest control center, the motor cortex, programmed into a movement program and sent to the motoneuron pool. The motoneuron pool activates the muscle, the muscle generates force and finally this results in a movement. The maintenance of appropriate levels of muscle tone facilitates the muscle's ability of make optimal response to voluntary or reflexive commands. Comprehension of the mechanisms utilized to alter muscle tone requires an ability to conceptualize the role of the central nervous system in the regulation of motor control. This research demonstrates that the abnormal motor behavior which characterizes spasticity can be modeled as response to a change in the equilibrium state of the motor system. The equilibrium point hypothesis of motor control, with its ability to it model the positional and velocity gains of the stretch reflex relative to a static or moving state of dynamic equilibrium at a joint, has important implications for disordered motor control flowing a CNS lesion.

2.1 Equilibrium Point Hypothesis

The equilibrium point hypothesis (EPH) or λ model of motor control suggests that descending commands from the CNS utilize muscle reflex mechanisms to facilitate changes in the activity of muscle reflexes, while also specifying the parameters of the reflexes (Latash, 1998). Muscle reflexes specify a relationship between muscle force and length – an invariant characteristic, IC (Figure 2.1). For a set descending command, constant external load and certain muscle length, there exists a point, the equilibrium point, where the muscle-load system is at equilibrium. Perturbations or changes in the external load yield changes in muscle length inducing changes in muscle activation levels via the tonic stretch reflex arc (Latash, 1998). Reciprocally, the resultant changes in muscle activation levels stimulate parallel changes in muscle force and length until a new equilibrium point is reached. According to the equilibrium point hypothesis, voluntary motor control or the control actions of muscles is not explicitly computed, but rather arises as a consequence of the interactions among moving equilibrium position, current muscle kinematics, and stiffness of the joint (Suzuki and Yamazaki, 2005).

The EPH is based on the principle that changes in descending signals to the spinal segmental apparatus may be described as setting threshold values of muscle length for the tonic stretch reflex (Latash, 2008). When the length of a muscle is below this threshold, the muscle is silent. In contrast, if the length of the muscle is over the threshold, the muscle is activated and the level of activation grows with the difference between the actual muscle length and the threshold value (Latash, 2008). The resulting muscle activation produces muscle contraction or shortening, bringing its length closer to the threshold value. Thus, muscle activation of motoneurons and the muscle fibers they

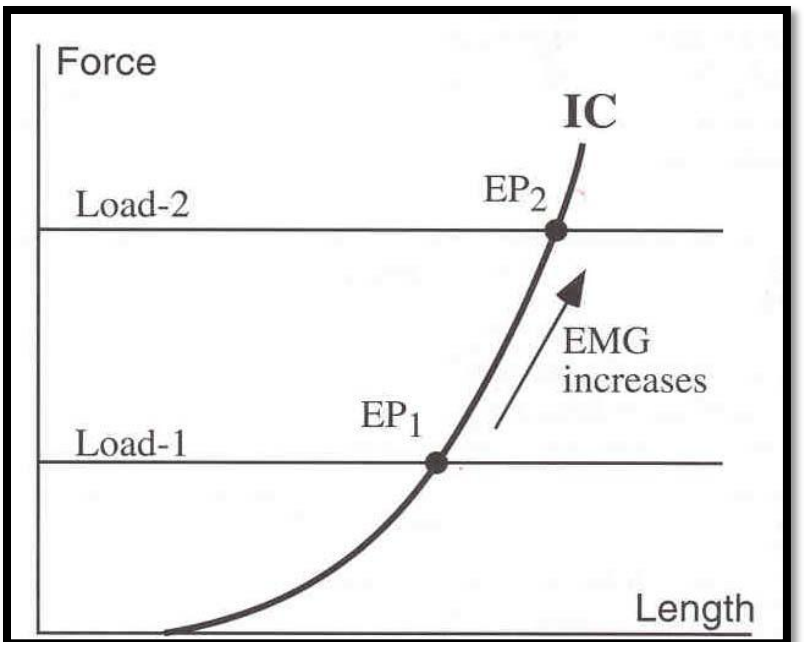

Figure 2.1 Relationship between muscle force and muscle length in EPH.
Source (Latash, 1998)

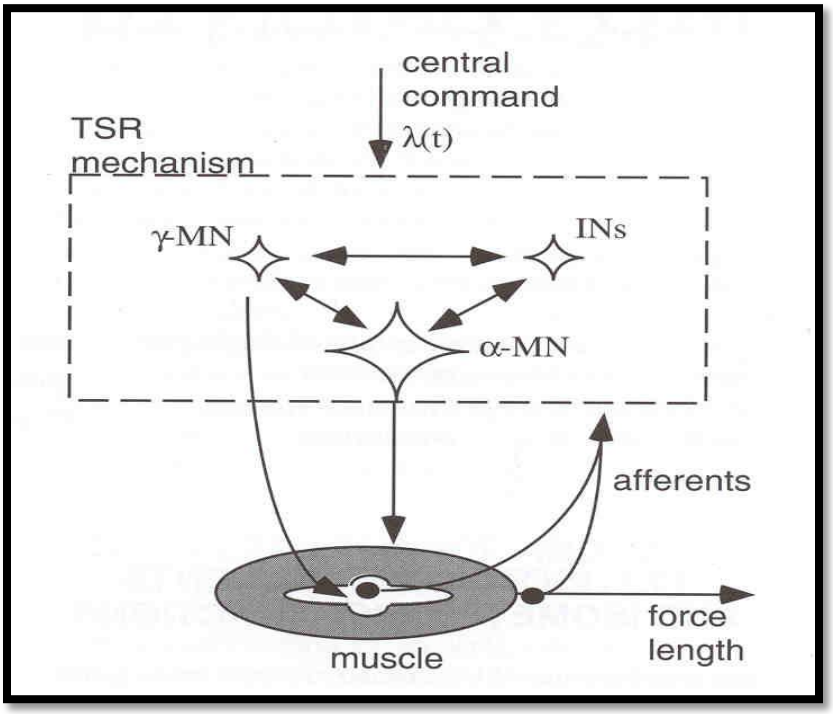

Figure 2.2 Balance of combination of descending signals to all groups of spinal neurons
Source (Latash, 1998)

innervate are controlled by the difference between the threshold position, defined by descending signals and actual muscle position, sensed by proprioceptors (Latash, 2008). The equilibrium point hypothesis presupposes that the central command represents a "balanced combination of descending signals to all groups of spinal neurons including α-motoneurons, γ-motoneurons, and interneurons", as shown in Figure 2.2 (Latash, 1998). The interaction between neural elements (descending command), muscle elements (muscle length) and environment (load) through mechanics & neural loops reduce the activity of motoneurons and minimize the difference between the actual position and the threshold position (Latash, 2008). The rationale of the EPH is that muscles try to achieve minimal activation compatible with external forces including those produced by other muscles.

2.2 Single-Muscle Control Within the EP-Hypothesis

For a single muscle, its steady-state is defined by two variables, length and force. The descending or "central command" is characterized by the variable λ, which represents threshold of tonic stretch reflex. This command defines the dependence between active muscle force and length by setting threshold for the tonic stretch reflex. Actual muscle force and length depend on λ and external load. For a specific λ and external load L, there exists a specific equilibrium point (EP1 in Figure 2.3A). If a muscle is at an equilibrium point (EP1) acting against the load L, its force magnitude equals L. Any deviation of the muscle from that point would result in a change in its activation such that the active muscle force will be higher than L, if the muscle is stretched, or lower than L, if the muscle is shortened (Latash, 2008).

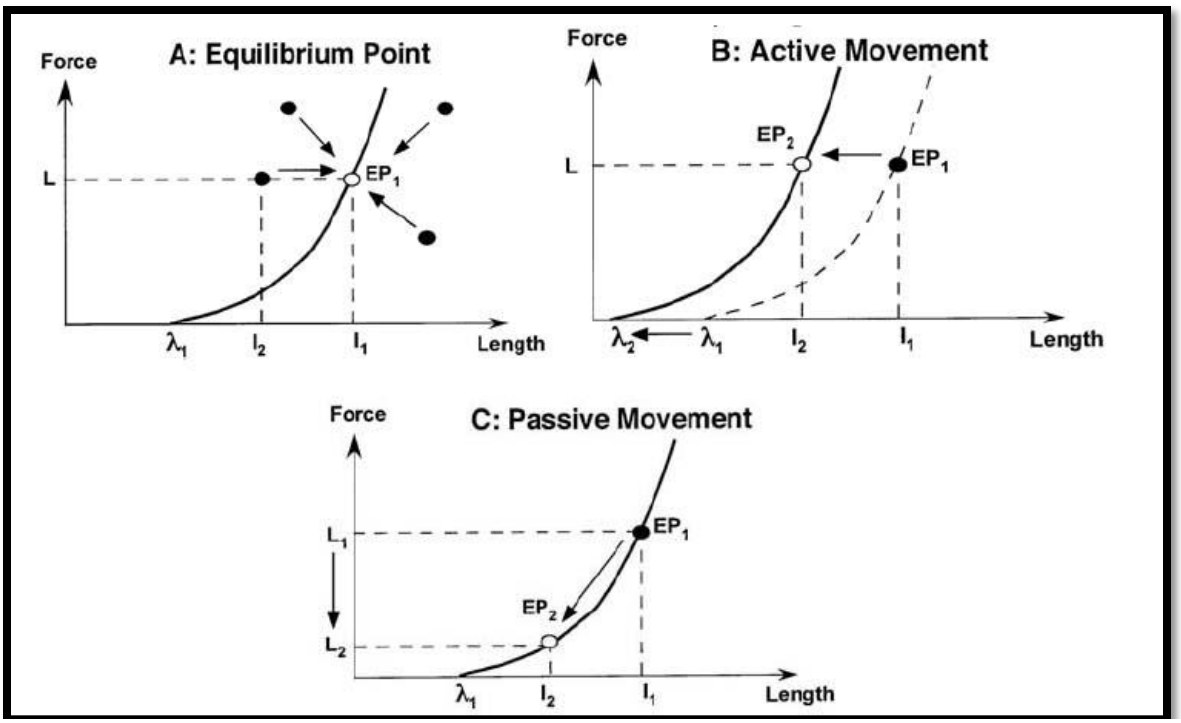

Figure 2.3 An illustration of single-muscle control within the EP-hypothesis. Source (Feldman, 2008)

Once the muscle is released its length changes and the muscle will go back to EP1 because no other equilibrium state has been defined. The equilibrium point hypothesis proposes that the threshold of the tonic stretch reflex, λ, is the only centrally supplied control parameter descending to the α and γ motor neurons (Bellomo, 1997). Central shifts in activation thresholds are the mechanisms utilized by the nervous system to produce movement. Within the framework of the equilibrium point hypothesis, movements can result from two causes. Passive or involuntary movement (Figure 2.3C) occurs as a result of a change in external load while keeping the voluntary command, λ, constant. This results in a change along the same force length curve due to a new combination of muscle force and length. Movements can also be produced by changing

threshold of tonic stretch reflex (Figure 2.2B), meaning change in λ. This is regarded as active or voluntary movement because λ is under CNS control (Latash, 2008).

2.3 EPH Applied to a Single Joint

Within the framework of the equilibrium point hypothesis single-joint movements can be simplistically controlled by at least a couple of muscles that develop force in opposing different directions. As opposed to the single muscle case, because muscle about joint causes rotation, mechanical variables of torque and angle are used to describe the state of joint control. Each muscle in the pair comprising the single joint is controlled with its own command variable, λ_{flx} for the flexor and λ_{ext} for the extensor. The $\{\lambda_{flx}; \lambda_{ext}\}$ pair defines the overall joint compliant characteristic, JCC (Figure 2.4), which represents the algebraic sum of the corresponding muscle characteristics (Latash, 2008).

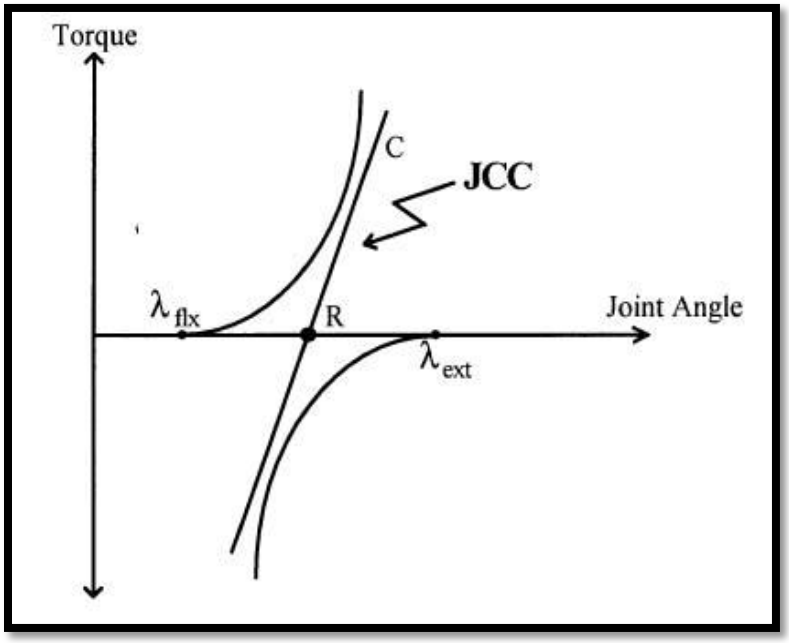

Figure 2.4 The joint compliant characteristic (JCC) curve.
Source (Bellomo and Inbar, 1997)

In the EPH control of this agonist/antagonist muscle pair is accomplished using two centrally descending commands which define the local behavior of the λs in each muscle, the reciprocal command, R and the coactivation command, C. The R command specifies the joint threshold angle R, at which the transition between agonist to antagonist activity or vice versa, occurs. It specifies a referent angle at which the active component of the net joint torque is zero, i.e., the point at which the joint is in equilibrium. The R command combines facilitation of agonist motorneurons with inhibition of antagonist motorneurons (Levin and Dismov, 1997). The coactivation or C command, specifies an angular range in which agonist and antagonist muscles may be simultaneously active (coactivation zone) if C>0 or silent (silent zone) if C<0 as shown in Figure 2.5. The ‘‘coactivation’’ command, C, simultaneously facilitates motoneurons of both muscle groups. Thus, the EPH can be scaled to represent a more realistic joint about which a number of muscles are active.

The value of the R and C commands defines a force-length relationship of the pair of antagonist muscles acting around the joint, the joint compliant characteristic (JCC), which is the algebraic sum of IC curves for the antagonist muscles. The JCC illustrates the dependence between the joint angle and torque (Figure 2.4). To control joint position, central commands can either define a pair of IC curves by specifying the flexor and extensor threshold angles (λ_{flx}, λ_{ext}), respectively, or by directly defining the JCC curve by specifying R & C (Bellomo and Inbar, 1997).

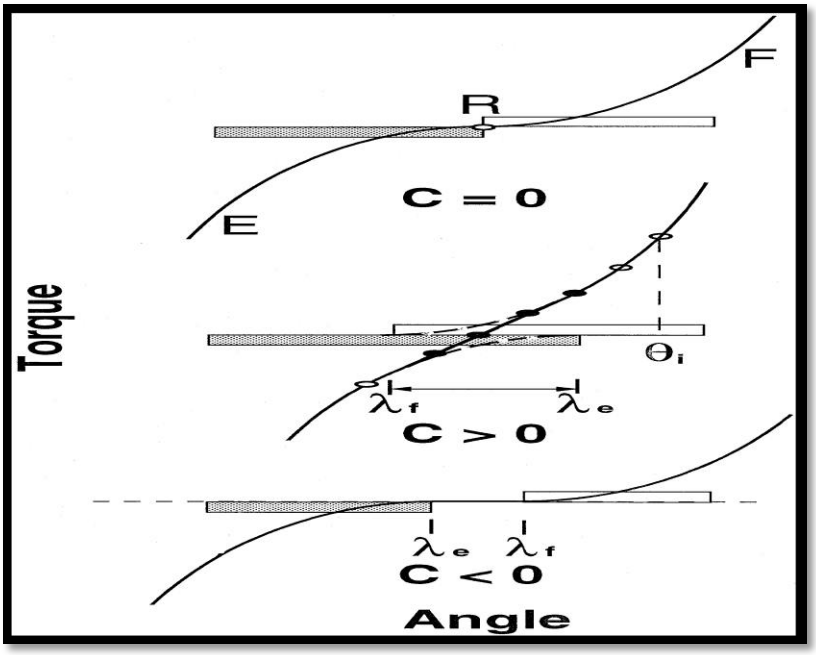

Figure 2.5 Spatial determinants (R and C) commands for the reciprocal and simultaneous activation of flexor and extensor muscles around a joint in the λ model.
Source (Levin and Dimov, 1997)

At the level of joint control the R command represents the equilibrium position of the joint in absence of external loads whereas the C command represents the stiffness level of the joint at the position, R (Bellomo and Inbar, 1997). As the JCC is the approximately linear sum non-linear IC curves its slope can be approximated as a constant, C, supporting the observation of McMahon (1985) that the combination of muscle spindle and golgi tendon organ signals produce a ratio of change in force over change in length, 'which appears to be fixed at a nearly constant value by the stretch reflex. McMahon explains that in this way, a joint presents a constant stiffness coefficient in spite of large non-linear variations in individual muscle characteristics. Voluntary joint motion and/or torque production result from shifts of λ_f and λ_e (Figure 2.5), which correspond to λ_{flx} and λ_{ext} in Figure 2.4. If λ_f and λ_e shift in the same direction along

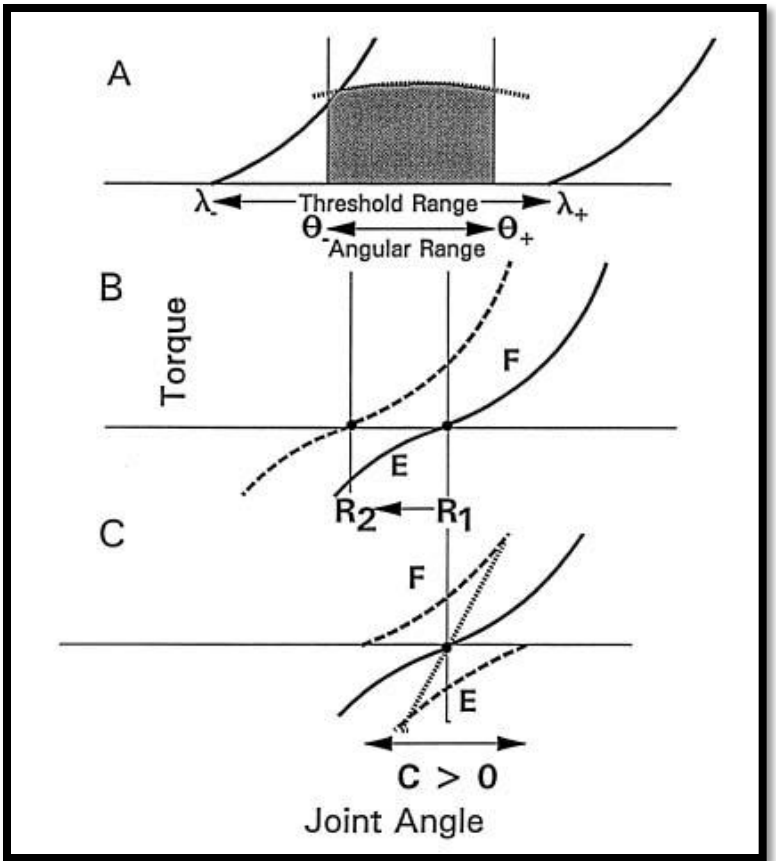

Figure 2.6 The regulation of joint angle (horizontal axis) and muscle torque (vertical axis) based on the control of the SR threshold in the framework of the λ model. Source (Levin et al., 2000)

angle axis, the mechanical characteristic of the joint shifts parallel along the axis without changing shape (Latash, 2008). The R command produces shifts in the λ's of flexor and extensor muscles in the same direction, allowing the CNS to facilitate shifts in the net joint torque/angle characteristic from one position R1 to another R2 (Figure 2.6B). This form of control suggests that one muscle is being activated and while relaxing the other. If λ_f and λ_e shift in the opposite direction along angle axis there is almost no change in location of the joint characteristic but a significant change in its slope. The C command causes the λ's to move in opposite directions (Figure 2.6 C) allowing for the modulation of the stiffness of the net joint characteristic curve (Levin, 2000). The greater the

command, the wider the λ separation and the higher the amount of agonist/antagonist coactivation. In essence the joint stiffens rather than moves. Thus, changing the C command does not affect the existing EP of the system nor does it affect shifts in the EP elicited by the R command (Levin, 2000). Since change in joint stiffness facilitates a reduction in limb movement about the joint for example, the C command influence shifts in the EP elicited by modulations in the external load. Therefore the λ model establishes a control system that distinguish between voluntary (R command mediated shifts in the EP) and involuntary (load perturbations) reactions (Levin, 2000). In order to account for the dynamics of voluntary movements, Levin and Feldman (1994) introduced the concept of a dynamic tonic stretch reflex (TSR) threshold defined as:

$$\lambda^* = \lambda - \mu V \qquad 2.1$$

where μ is a constant and V is the speed of muscle stretching (Latash and Gutman, 1994). The parameter μ, was introduced to represent the contribution of the group Ia afferents that are sensitive to the rate of change of muscle length (Bellomo and Inbar, 1997). This relation is theorized to reflect the dynamic sensitivity of muscle spindles. The dynamic threshold, λ* represents the joint angle at which recruitment of the α-motor neurons begins due to phasic responses in muscle resulting from fast changes in the muscle length. When the muscle length is greater than λ*, its instantaneous activity (EMG) is proportional to the difference between its length and the value of λ*. The activation threshold, λ*, has a component (λ) that is determined by central control influences that are independent of proprioceptive feedback as well as components that are dependent on it (Feldman and Latash, 2005).

2.4 Trajectory Formation Within the EPH

The previous section describes how within the framework of the EPH voluntary joint position can be controlled by directly setting the joint compliant characteristic, JCC, by setting the commands R and C. The R command represents the equilibrium point of the joint when no external forces are acting on it, and "C" represents the stiffness level of the joint at the position indicated by R (Latash et al., 1991). For a given R & C the joint behaves like a non-linear spring with an equilibrium state and mechanical behavior dependent on the external load (Latash, 1992). Neville Hogan (1985) and Tamar Flash (1987) expanded the original concept of joint position control within the EPH to describe multi-joint arm motion as occurring by shifts in the equilibrium position defined by neuromuscular activity. A centrally induced change in position, R, or slope, C leads to a difference between actual joint position and equilibrium position. This difference creates muscle activation and generates joint torque designed to move the joint to a new equilibrium point (Latash, 1992).

Gomi and Kawato (1996) expand on this concept of moving between equilibrium points by describing how in reaching task, the brain sends an "equilibrium point trajectory," which is similar to the desired trajectory, to the periphery as a motor command. They describe the equilibrium-point trajectory as "a time series of equilibrium points, each of which would be realized because of the mechanically stable elastic properties of the muscles and reflexes, if the motor command at some instant were maintained indefinitely". Latash (1992) expands this concept of the equilibrium-point trajectory by describing it as a "virtual trajectory". In the context of single joint movement, the virtual trajectory is trajectory that would be followed by a massless limb

without damping and changes in the external load (Latash and Gottlieb 1991). According to this definition, any central shift in the equilibrium point would lead to the development of a non-zero joint torque that would, in turn, lead to infinite acceleration of the limb immediately bringing it to the new equilibrium position (Latash, 1992). Thus descending commands control voluntary movement by specifying a time pattern of the control parameters (Bellomo and Inbar, 1997). A time pattern of R represents the virtual trajectory, "a pre-planned quasi-static movement trajectory defined by the descending commands" (Bellomo and Inbar, 1997). These simple trajectories can be planned without complex computation.

During central shifts in R there is a lag between the equilibrium position and the actual instantaneous position of the joint (Latash, 1992). This lag is due to several factors including the dynamic properties of the limb and changes in the external force field (Latash, 1998). Therefore, the virtual trajectory is the centrally desired trajectory that becomes altered in order to produce an actual trajectory by the processing of neural signals, activity of the muscles, and load.

2.5 Spasticity and the λ-Model

Reflex and motor deficits such as spasticity, limitations in force regulation, inappropriate agonist/antagonist coactivation and movement segmentation are common outcomes of central nervous system lesions (Levin, 2000). The regulation of thresholds as well as positional and velocity gains of the stretch reflex are essential results of supraspinal action and may have important implications for disordered motor control following CNS lesions. The λ model provides an explanation of the motor deficits, which characterize spasticity, in terms of the CNS' ability to regulate the stretch reflex (SR) threshold.

According to the λ model, the range in which muscle force and joint position are controlled is a consequence of the specification of SR thresholds at the muscle level and their coordinated regulation at the joint level (Levin et al., 2000). In the absence of external force slow active flexor movements against gravity can be produced by a decrease in the flexor SR thresholds. Prevention of extensor muscle activation due to stretching would require parallel diminution of extensor SR thresholds.

Within healthy populations, the SR threshold can be specified at any point within the physiological range of the joint. The λ model postulates that normally, the threshold range of λ (λ-to λ+; Fig. 2.7) should extend beyond the physiological limits of the joint for healthy individuals. Levin et al., (2000) suggest that this SR control mechanism in healthy individuals allows for complete relaxation when muscles are fully stretched (flexor $\lambda+ > \theta+$) and complete activation of the muscle when it is in the fully shortened position (flexor $\lambda- < \theta-$). Levin tested this concept by stretching muscles of the elbow in pediatric and adult hemiplegic patients at different velocities. Stretches were applied to the forearm immobilized in a manipulandum coupled to a torque motor, in either the flexion or extension direction to determine the SR thresholds of flexor and extensor muscle groups. The dynamic thresholds, λ*, at each velocity were determined from the responses in patients, as the angle at which stretch reflex activity first appeared in the stretched muscles. In healthy subjects at rest, since even rapid stretches evoked no reflex activity in either elbow flexors or extensors, no static SR thresholds lay within the physiological joint range.

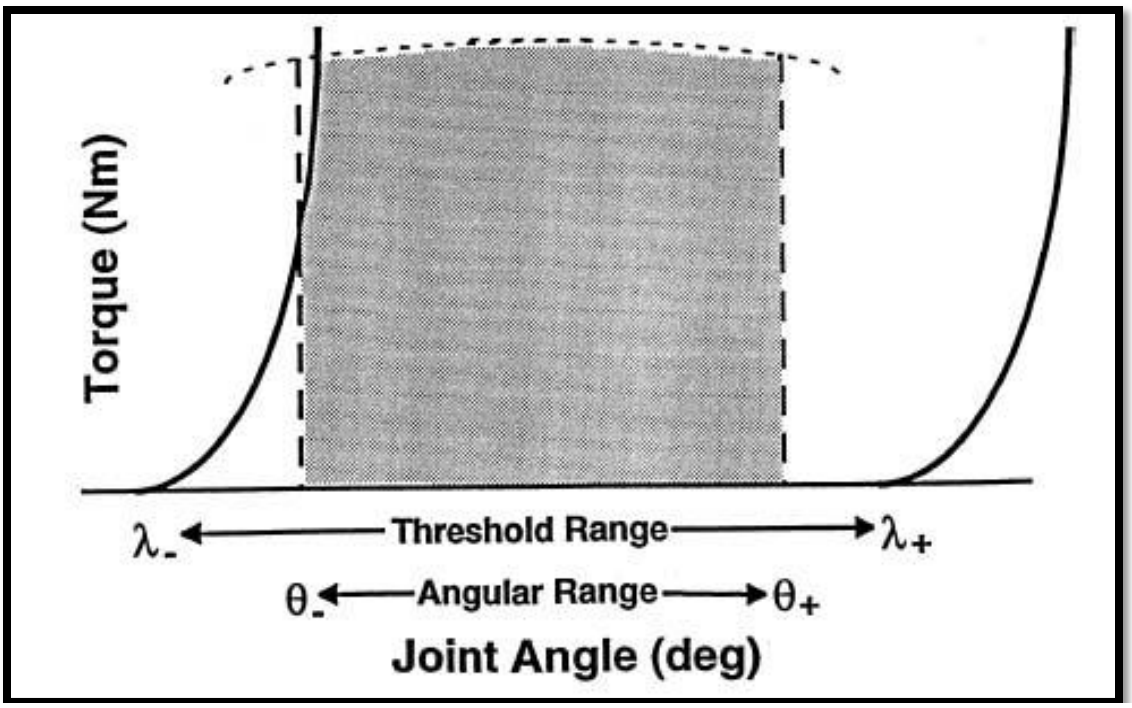

Figure 2.7 Regulation of joint angle (horizontal axis) and muscle torque (vertical axis) based on the control of the SR threshold in the framework of the λ model.
Source from (Levin et al., 2000)

Studies have suggested that spasticity may be related to problems in regulating stretch reflex (SR) thresholds in specific muscles. In the same study by Levin (2000), data from a spastic hemiparetic child in whom the upper border of the stretch reflex, λ+, for flexors was found to lie within the physiological range (i.e., θ- < λ+ <θ+,) of the joint (Fig. 2.8A). The data from elbow flexor muscles in almost all the pediatric and adult hemiparetic subjects tested, the threshold fell within the joint range. The implication of these results suggests that the threshold cannot be shifted further to the right of value λ+. When the arm is placed or stretched to the right of λ+, the flexor muscles cannot relax immediately, which can be interpreted as the presence of muscular hypertonicity (Levin, 2000). Levin's work reinforced earlier research by Levin and Feldman (1994), which tested the hypothesis that in spastic hemiparetic subjects, there is a change in the

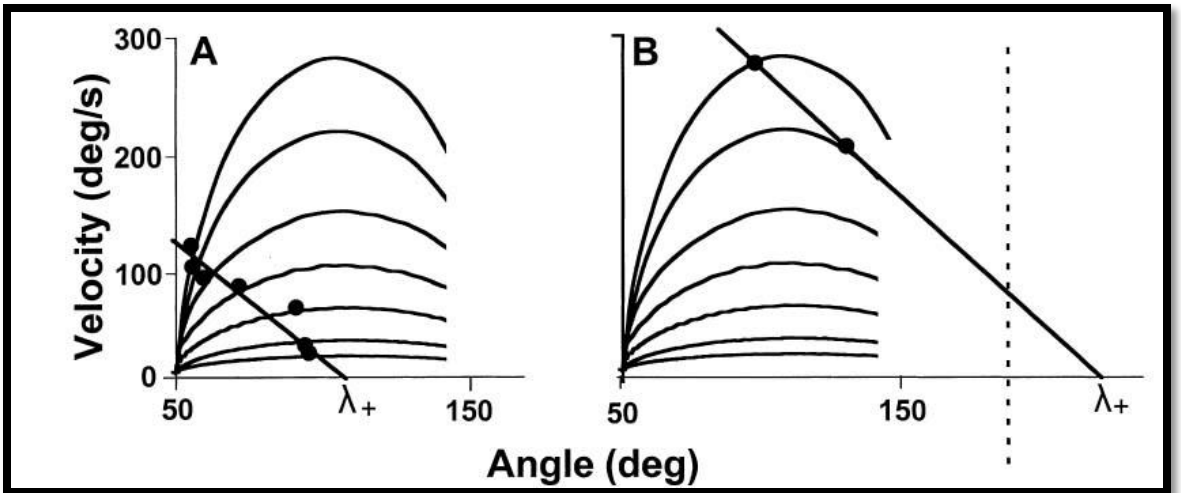

Figure 2.8 Velocity/angle phase diagrams for two children (A and B) with CP. Source (Levin, 2000)

parameters of static and dynamic stretch reflex threshold regulation. Stretch reflex threshold regulation was compared in eleven spastic hemiparetic and six normal subjects. Subjects sat with their arms fully supported in a forearm and hand mold attached to a manipulandum mounted on and controlled by a torque motor. Displacement and velocity of the forearm were measured as well as EMG signals from two elbow flexors and two elbow extensors, when the elbow flexors were stretched at each of seven velocities (Levin and Feldman, 1994).

The main findings of their study were that static and dynamic stretch reflex thresholds were decreased in spastic hemiparetic compared to normal subjects and that the thresholds depended on velocity. Utilizing the lambda model as the foundation of the rationalization of their results Levin and Feldman (1994) theorized that healthy subjects were able to relax at the initial elbow position due to an "increase in the threshold which precluded muscle activation in the whole physiological range of arm displacement". In contrast spastic patients were unable to increase the stretch reflex threshold to prevent muscle activation during even slow velocity stretching.

Comparison of the stretch reflex responses between healthy and spastic populations led to the conclusion that the regulation of the stretch reflex threshold is an essential mechanism of motor control which may be impaired in spastic patients. According to the λ model, when descending influences to motoneurons and spinal interneurons are held constant, motoneuronal recruitment begins when muscle length reaches the threshold length and increases with further muscle stretch leading to an increase in active torque (Levin and Feldman, 1994). Hence in patients with CNS lesions, abnormally increased tone is present and muscles cannot relax with in the short time frame characteristic of healthy subjects.

The equilibrium point hypothesis is a theory of active motor control which provides a framework to describe the control of a joint by three physical parameters:

1. Stiffness, C
2. Rate of change in muscle length, μ
3. Trajectory, R

These three parameters allow for differentiation in the trajectories of motion of individuals with and without spasticity. The sequent chapters will outline how a forward model of passive movement can be built using these three parameters that has strong physiological justifications.

CHAPTER 3

PASSIVE PENDULUM MODEL OF KNEE MOTION

3.1 Origin of Original Pendulum Model

The pendulum test was first modeled by Badj and Bowman (1982) and Vodovnik et al. (1984) using the linear elements of a stiffness, damper, and inertia combined to make an underdamped second order system. The motion of the passive normal knee can be described by the following differential equation:

$$I\ddot{\Theta} + B\dot{\Theta} + K\Theta = mgl_c\sin\Theta \tag{3.1}$$

where I is the moment of inertia, $\ddot{\Theta}$ is angular acceleration, B is the damping coefficient, $\dot{\Theta}$ is angular velocity, K is the stiffness coefficient, Θ is trajectory of the knee joint, m is segment mass (defined as the mass of the shank+foot), g is gravitational acceleration, and l_c is the length to the segment's center of mass. The advantage of the Badj and Vodovnik model is that the stiffness and damping, K and B, of the model accounts for the lumped mechanical properties of both agonist and antagonist muscle groups as well as all of the passive structures in the knee (Lin and Rymer, 1991).

While this model represented the non-spastic knee trajectory reasonably well, it failed to sufficiently represent the spastic knee trajectory. As a potential solution, Vodovnik et al. (1984) proposed the use of additional torques with the model to fully represent the spastic trajectory. As the anti-gravity reversals in the trajectory were accompanied by EMG bursts, signifying active muscle–generated torques, this new

model was augmented by carefully chosen pattern of torque pulses that were timed to coincide with the measured EMG signals. Using this time varying pattern of torque, Vodovnik et al., propose a new model equation to describe both spastic and non-spastic limb motion during the pendulum knee drop:

$$I\ddot{\Theta} + B\dot{\Theta} + K\Theta + T_h(t) = mgl_c\sin\Theta \tag{3.2}$$

Where $T_h(t)$ represents a step function of limited duration introduced as an approximation of the quadriceps force indicated by the burst of EMG present during the falling of spastic limbs. To allow the model the robustness to describe the pendular swings of non spastic limbs as well, $T_h(t) = 0$.

Lin and Rymer (1991) developed a model of pendular motion using the same framework established by Vodovnik et al.. In their preliminary analysis of passive limb motion Lin and Rymer proposed determining the parameters, K and B of Equation 3.1 for each half-cycle of motion. This was believed to be a better reflection of the asymmetry of limb motion (Lin and Rymer, 1991). Whereas the Vodovnik et al., model, expressed in Equation 3.1, predicted constant relationships between stiffness coefficient K, damping coefficient, B and angular displacement and velocity respectively, Lin and Rymer found that the stiffness and damping parameters were not constant throughout the motion, indicating significant nonlinear behavior (Lin and Rymer 1991). The varying values of K and B suggest that the parameters could depend upon motion amplitude, velocity, or direction of swing (Lin and Rymer, 1991). On the surface, Lin and Rymer's observations suggest that changes in either motion amplitude, velocity of swing or direction of swing

can bring about physiological changes in both stiffness and damping. It can be reasonably hypothesized that Lin and Rymer's model, as presently constructed, may be missing an additional parameter and that the changes in stiffness and damping are simply compensation for that missing model parameter.

To expand the model to describe the trajectory of spastic limbs Lin and Rymer proposed a piecewise change in the model parameters, K and B driven by an EMG signal used as an input to determine how the systems Equation (3.1) should change as result of muscle activation. Rather than explicitly defining a stepwise torque to correspond with the timing of the observed EMG as in Equation 3.2, this technique modulates the gain of K and B separately at three time periods. For each trial, the values of K and B which produced the least squared error were found for the interval before EMG activity. Then the values for the gains were found for the interval after EMG onset and the end of the first half-cycle (Lin and Rymer, 1991). Each successive half-cycle was analyzed similarly with the computed gains for K and B from the previous half-cycle used as initial inputs for the next half-cycle. Lin and Rymer found that this piecewise change in K & B alone was insufficient in reproducing the motion of the spastic leg mainly due to the leg's inability to cross the vertical plane (0^o) during the first downward swing. The deviation from pendulum-like motion shown by the spastic suggested that additional active torque inputs must be influencing joint motion (Lin and Rymer, 1991). Their solution was to incorporate Feldman's lambda model to reproduce a spastic trajectory with a step-wise adjustment of the zero length of the spring represented by the stiffness term. Under this model, Lin and Rymer proposed that the angle at which EMG activity is initiated, which

is where the stretch reflex threshold is reached, approximates the new rest length, of the model spring, transforming Equation 3.2 to:

$$I\ddot{\Theta} + B\dot{\Theta} + K(\Theta - \Theta_R) = mglsin\Theta \quad (3.3)$$

where Θ_R is the new zero-length of the muscle modeled as a spring (Lin and Rymer, 1991). The zero-length, Θ_R was held constant once EMG stated and the timing of the step changes in K and B utilized the same sequenced described previously.

In a different approach to modeling the spastic pendulum knee motion, He et al. (1997) proposed a more complex model that included explicit representations of the muscles acting on the knee along with their muscle spindles. By varying the thresholds and the gains of the feedback loops, they were successful in modeling the trajectory of the spastic pendulum knee drop. Fee and Foulds (2004) developed two active models utilizing external torques to reproduce angular motion trajectories closely matching the experimental knee trajectories of subjects with spasticity due to cerebral palsy. The first model allows for the direct application of toques to the passive model, similar to the representation of Equation 3.2. The second model provides additional torque to the passive model through velocity feedback. The velocity feedback model of active torque reflects the physiological characterization of spasticity as velocity dependent and the knowledge that muscle spindle Ia afferent signals provide velocity-related information to the alpha motor neuron (Fee and Foulds, 2004). In contrast to previous models which depended on EMG timing to set the active step gain for stiffness, K and damping B, the velocity feedback model relies upon an optimization algorithm to specify the timing and

amplitude of torques that can be introduced to improve the performance of the best fitting passive model (Fee and Foulds, 2004).

3.2 Trajectory-Based Pendulum Model

Simon and Foulds in 2004 first introduce the idea that in the spastic pendulum knee drop data the limb appears to be oscillating about an exponential trajectory that passes through the points of max velocity in the oscillations, both positive and negative; corresponding to the location of the inflection points of the curve (Figure 3.1). The significance of the observation is that it proposes that in addition to the model stiffness parameter, K, and damping parameter, B a third parameter, the trajectory about which the limb oscillates, can be used in the differentiation of limb motion between non-spastic and spastic subjects. It was proposed that an exponential equation, Ae^{-st} where "A", represents the initial angle of release and "s" represents the decay constant, can modeled as a trajectory fitting through inflection points of the PKD trajectory. It was theorized that the decay constant represents the steepness of exponential decay and therefore could be used as a measure distinguishing non-spastic limb trajectory motion from spastic limb motion. This represented a step forward from the analysis of spasticity using the relaxation index which focused on the initial drop amplitude and final rest angle.

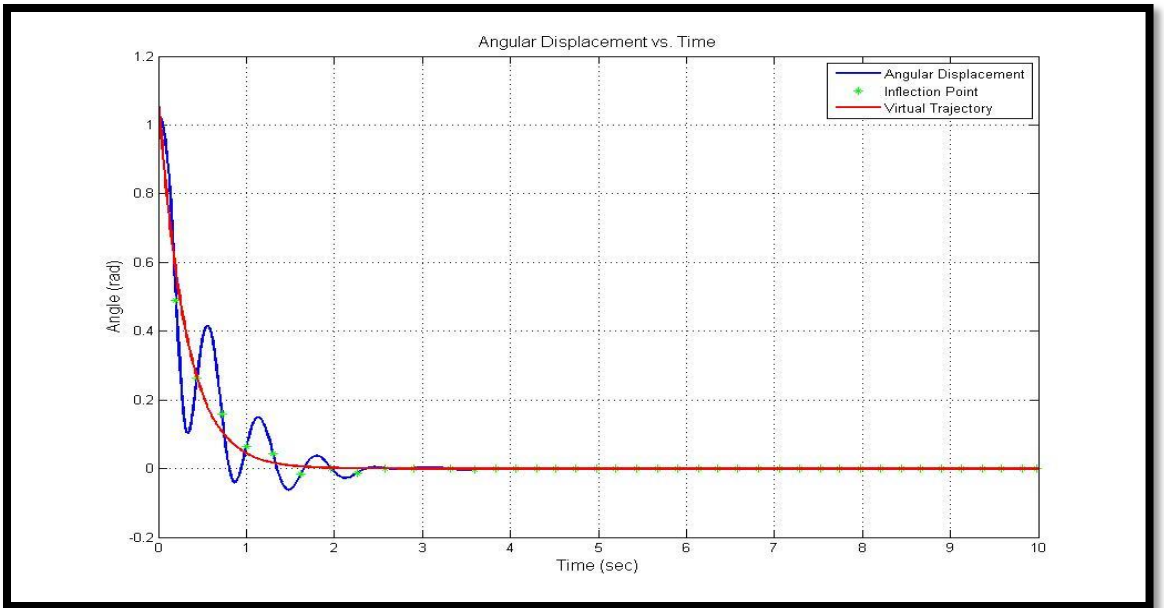

Figure 3.1 Pendulum knee data of spastic subject with exponential VT through inflection points.

Swift et al. (2006) expands on the idea of the trajectory analysis of the spastic pendular motion by creating an inverse dynamic model of pendulum knee drop motion. Utilizing the equilibrium point hypothesis she redefines the original by Badj and Bowman equation to incorporate a relative stiffness term:

$$I\ddot{\Theta} + B\dot{\Theta} + K(\Theta - \Theta_o) = mglsin\Theta \tag{3.4}$$

where Θ_o is the trajectory about which the leg oscillates. This suggests that the dynamic stiffness, modeled from the pendulum knee drop data, is a function of the difference between the actual trajectory of the limb and the trajectory specified by the CNS Using an inverse dynamic model, this paper showed that the curve through the inflection points closely matched a sequence of local equilibrium points of the spastic trajectory.

Motion along a sequence of equilibrium points has long been used to define voluntary or active movements. In the previous chapter, the idea of virtual trajectory control of motion was introduced. With the framework of virtual trajectory control, the system dynamics are not computed explicitly in the CNS, but the planned trajectory is fed directly to the muscle as desired equilibrium lengths (Schweighofer et al., 1998). Hogan (1984) presented a mathematical model, incorporating a virtual trajectory control strategy to predict qualitative and quantitative features of a class of voluntary movements in the upper limb. The model was based on observations of both unperturbed and perturbed large amplitude voluntary single plane elbow movements performed at intermediate speeds by intact and deafferented monkeys. Hogan's research laid the foundation for the application of virtual trajectory control to human subjects performing unconstrained voluntary arm movements in the horizontal plane. Flash (1987) tested the virtual trajectory hypothesis within the context of reaching movements. Using joint stiffness parameters derived from experimentally determined static stiffness values, Flash successfully developed a mathematical simulation of actual arm movements based on hypothetical equilibrium trajectories. Empirical studies in support of view suggest that the equilibrium shift is gradual (Bizzi et al.. 1984), that it is similar in form to the actual movement (Won and Hogan 1995), and that it ends substantially before the end of the movement (Feldman et al.. 1995).

While there have been several studies illustrating the application of the virtual trajectory hypothesis in active movements, the outstanding question still remaining is whether there is a framework within the EPH to describe passive motion along a trajectory of equilibrium points? Recall from chapter two, the equilibrium point

hypothesis describes passive movement occurring as a result of a change in load along a constant λ (Figure 2.3 C). Such change in load results in the previous equilibrium point, (EP1), becoming non-equilibrium and movement occurs to a new equilibrium point (EP2) where the active force of the muscle equilibrates the external load (Latash, 2008). A timed sequence of these transitions between equilibrium points is consistent with the concept of a control or virtual trajectory (Latash, 2008).

This chapter outlines the evolution in development of models analyzing pendulum knee data. Originally, forward models were developed that needed additional burst of torque to match spastic data. Trajectory-based modeling of pendulum knee trajectory began observe that the spastic trajectory oscillates about an exponential-like curve. Swift 2006) showed that such a curve approximates the equilibrium points of the spastic trajectory. Previous research incorporating virtual trajectory control in driving active movements provides a framework for the development of a forward model capable of describing the passive spastic trajectory in terms the stiffness parameter K, damping parameter B, and a virtual trajectory.

CHAPTER 4

METHODOLOGY

4.1 Theoretical Framework

The objective of this dissertation is to develop a model of passive knee motion that can merge Lance's (1980) original characterization of spasticity as a "velocity dependent increase in tonic stretch reflex activity" with Burne's (2005) observation of increased passive resistance in spastic limbs even at rest. The framework of this research is outlined in the overarching research questions proposed in Chapter 1:

1. Can we create experimental measures to develop a model of spasticity that can be interpreted within the framework of a general theory of motor control?
2. Can the underlying motor control framework provide a unique parameter capable of describing both normal and altered/abnormal movement?
3. Can the model be robust enough to explain active as well as passive movement?

The previous chapter illustrates the evolution of models describing the passive motion of the knee joint. Badj et al. (1984) established a model that can reasonably characterize the motion of the knee joint by lumping the stiffness and damping of all the knee joint structures into two single model parameters of K and B. The inability of the model to account for the nonlinear property of muscle provided limits to the overall accuracy of the model for non-spastic subjects and these limits were exacerbated in the modeling of spastic knee joint motion. Rather than using models requiring piece-wise approximation for stiffness, K and damping, B or additional burst of torque to model spastic knee trajectories, the equilibrium point hypothesis can provide the basis of a forward model that incorporates parameters of K and B, from earlier second order models, while introducing the concept of a virtual trajectory parameter, VT.

Simon and Foulds (2004) and Swift et al. (2007) introduce a virtual trajectory-based pendulum model of knee motion. These models offered a unique way to incorporate the nonlinear nature of knee joint motion through the incorporation of the equilibrium point hypothesis. The models focused on an exponential curve, $\Theta_s e^{-at}$, that passes through the equilibrium points of the pendulum knee angular trajectory. The equilibrium points correspond to the places where the sum of the torques about the knee joint equals the moment of inertia multiplied by angular acceleration or $\Sigma T = I\ddot{\Theta} = 0$.

The EPH defines a single-joint system as being in static equilibrium when the torque produced by the flexor is equal and opposite to the torque produced by the extensor, in the absence of external torque (Flanagan et al., 1993). The R command governs the equilibrium point, EP, of the joint through its ability to shift λ_{flx} and λ_{ext} in the same direction. Thus R represents the equilibrium joint angle, is specified by the combined actions of both muscles and corresponds to the angle at which the net joint torque is zero (Flanagan et al., 1993). R only represents the actual angle when there is no load. This is not the condition that defines the analysis of the dynamics present during the pendulum knee drop. Referring back to Equation 3.4, the sum of the moments about the knee joint does not equal zero but rather equals the torque resulting from gravity, $mgl\sin\Theta$. This suggest that rather than a virtual trajectory, as defined by the equilibrium point hypothesis, the trajectory molded by Simon and Foulds (2004) and Swift et al. (2007) is the system equilibrium trajectory, as the trajectory actually passes through the system's equilibrium points defined by load=$mgl\sin\Theta$. Figure 4.1 illustrates the difference between a hypothetical virtual trajectory which is defined centrally, and the system

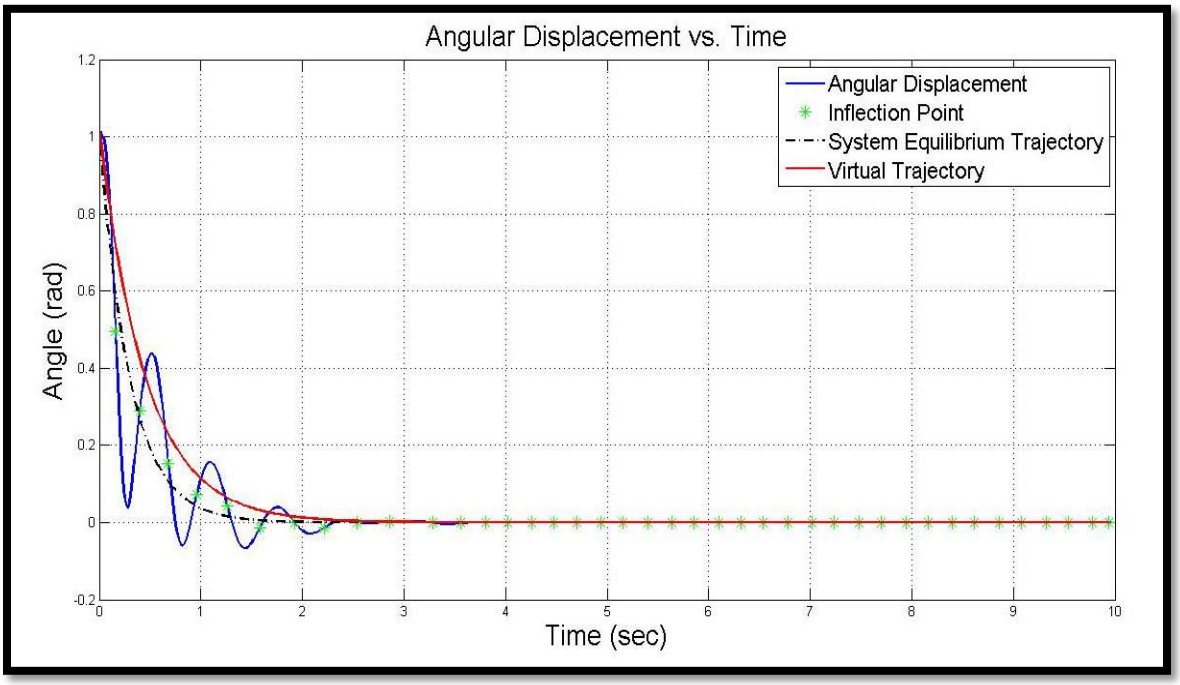

Figure 4.1 Spastic pendulum drop about system equilibrium trajectory (SET) and virtual trajectory.

equilibrium trajectory (SET) which incorporates the role that external forces and internal forces, such as muscle activation, has on movement. The framework of this dissertation is the utilization of the pendulum knee test to define knee joint motion based on the extraction of three broad parameters: damping coefficient, B, stiffness coefficient, K and the virtual trajectory VT. Rather than specifying an exponential curve through the points of inflection defining the system's equilibrium trajectory, a forward model is initially created with an optimized exponential curve to represent the centrally driven virtual trajectory. Thus, the virtual trajectory represents the centrally defined objective. The presence of both external and loading causes the limb to follow a system equilibrium trajectory.

The link between a model capable of describing spastic limb motion and the equilibrium point hypothesis lies in the EPH's interpretation of the role of the CNS in muscle activation. In previous spasticity research utilizing the pendulum knee drop, electromyorgraphic, EMG, data has shown that muscle activity appearing as torque burst in the form of a reflex is present which subsequently alters limb motion. The EPH specifies however, that the CNS does not specify the torque bursts, but they are the result of the interaction between K and B and a third important parameter of motor control, the VT. Thus, the remainder of this dissertation will show that timed bursts of torque need not be explicitly specified, but are the direct result of changes in the VT that are can be linked to spasticity.

4.2 Exponential Forward Model

Originating from the equation of motion of the leg-foot segment about the knee joint, developed by Badj, Vodovnik, and Bowman, the equation; $I\ddot{\Theta} + B\dot{\Theta} + K\Theta = mgl\sin\Theta$, is rewritten as model formula:

$$I\ddot{\Theta} + B(\dot{\Theta} - \dot{\Theta}_o) + K(\Theta - \Theta_o) = mgl_c\sin\Theta \tag{4.1}$$

The moment of inertia, I, shank mass, m, center of mass shank length, l_c were calculated from anthropometric data. The virtual trajectory Θ_o is calculated from the following exponential equation:

$$Ae^{-(st)} \tag{4.2}$$

where "A" is the angle trajectory start position, Θ_{start} and "s" represents the decay constant. This model distinguishes itself by extending the equilibrium point hypothesis by to include calculation of relative damping $B(\dot{\Theta} - \dot{\Theta}_o)$ (de Lussanet et al., 2002). Relative damping proposes replacing the damping relative to the environment (absolute damping) with damping with respect to the velocity of the equilibrium point (de Lussanet et al., 2002). This model builds on the non-linear spring concept of muscle dynamics by incorporating analysis of the equilibrium states within muscle force-movement relationship. Model implements the EPH to explain spastic torque behavior, hypothesized to be the active reflexes in spasticity. The incorporation of relative damping with the EPH has been shown to be important in modeling of active joint movements (Chen and Foulds, 2010; Chen et al., 2009).

4.2.1 Simulink Representation of Model

A feedback model of Equation 4.1 and incorporating Equation 4.2 was developed using Simulink (Mathworks, Inc., Natick, MA) which supports linear and nonlinear dynamic modeling. The model adheres to Newton's second law of motion, with respect to rotation where the sum of the moments equals the moment of inertia multiplied by angular acceleration. The model isolates three moments affecting the total rotation about the knee being gravitational, stiffness, and damping moments. As shown in Figure 4.1, the model represents the moments acting on the knee as follows:

- Gravitational – $mgl_c\sin\Theta$ term in Equation 4.1, Gravitational Torque orange function box in Figure 4.2
- Damping – $B(\dot{\Theta} - \dot{\Theta}_o)$ term in Equation 4.1, B_{rel} group of yellow icons in Figure 4.2.
- Stiffness - $K(\Theta - \Theta_o)$ term in Equation 4.1, K_{rel} group of green icons in Figure 4.2

The virtual trajectory, Θ_o is represented in the model by a function block, 'Decaying exponential model of VT' (Figure 4.2), which utilizes Equation 4.2. The derivative of this function is used to calculate the damping moment shown above. Anthropometric tables are used to calculate moment of inertia, segment mass, and segment length. The calculations used to produce the moment of inertia, I, in Equation 4.1 are represented in the subsystem box '1/Inertia', in red shown in Figure 4.2. The content of this subsystem is shown in Figure 4.3. The Simulink model takes this subsystem output and incorporates its value into the main model.

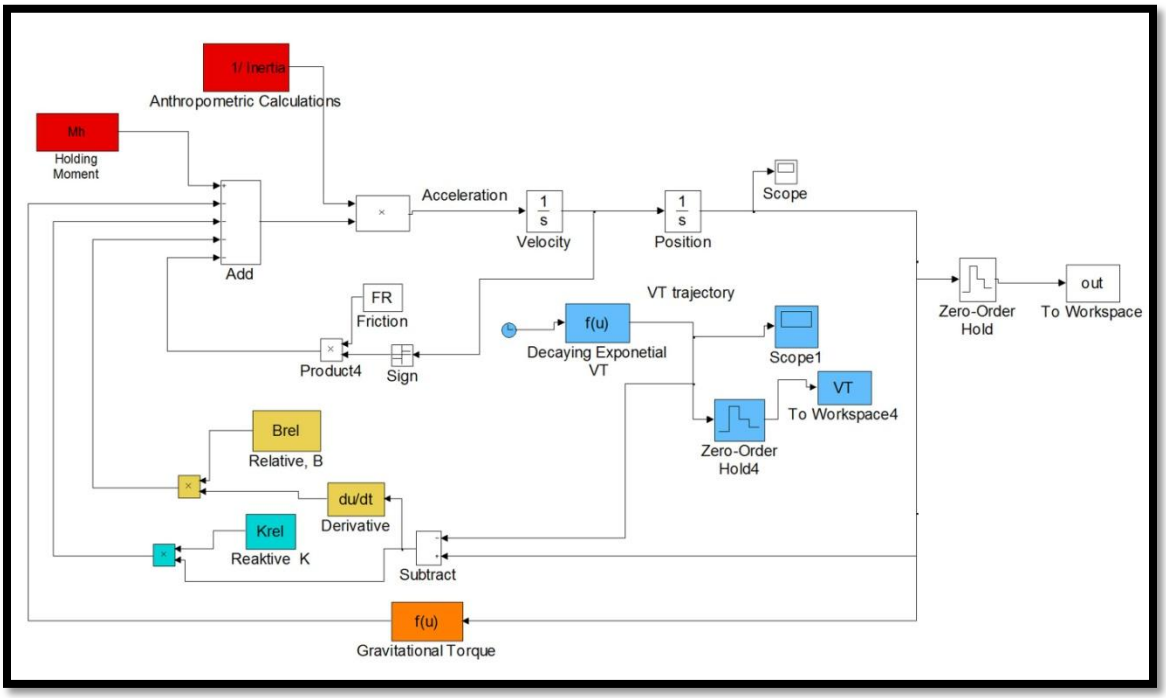

Figure 4.2 Simulink pendulum knee forward model.

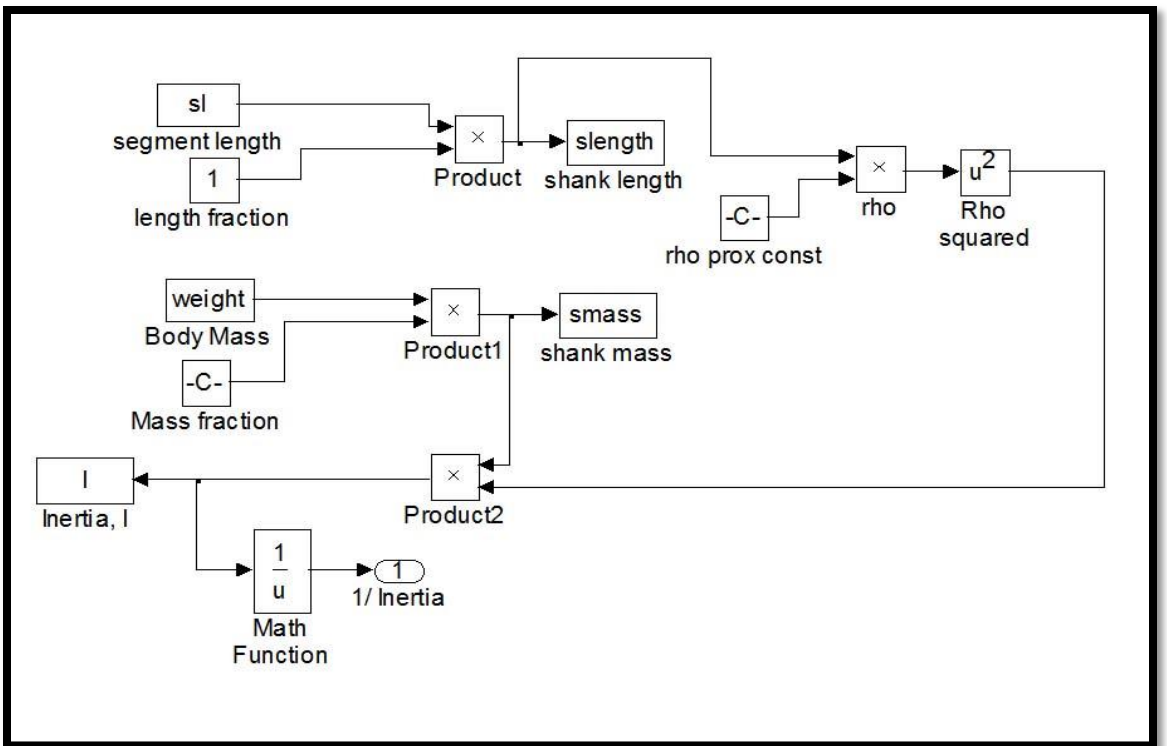

Figure 4.3 Simulink subsystem model for moment of inertia, I and its inverse, 1/I.

4.2.2 Operation of Simulink Model

A Levenberg-Marquardt method based gradient-descent optimization program was developed in MATLAB, which recursively uses Simulink to optimize the model parameters of Equation (4.1). This program passes initial parameters to the Simulink models, records the output of the models, and performed an optimization of the parameter variables (Grace, 1990). The output from the '1/Inertia' subsystem is multiplied by the sum of the moments acting on the knee discussed in the previous section. This product generates the angular acceleration of the leg as it is falling during the pendulum knee test. The acceleration is differentiated once to produce velocity and then again to produce the position of the limb. The output of the model is limb position in space, measured in radians.

Four parameters are optimized in the model: stiffness and damping coefficients, B_{rel} and K_{rel} respectively, from Equation 4.1 and start angle and decay slope, variables "A" and "s" respectively from, Equation 4.2. In order to determine a reasonable value to serve as an initial guess for variables, "A" and "s", used in the optimization program, the calculated inflection points in the angle data were fit with an exponential parametric model in MATLAB. Using the inflection point times as the input and the inflection point angle values as the output, a non-linear model in the form of $y=Ae^{-bx}$ was created where "A" and "b" are coefficients. The value of these coefficients, "A" and "b" in the Matlab fit model were then assigned as values to variables "A" and "s" from Equation 4.2 and used as the initial guess for these variables in the optimization routine.

The model variables, "K_{rel}", "B_{rel}", "A" and "s" are the parameters of the proportional integral derivative (pid) controller (Grace, 1990), which is the Simulink model shown in Figure 4.2. The variables are optimized based on a user-defined order scheme. The program selects the first parameter to be optimized, assigned the controller variable, pid(1), changes that parameter, evaluates the level of either increase or decrease in the cost function, and finally decides whether to keep or reject the new value (Fee and Foulds, 2004). The cost function is based on the sum-squared error, SSE, of a sample-by-sample comparison of the model output with experimental data (Winter, 2005). Once the SSE resulting from the variation in a parameter reaches a minimum value, determined by user-defined criteria, another the next variable, which has been assigned the controller variable, pid(2) is chosen and the process is repeated. The program iteratively cycled through the set of variables until the SSE reached a minimum value and would go no

lower. This final SSE is taken as a measure of the goodness of fit of that model's output to the experimental data (Grace, 1990).

4.2.3 Validation of Exponential VT Model

The output of the developed forward model is the simulated pendular trajectory of motion occurring from the pendulum knee drop. The goal of model validation is to demonstrate that by using an exponential virtual trajectory, VT, plus optimized values of damping, B and stiffness, K, the model can produce a trajectory of motion which accurately reflects the actual experimental data. The data analyzed consists of the time course of the knee's angular displacement collected from the pendulum knee drop test of six subjects; three with cerebral palsy and three subjects without clinical signs of cerebral palsy or spasticity.

Three of the subjects are identical male triplets of whom two (BX and CX) have cerebral palsy with mild spasticity and one (AX) shows no clinical signs of cerebral palsy or spasticity. Their pendulum knee data was provided by James Fee from the A. I. duPont Hospital for Children. The pendulum tests of the triplets were originally conducted at the A.I. duPont Hospital for Children, Wilmington, DE, with the cooperation of the Department of Orthopedics (Fee and Foulds, 2004). The triplet data was obtained with the approval of the Hospital's Institutional Research Review Committee. The remaining three subjects consisted of a thirty-two year old male with cerebral palsy and two young adults with no history of cerebral palsy or spasticity. Pendulum knee tests were performed for these subjects at the Neuromuscular Engineering Laboratory at NJIT. Subjects provided informed consent approved by the NJIT Institution Review Board.

4.2.4 Experimental Procedure

Anthropometric analysis (Winter, 1990) was used to calculate the shank mass, moment of inertia, and shank center of mass for all of the subjects. These calculations later served as input into the forward model. For the test regime, the subjects sat on a specially designed seat which allowed the lower limb to swing freely. The rotation of the shank about the knee during the pendulum knee test of the male identical triplets was measured using an electromagnetic sensing device, the 3SPACE Isotrak by Polhemus, Inc. The angular rotation data of the triplets was collected at a 50Hz sampling rate.

The limb position data for the three subjects test at the Neuromuscular Engineering Laboratory at NJIT was recorded at a sampling rate of 100Hz using a different magnetic sensing device, the 3DGuidance trakSTAR by Ascension Technology Corporation (Figure 4.4). The trakSTAR is an electromagnetic tracker that uses pulsed DC technology to determine the position and orientation of a sensor relative to a source. The transmitter sequentially generates magnetic fields and the sensor instantly measures the transmitted field vectors at a point in space. The source was placed on a fixed stand beside the subject, as shown in Figure 4.5. The trakSTAR determines six degrees-of-freedom (6DOF) position and orientation (X, Y, Z, Azimuth, Elevation, and Roll) of one or more sensors referenced to a fixed transmitter. The transmitter sequentially generates magnetic fields and the sensor instantly measures the transmitted field vectors at a point in space. From theoretical knowledge of the transmitted field, the tracker accurately deduces the real-time location of the sensor(s) relative to the transmitter (Ascension Manual, 2009). The data acquisition method employed with the trakSTAR replicates as closely as possible the method utilized by the 3Space Isotrak by Polhemus.

Figure 4.4 trakSTAR device introduction from Ascension Technology.
Source: Ascension Technology Corporation Official Website.
http:// www.ascension-tech.com/medical/pdf/TrakStarSpecSheet.pdf, accessed August 21, 2011

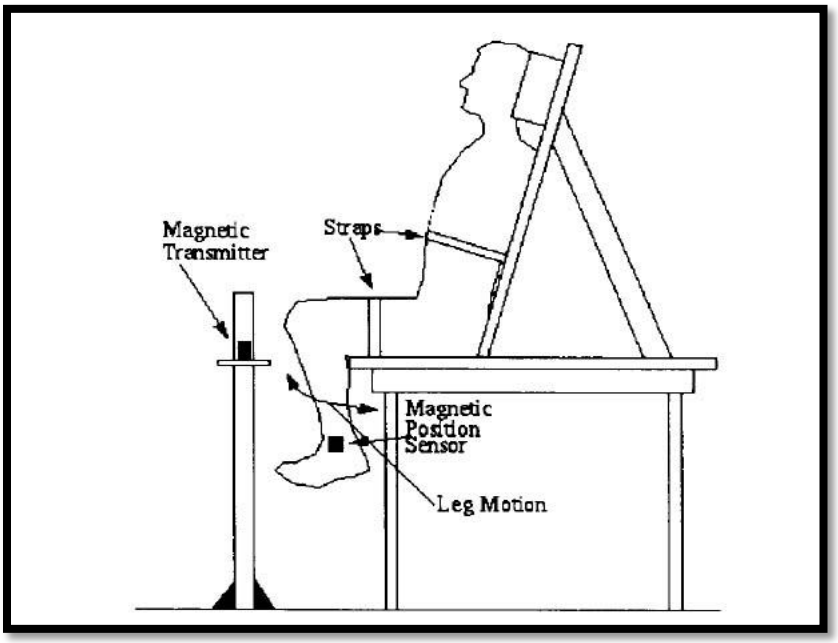

Figure 4.5 Subject in Test Position.
Source (Fee and Samworth, 1995)

For each test, the upper leg was held fixed and a sensor was placed along the long axis of the shank above the malleolus. In order to measure the amount of force necessary to slowly raise the limb and hold the limb before release, a force transducer, the mini 40 by ATI Industrial Automation was also secured on the shank by a light strap attached to a specially designed mounting. The transducer converts force and torque into analog strain gage signals. EMG was monitored with surface electrodes located over the quadriceps and hamstrings. EMG signals were amplified (×1000) using a multi-channel electromyography card (PCI-6024E made by National Instruments®), band-pass filtered at 55-600 Hz by a 4th-order zero-lag Butterworth filter. Angular and EMG data were synchronized for later analysis.

To perform the test, the lower leg was gradually extended by a string attached to the mounting of the force transducer, to a point of maximal tolerated resistance, that is, as far as the subject would allow without expressing discomfort. The movement was performed in a manner where the string was pulled in a direction perpendicular to the limb segment. The subject was then told to relax, and the limb was then allowed to fall to its resting position. A lab written MATLAB program, integrated the trakSTAR, force transducer, and EMG; recording both angle and force data at rate of 100 Hz and EMG at 1000Hz. The entire testing regimen consisted of 5 pendulum knee drops per subject with an average of two minutes between each successive knee drop.

The pendulum model defined by Equation 4.1, used in the previous analysis, arises from the rotational analog of Newton's second law of motion. The net torque acting on an object has a moment of inertia, I, causes an angular acceleration α. The introduction of a force transducer to measure the force involved in lifting and holding the

limb before release gives us the ability to calculate the holding moment, Mh. The holding moment is the product of the force, in Newtons, measured by the transducer, and the distance along the shank from the bony prominence of the knee to the place of attachment of the transducer. This creates a modification of Equation 4.1 to incorporate into the model the contribution of the holding moment, as shown previously in Figure 4.2:

$$I\ddot{\Theta} + B\left(\dot{\Theta} - \dot{\Theta}_o\right) + K(\Theta - \Theta_o) + Mh = mgl_c \sin\Theta \quad (4.3)$$

The novelty of this method is that all of the forces and moments acting upon the limb during the entire phase of motion, including the initial lift are accounted for in this model. It is recognition of the coupling between the person performing the test and the test subject. This serves as the only model that breaks down the mechanics of the pendulum test and examines the impact that this coupling between examiner and subject has on the outcome of the test.

4.3 Transition Towards New Trajectory Model

The distinguishing feature of the previous model is the incorporation of an exponential curve to represent the virtual trajectory in a trajectory-based pendulum model of knee motion. A main appeal of the EPH is that the control signals that underlie the point-to-point movements are simple and monotonic in form (Feldman et al., 1995; Adamovich et al., 1997). In applying the EPH to a single joint model central commands have been assumed to vary over time in a simple fashion. The equilibrium point, specified by the R-command, has been shifted at a constant rate from the start position to the final position; the C-command has been increased at the start of movement and then gradually

decreased after the movement (Flanagan et al., 1993). This would seem to suggest that the virtual trajectory, described by Feldman and others, is comprised of a series of straight line transitions from equilibrium point to equilibrium point. Rather than specifying a complex trajectory such as an exponential curve, it is likely that the CNS, in the context of the equilibrium point hypothesis, specifies a simple VT, but neural signal transmission and system dynamics result in an exponential-like appearance in the trajectory.

Lin and Rymer (1991) discuss an anomaly at the start of the pendulum knee drop where they indicate an unexplained hesitation. They noticed that instead of the leg immediately accelerating to a finite negative value, due to the influence of gravity, there was a delay in the leg obtaining maximum acceleration. This delay was measured as more than 60ms from the time the angle position starts to change (Lin and Rymer, 1991). In their analysis of this delay Lin and Rymer offers two possible explanations. They offer a brief discussion on the research of Brown et al. (1988) investigating the impact of thixotropic properties in muscle on limb acceleration. Thixotropic properties of muscle refer to the history-dependent change in the short-range elastic component of muscle (Kellermayer et al., 2008). Brown's research theorized that during the pendulum knee test, when the leg is held in a relaxed position for a few seconds before release, muscle thixotropic properties develop causing nonlinear behavior in limb acceleration, period and damping during the first cycle of swing.

Lin and Rymer extend this analysis by rationalizing that the thixotropic properties not only create abnormal mechanical changes while the leg is held but the effects of these changes are evident during the rest of the leg swings. The implication of this idea is that

the varying values of stiffness, K and damping, B during each half cycle, obtained from modeling the angular data from the pendulum knee test, can be attributed to muscle thixotropic changes (Lin and Rymer, 1991).

An alternate explanation offered by Lin and Rymer for the delay in leg acceleration is that the load on the leg may not have been applied instantaneously. This rationale suggests that the leg may not have been released cleanly, causing abnormalities in the acceleration of the limb (Lin & Rymer, 1991). Though offered as a source of potential error, Lin and Rymer concluded that the magnitude of this method of error was small due to the relative quick release of the limb, 10ms in most cases. They also observed that the difference between actual acceleration of the limb and the theoretical calculation of limb acceleration is significantly greater than limb acceleration that could be attributed solely to the noninstantaneous release of the limb.

Lin and Rymer's observation combined with the reaffirmation of Feldman's characterization of a virtual trajectory created by moving λ along a straight line simple curve suggest that a new model to analyze pendulum knee data was needed. In order to merge the concepts of a trajectory consisting of simple straight line transitions between equilibrium points and the natural delays that occur during processing of movement signals, an ideal model virtual trajectory model for pendulum knee data would have three components: a constant position segment representing a time delay, a straight line sloping virtual trajectory followed by a second constant position segment representing the settling of the limb position at the limb resting angle. Figure 4.6 illustrates this new theoretical conception of the ideal virtual trajectory that the CNS would try to create within the frame work of the equilibrium point hypothesis.

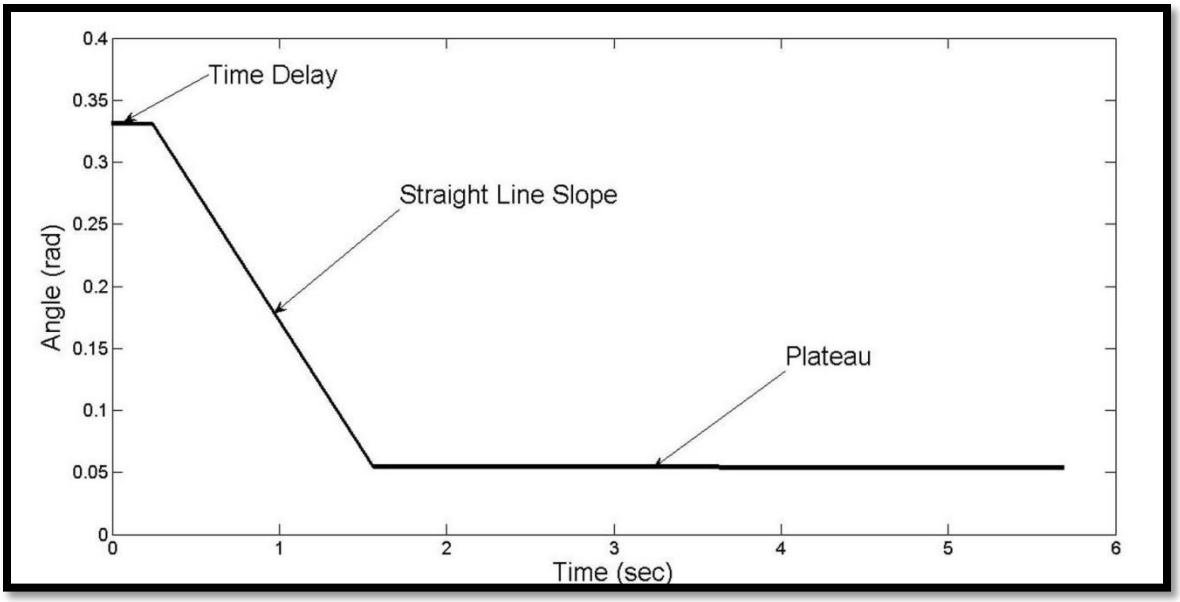

Figure 4.6 Idealized representation of the CNS equilibrium point hypothesis based-VT.

The goal is to this dissertation is to create mathematical representation which can approximate the virtual trajectory illustrated in Figure 4.6. In addition to maintaining theoretical consistency with Feldman's (1995) characterization of a monotonic shift between equilibrium points, the mathematical equation must also encompass the idea of CNS signal changes that naturally occur during neural transmission, well as system dynamic induced changes in the CNS signal. The trajectory represented in Figure 4.6 provides the appearance that shifts between components of the trajectory happen instantaneously. The delays naturally occurring in neural transmission and overall system dynamics would ultimately tend to modify the initial CNS signal to a modified form represented in Figure 4.7. This modified representation of the CNS signal demonstrates how the delays neural transmissions and system dynamics would give the signal a more curve-like appearance. Implementing the CNS signal into a virtual trajectory model requires the development of a mathematical equation that is theoretically consistent with

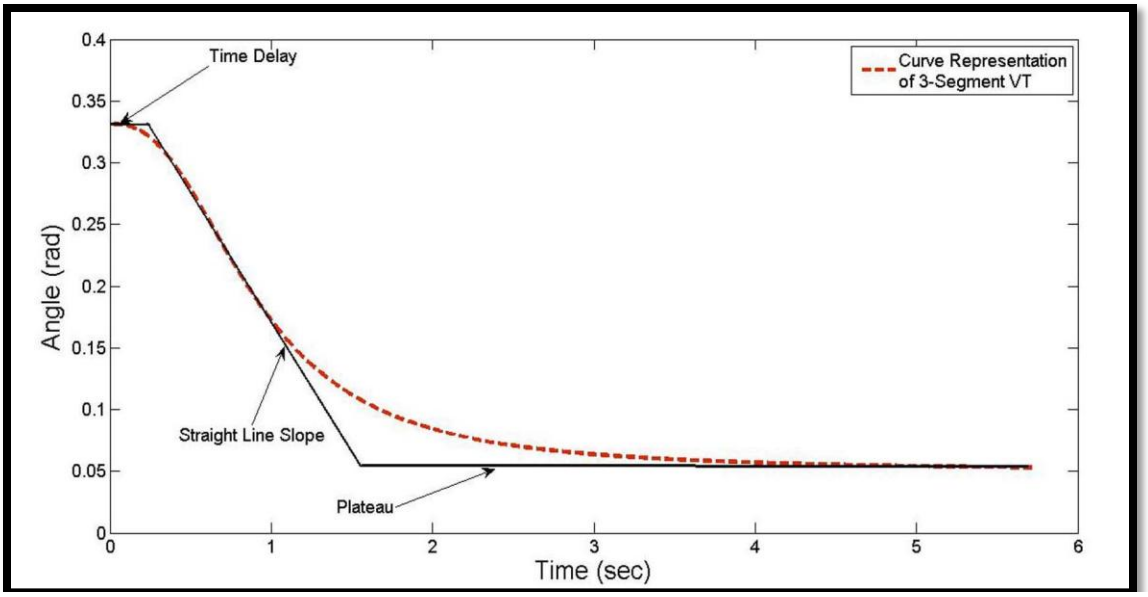

Figure 4.7 CNS signal with signal modified curve representation.

the three segment monotonic VT shown in Figure 4.6 yet also acknowledges the change that would occur in the CNS signal due to system dynamics demonstrated in Figure 4.7. The mathematical equation of a sigmoid function can act as representation of the CNS virtual trajectory first shown in Figure 4.6 with the curves as shown in Figure 4.7, incorporating the signal changes due to system dynamics.

4.3.1 Sigmoid Model Components of the Virtual Trajectory

The sigmoid equation is an easy to use mathematical function that produces a smooth virtual trajectory, without sharp discontinuities, that has the desired characteristics of a flat top, during the signal feedback delay, a quasi-linear slope and a flat bottom. The virtual trajectory equation, Θ_o originally defined in Equation 4.2 becomes:

$$\Theta_o = \text{Bottom} + \left((\text{Top} - \text{Bottom}) / \left(1 + \left(\frac{x}{k} \right)^n \right) \right) \tag{4.4}$$

where Bottom and Top are the bottom and top of the sigmoid curve respectively, k is the inflection point time of Θ_o, and n is the slope of the sigmoid curve. Using the equation of a sigmoid curve as an approximation demonstrates the ability of the equilibrium point hypothesis to provide a comprehensive explanation of the observations of Lin and Rymer. During the pendulum knee test, when the leg is held at a constant angle, Θ, the virtual trajectory angle, Θ_o moves to the holding angle. When the leg is released, Θ_o will be held at the holding angle until the spindle feedback tells the spinal cord/CNS that the leg is falling. Then after that feedback delay time, Θ_o is allowed to follow Θ, forming a passive VT. The simplicity of this technique lies in its ability to differentiate the knee joint motions based mainly on three overriding parameters: The virtual trajectory, Θ_o, relative damping coefficient, B, and stiffness coefficient, K. The sigmoid-based trajectory eliminates the need for the complex equilibrium-point trajectories used in standard models in order to reproduce simple motions such as Latash's N-shaped trajectory (Latash,1998) or the exponential trajectory suggested by Simon and Foulds (2004).

Having established a mathematical equation capable of representing the VT, incorporation of this equation into the forward model shown in Figure 4.2 is accomplished by replacing the equation defined in the 'Decaying Exponential' box in Figure 4.2, with the variables representing Equation 4.4. Though four variables are defined within Equation 4.4, only three variables are optimized. The variable, "Top" in Equation 4.4 is assigned in the forward model as the variable, Tp. The variables "k" and "n" from Equation 4.4 remain unchanged in the equation defined for the VT in the forward model. The variable "Bottom" from Equation 4.4 is assigned the variable, "Bt" in the forward model. However as a simplification of the forward model, when the leg

finally comes to rest after several oscillations, the virtual trajectory, Θ_o equals the actual trajectory, Θ. Thus the variable, "Bt" used in the forward model equals the angular position, Θ_{rest}, when the leg comes to rest, which is given by the position data collected from the trakSTAR.

The virtual trajectory shown in Figure 4.8 essentially consists of a time delay, a straight line slope and then a plateau. The representation of these sigmoid function features as curves is physiologically reasonable as the nature of muscle-force feedback systems include system dynamics which prevent the instantaneous change in position or velocity.

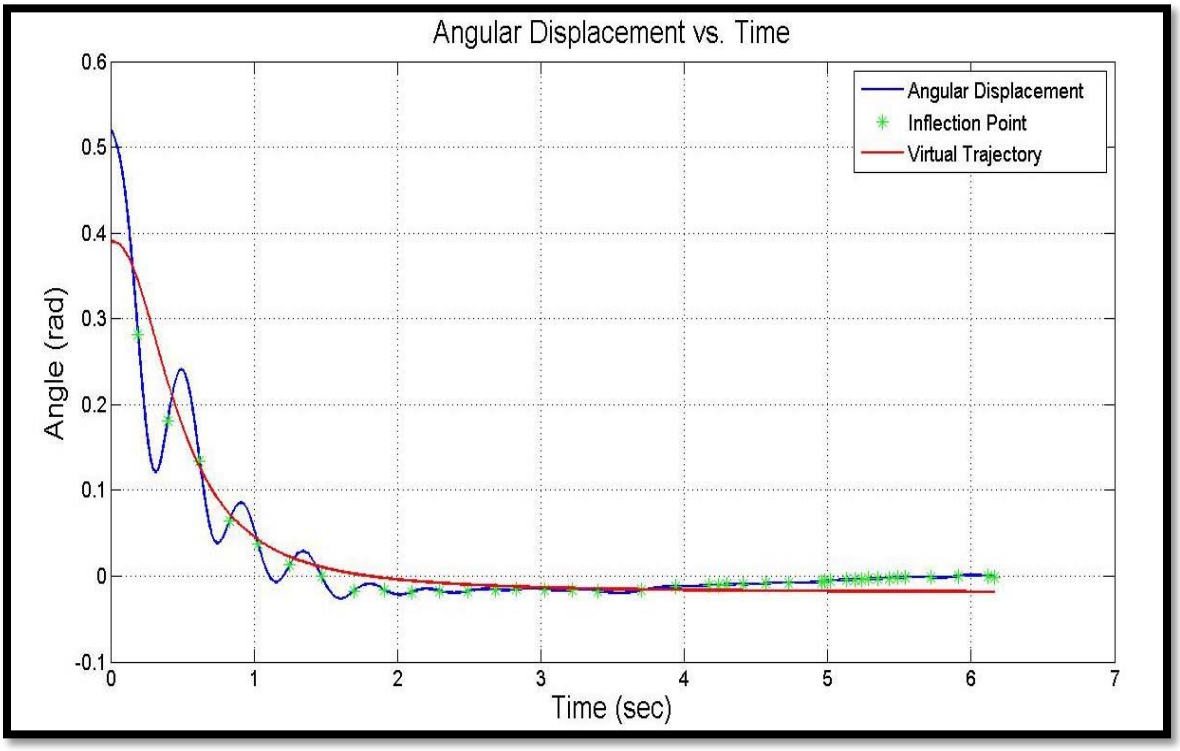

Figure 4.8 Pendulum knee data of spastic subject with sigmoid hypothetical VT.

4.3.2 Assessment of Sigmoid Virtual Trajectory Model

The effectiveness of this new definition of virtual trajectory was assessed using the same validation methods describe previously in section 4.2.3. The objective of the assessment is to establish the model's ability to accurately represent the experimental pendulum knee test data through the optimization of the parameters representing the sigmoid VT, plus B and K. Additionally, it is expected that the model implementing the simpler, constant slope, sigmoid trajectory, which aligns conceptually with the concept of the virtual trajectory described in the EPH, will provide a SSE that is as low as the model output of the exponential VT.

4.3.3 Cluster Analysis of Parameters

Cluster analysis is a technique used for classification of data in which data elements are partitioned into groups called clusters that represent collections of data elements that are proximate based on a distance or dissimilarity function. It is a discovery tool that reveals associations, patterns, relationships, and structures in masses of data. Cluster analysis aims to sort objects into groups such that there is a maximum degree of similarity between objects belonging to the same group and minimum association to objects in other groups (Donnelly, 2006). In cluster analysis there is no a priori information about the group or cluster membership for any of the objects. Groups or clusters are suggested by the data, not defined a priori.

Cluster analysis was applied in order to understand the relationship among the variables optimized by the model. The goal in this research was to detect interrelations among the optimized parameters: B, K, and the sigmoid VT parameters: Tp, n, and k. The goal of clustering variables in this research was to reduce the number of variables

required to describe the output of the model. In this way, the dynamics of the pendulum knee model could be defined by a smaller grouping of variables. Minitab was used to perform an agglomerative hierarchical method that begins with all variables separate, each forming its own cluster. In the first step, the two variables closest together are joined. In the next step, either a third variable joins the first two, or two other variables join together into a different cluster. This process will continue until all clusters are joined into one. Clusters were formed utilizing the linkage criteria of minimization of within cluster variance. Based on this criterion, Ward's method was chosen for the analysis. For each cluster, the means for all the variables are computed. Then, for each object, the squared Euclidean distance to the cluster means is calculated:

$$d_{Euclid^2}(\mathrm{x}, y) = \sum_i (x_i - y_i)^2 \tag{4.5}$$

These distances are summed for all the objects. At each stage, the two clusters with the smallest increase in the overall sum of squares within cluster distances are combined. In Ward's method, the proximity between two clusters is defined as the increase in the squared error that results when two clusters are merged.

4.4 Summary

This chapter outlined the development of forward model that incorporates parameters from previous models, K and B, and a virtual trajectory parameter, Θ_o which incorporates the equilibrium point hypothesis. As an initial approximation, the virtual trajectory was modeled as an exponential curve for validation with pendulum knee data from six subjects. However, the virtual trajectory, as discussed by Feldman and others, is a simple curve resulting from point to point monotonic shifts and thus suggest that the CNS is not likely to specify a complex curve like an exponential. This fact combined with Lin and Rymer's observation of a delay in falling of the leg upon initial release necessitated a new definition for the virtual trajectory to be used in the model. A sigmoid function was chosen because it represented a combination of a time delay, straight line VT, with the ability to adjust its starting and ending angles. This new model was tested with the pendulum knee test data from previous six subjects.

CHAPTER 5

RESULTS AND DISCUSSION

The pendulum knee drop test was performed on six subjects, as described previously. Figure 5.1 shows the movement trajectories for the three triplet subjects of whom two (BX and CX) have cerebral palsy with mild spasticity and one (AX) shows no clinical signs of cerebral palsy or spasticity. The trajectory for the non-spastic sibling, AX, shows the expected smooth swinging, damped pendular movement (Figure 5.1A). The two subjects with spasticity (BX and CX Figure 5.1B and C) show the characteristic spastic trajectory characterized by a downward trends due to gravity with upward movements due to muscle activity (Fee and Foulds, 2004).

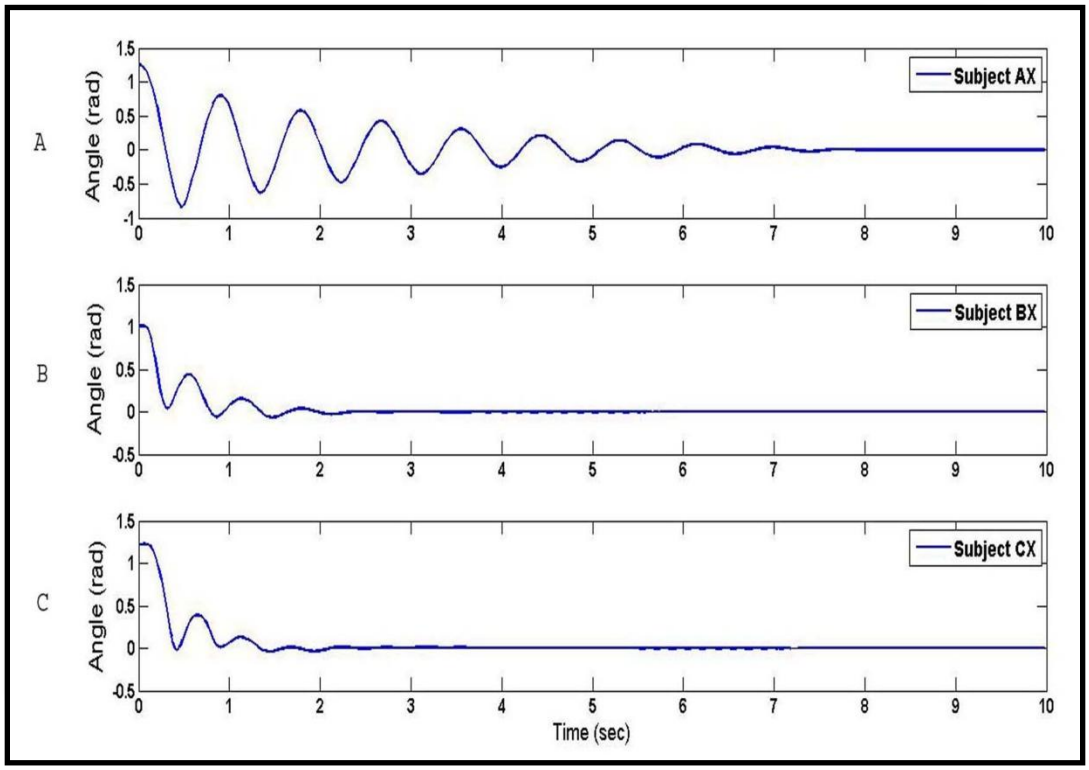

Figure 5.1 Representative movement trajectories for triplet subjects.

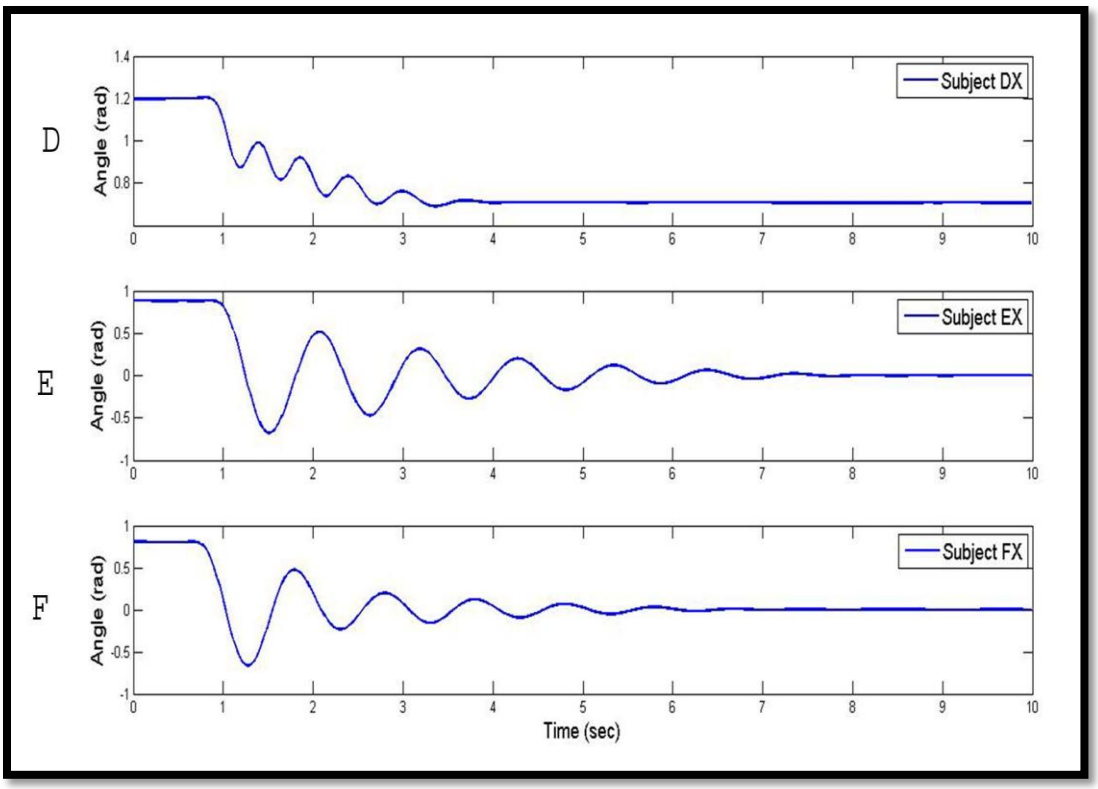

Figure 5.2 Representative movement trajectories for subjects tested at Neuromuscular Engineering Lab at NJIT.

Figure 5.2 displays the pendulum knee test angular trajectories of the three subjects tested at the Neuromuscular Engineering Lab at NJIT. Subject DX, is a thirty-two year old male with cerebral palsy. The angular trajectory data of subject DX (Figure 5.2 D) is similar in appearance to the two cerebral palsy children, subjects BX and CX, tested at the A.I. duPont Hospital for Children, shown in Figures 5.1B and C respectively. The angular trajectory of subjects EX and FX, (Figures 5.2E and F) is of two young adult subjects with no history of spasticity. Their angular data looks similar to the non-spastic sibling, subject AX, shown in Figure 5.1A.

5.1 Exponential VT Model

The forward model described previously, was designed to be utilized in a gradient-descent based optimization program, which recursively uses Simulink to optimize the model parameters of Equations 4.1 and 4.2. This program passed initial parameters to the Simulink model, recorded the output of the models, and performed a non-linear least-squares optimization of the parameter variables. Figures 5.3 and 5.4 show the model output superimposed on the experimental angular trajectories of a subject with and without spasticity respectively. In addition each figure shows the resulting optimized exponential virtual trajectory, Θ_o developed from the optimized parameters, *A* and *s* from Equation 4.2. The figures show the goodness of fit of the model, R^2, and the sum of squares due to error, SSE, of the model.

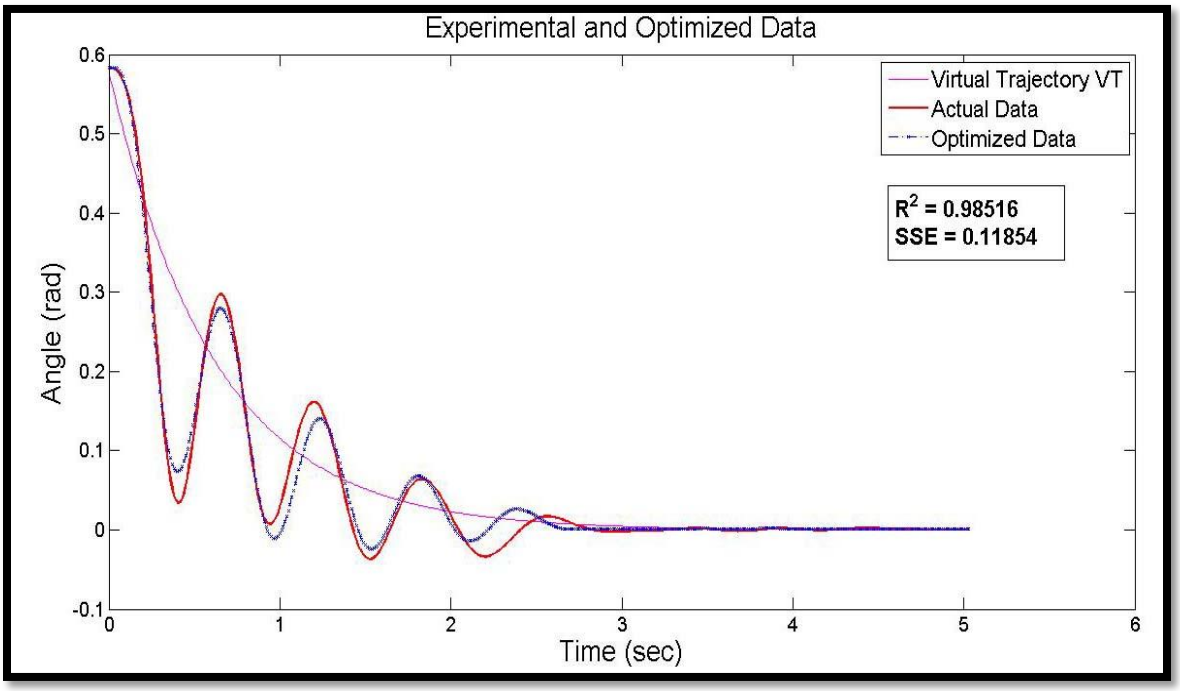

Figure 5.3 Exponential VT model of spastic subject, DX.

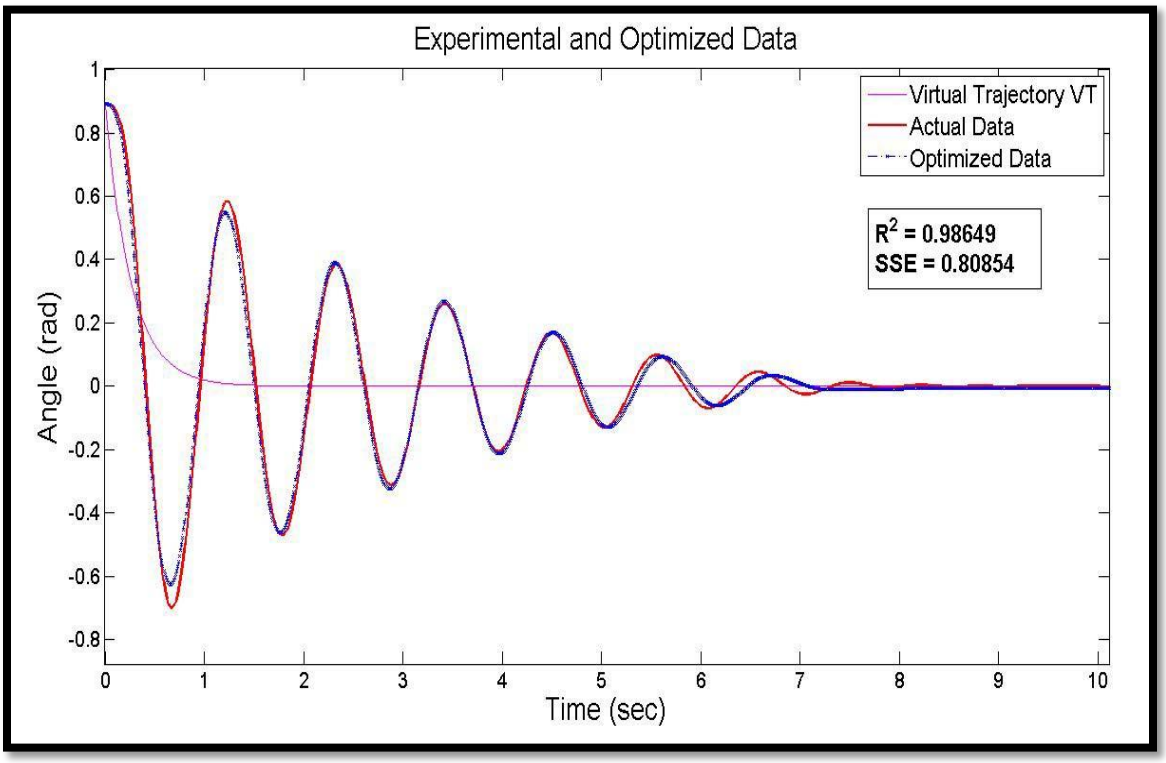

Figure 5.4 Exponential VT model of non-spastic subject EX.

Four parameters were optimized by the model; stiffness and damping, K_{rel} & B_{rel}, corresponding to K and B from Equation 4.1, and Θ_o variables, "A" and "s" from Equation 4.2. Tables 5.1 and 5.2 show the average optimized parameters for the subjects with spasticity and without spasticity respectively. The results of optimizations of the model present an assessment of the model's ability to reproduce the experimental data from the six subjects. Figures 5.3 and 5.4 demonstrate the model's accuracy. The measure of goodness of fit for the model with its best set of parameters was determined by an SSE computation of the models' output compared on a sample by sample basis with experimental data. In Figure 5.4, which represents the modeling of the pendulum knee data for non-spastic subject, EX, even with a high R^2 value, the model output data

Table 5.1 Spastic Subjects Model Parameters for Exponential VT Model.

Subject	B_{rel}	K_{rel}	Θ_o Variables		R^2	SSE
			A	b		
BX	0.2514	7.6013	1.2561	2.2421	0.9834	0.2928
CX	0.2643	8.1727	1.2855	2.6573	0.9898	0.1504
DX	0.7167	64.0190	0.5271	1.4249	0.9866	0.0965
Note: Units for B_{rel}: N-m-sec/rad, K_{rel}: N-m/rad						

Table 5.2 Non-Spastic Subjects Model Parameters for Exponential VT Model.

Subject	B_{rel}	K_{rel}	Θ_o Variables		R^2	SSE
			A	b		
AX	0.0525	2.3565	0.8015	1.5989	0.9946	0.2192
EX	0.2981	6.3082	0.8781	3.8698	0.9863	0.7374
FX	0.1659	1.9727	0.8035	4.2887	0.9754	0.9814
Note: Units for B_{rel}: N-m-sec/rad, K_{rel}: N-m/rad						

slightly undershoots of the experimental data. Qualitatively, pendulum knee test data of subjects with spasticity produce trajectories that are characterized as being more damped, having higher stiffness and exhibiting the appearance of an exponentially shaped system equilibrium trajectory compared to the trajectories of non spastic subjects. The optimized parameters of the damping coefficient, B_{rel} and stiffness coefficient, K_{rel} shown in the previous tables provide quantitative support of this qualitative analysis by producing higher values of B_{rel} & K_{rel} in the spastic data compared to the non-spastic subjects.

5.2 Sigmoid VT Model

The sigmoid VT model was optimized in a similar manner as the exponential VT model. The rationale of sigmoid function is its ability to combine a time delay, straight line virtual trajectory, with an ability to adjust its starting and ending angles. In addition to the parameters of stiffness and damping, K_{rel} & B_{rel}, corresponding to K and B from Equation 4.3, the parameters which define the sigmoid curve, Θ_o, are optimized by the forward model: Top (Tp), slope (n) and inflection point time (k). Figures 5.5 and 5.6 demonstrate the model's ability to accurately reproduce the experimental data through the gradient descent optimization techniques described previously.

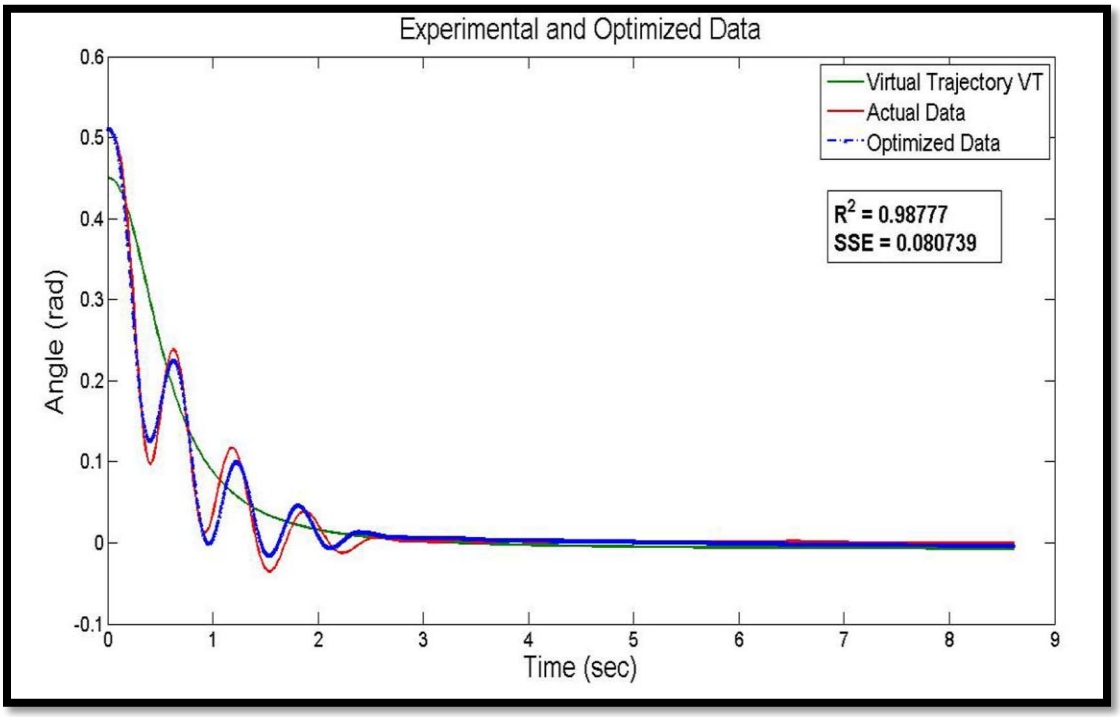

Figure 5.5 Sigmoid VT model of spastic subject DX.

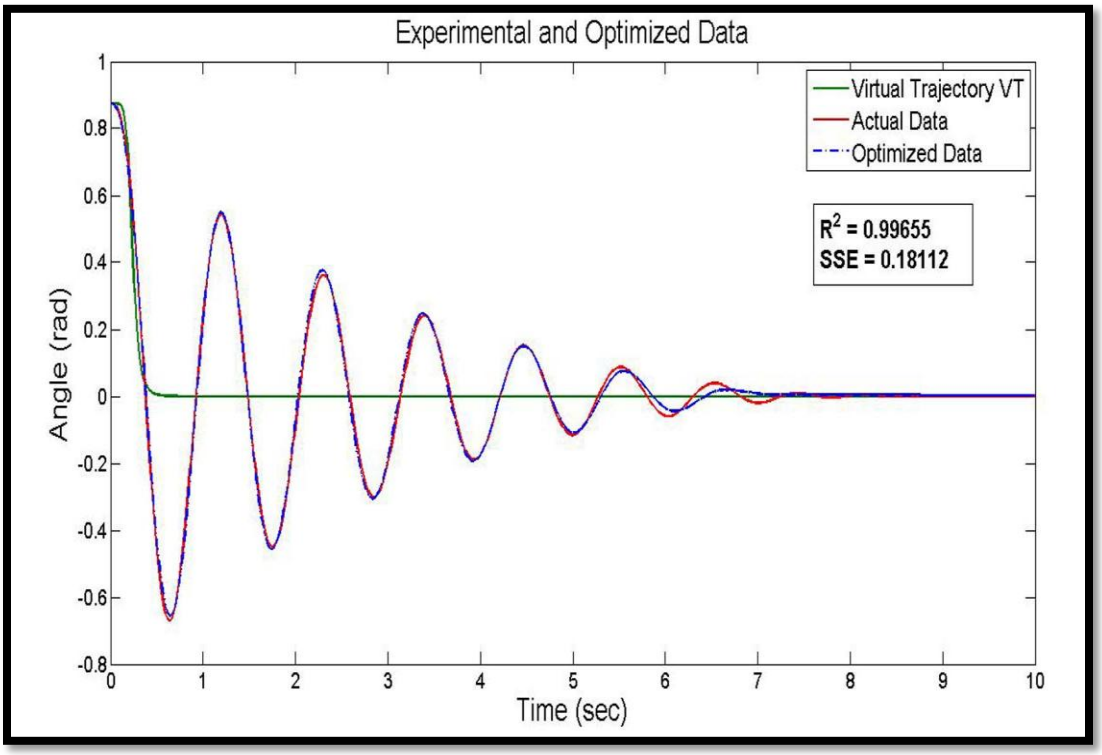

Figure 5.6 Sigmoid VT model of non-spastic subject EX.

Figure 5.5 shows a virtual trajectory for a spastic subject that is below the actual angle trajectory at the point of limb release. The significance of this outcome is that it supports the theory described in Levin's (2000) research that the equilibrium point hypothesis can describe spasticity as the inability to regulate the stretch reflex threshold throughout the entire physiological range. This outcome also supports the concept of the virtual trajectory lagging the actual trajectory as described in Latash's (1992) research. As the limb is raised to near max extension, held and then release, the virtual trajectory initiated by the CNS lags the actual trajectory of the limb. Figure 5.5 shows that in subjects with spasticity, at the point of release of the limb, the model predicts a VT that has not reached the actual trajectory angle.

In contrast Figure 5.6, which shows the model output for a subject without spasticity, the VT is equal to the actual trajectory at the point of limb release. This outcome is consistent with Levin's view that individuals without spasticity have the ability to regulate the stretch reflex threshold throughout the entire physiological range. In the context of Latash's (1992) theory that everyone exhibits a VT which lags the actual trajectory, Figure 5.6 demonstrates that at the time the limb was released following being held momentarily, the modeled VT has in essence, caught up to the actual trajectory. By extension, the result suggests that there is a greater lag the VT relative to the actual movement trajectory in subjects with spasticity. The model output for the non-spastic subjects closely match the experimental pkd as evidenced by the lack of overshoot in the model data, shown in Figure 5.6 and low SSE value.

Previous research in passive limb oscillations (Vodovnik et al., 1984; Lin and Rymer, 1991; He et al., 1997 and Fowler et al., 2000) modeled data from pendulum knee drop test of non-spastic subjects with an equation of motion, Equation 3.1, only using the parameters of stiffness, K and damping, B, with respect to gravitational 0. Viewing this previous research within the context of the equilibrium point hypothesis, Figure 5.6 allows for the rationale that the results of the earlier models achieved a good level of accuracy because the VT drops toward gravitational zero quickly. Figure 5.7 demonstrates what the output of a model of the same subject (EX shown in Figure 5.6) without adding a VT parameter and using the parameters of K and B. While the level of accuracy is high as shown by the coefficient of determination, R^2 value of 0.95, the accuracy is still lower than the levels produced by the exponential and sigmoid VT models used in this research, R^2 = 0.98 and 0.99 respectively.

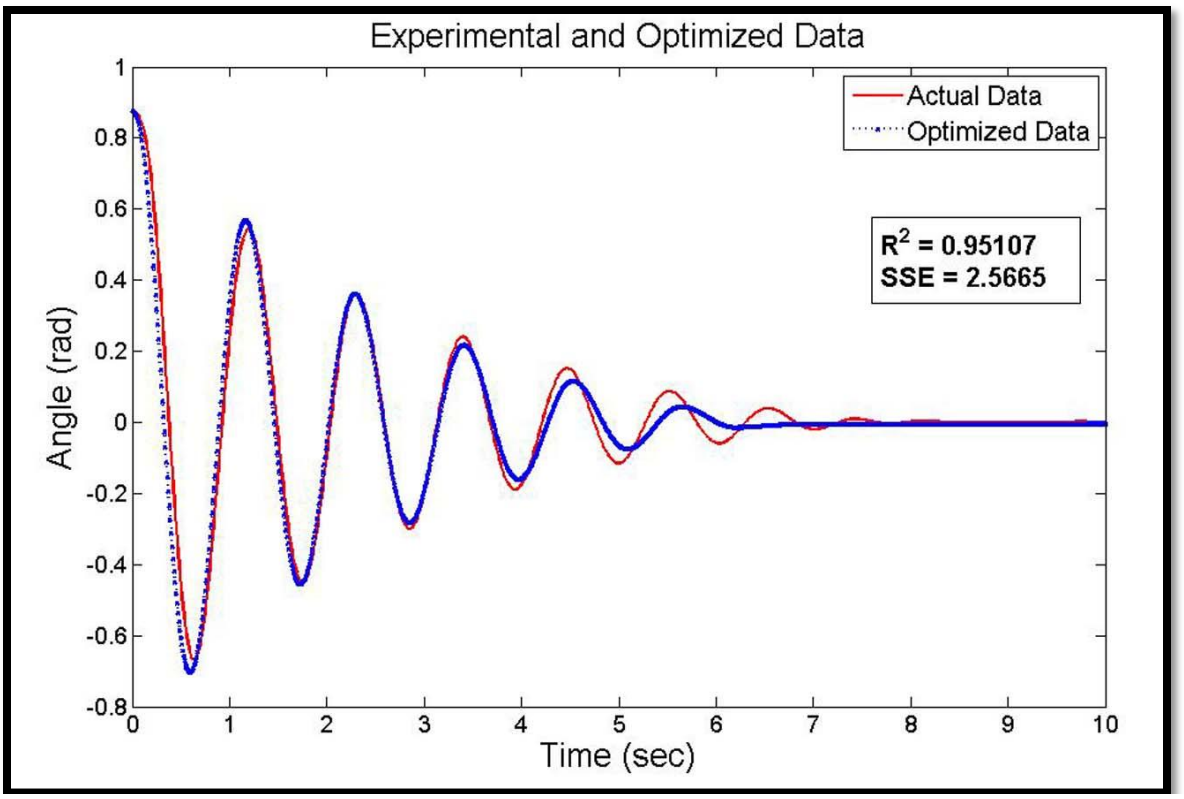

Figure 5.7 Comparison of model output data with experimental pkd data for subject, EX using a non-VT based model.

The SSE for the subject EX when modeled with a VT parameter is also higher, 2.5665, compared to 0.7373 and 0.2359 in the exponential and sigmoid VT models respectively. The increased SSE displayed in Figure 5.7, represents a model that can effectively reproduces first few seconds of the experimental data but has increasing difficulty matching experimental data beyond the first few seconds. Previous models of spasticity utilized measures such as the Relaxation Index which was calculated analyzing only data from the first drop and the final resting angle, which minimized the need to analyze the entire trajectory of the pkd.

The comparison between the output of models with and without a VT, (Figures 5.5, 5.6 and 5.7) make the case that in the limb motion data of non-spastic subjects can be modeled without a VT parameter but the model can be markedly improved with the inclusion of a parameter representing a virtual trajectory. While the VT can be ignored in the non-spastic case, it is much more important in the spastic case. A model implementing a VT parameter not only improves the data fit for non-spastics but is robust enough to accurately model the motion data of spastic subjects as well.

The distinguishing feature of the sigmoid-based VT model compared to the exponential VT model is the ability to segment the virtual trajectory into three unique phases, as illustrated in Figure 5.8. The top (Tp) or plateau region of the modeled sigmoid curve represents the time delay portion of the sigmoid function. This is consistent with the delay observed by Lin & Rymer (1991) in which they described an "unexplained hesitation" immediately after the release of the leg during the pendulum knee test. The rounding between the top section of the sigmoid and the second region, the slope, incorporates the physiological neural delays that exist in signals initiating movement and the beginning of movement. The bottom of the sigmoid trajectory curve settles with the actual position of the limb, demonstrating the ability of the virtual trajectory to follow the actual trajectory of motion, as described within the previous analysis of the equilibrium point hypothesis.

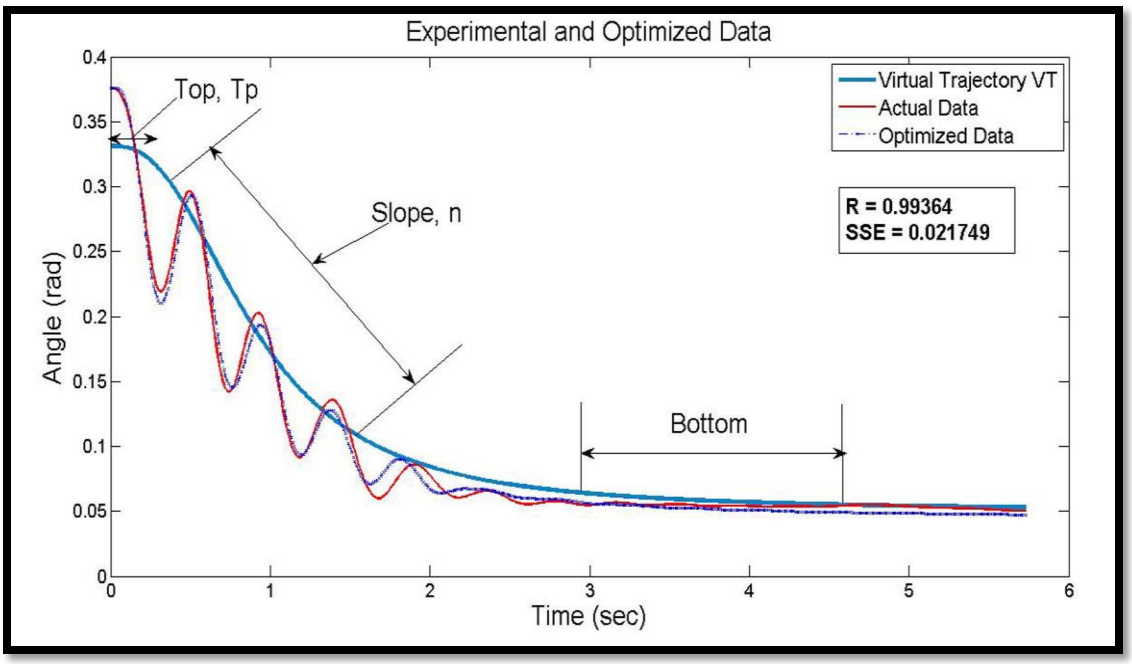

Figure 5.8 Components of sigmoid VT produced by model of spastic data.

Tables 5.3 and 5.4 summarize the average values of the model parameters for both populations of subjects in the study. The values optimized for the damping parameter, B_{rel} and stiffness, K_{rel} in the sigmoid VT model compare very favorably with the values for these same parameters optimized in the exponential VT model. The comparative agreement in stiffness & damping parameter calculations was seen in both the spastic and non-spastic data.

Closer examination of the data shows that the average optimized values for the parameters B_{rel} and K_{rel} for non-spastic subject, EX are close in value to the optimized values for the same parameters in the data from spastic subjects, BX and CX. This result was also shown in the optimized data utilizing the exponential VT model (Tables 5.1 and 5.2). It is know from previous research in pendulum knee models that the impedance values of K and B are generally higher in spastic subjects than subjects without spasticity (Vodovnik et al., 1984; Lin and Rymer, 1991; He et al., 1997 and Fowler et al., 2000).

Table 5.3 Spastic Subjects Model Parameters for Sigmoid VT Model.

Subject	B_{rel}	K_{rel}	Θ_o Variables			R^2	SSE
			Tp	n	k		
BX	0.1733	6.9582	1.1575	2.6823	0.4108	0.9869	0.2449
CX	0.1849	8.3314	1.0947	2.3389	0.3512	0.9858	0.2254
DX	0.6277	63.4455	0.5095	1.5502	0.5544	0.9871	0.0951

Table 5.4 Non-Spastic Subjects Model Parameters for Sigmoid VT Model.

Subject	B_{rel}	K_{rel}	Θ_o Variables			R^2	SSE
			Tp	n	k		
AX	0.0514	2.3529	0.7179	1.7571	0.4754	0.9951	0.2008
EX	0.3414	6.8828	0.8771	5.8820	0.2313	0.9956	0.2359
FX	0.1890	2.1802	0.8039	6.3654	0.2327	0.9862	0.5773

The differences in ages of the subject populations necessitated an examination of the impedance parameters, K_{rel} and B_{rel} relative to the moment of inertia of each subject. Table 5.5 shows a comparison of parameters K_{rel} and B_{rel} normalized to the moment of inertia of each of the subjects. The normalized values of B_{rel}/I and K_{rel}/I show a more defined separation between the group of subjects with spasticity and the group of subjects without spasticity. When viewed in this manner, it can be concluded that there is indeed increased impedance in subjects with spasticity compared to subjects without. The normalization of Brel and Krel also shows that within the spastic subject data set, Subject DX, an adult, has virtually the same B_{rel}/I value compared to the children with cp, BX and CX but much higher K_{rel}/I, attributable to an increased level of spasticity.

Table 5.5 Normalized Calculations of Impedance Values From Sigmoid VT Model.

	Subject	Moment of Inertia, I	B_{rel}	B_{rel} / I	K_{rel}	K_{rel} / I
Non-Spastic	**AX**	0.1130	0.0514	0.4549	2.3529	20.8255
	EX	0.6329	0.3414	0.5395	6.8828	10.8747
	FX	0.2078	0.1890	0.9094	2.1802	10.4900
Spastic	**BX**	0.1130	0.1733	1.5334	6.9582	61.5865
	CX	0.1130	0.1849	1.6365	8.3314	73.7407
	DX	0.4063	0.6277	1.5448	63.4455	156.1383

The Θ_o parameters optimized in the sigmoid VT model were, Tp, n and k. Tp represents the top or maximum plateau of the sigmoid curve, whereas, n and k represent the slope of the curve and time at the curve inflection point respectively. The parameters that define Θ_o establish the ability of the virtual trajectory to follow the actual trajectory. The results of the model demonstrate higher values of the slope, n, and lower values time at inflection point, k in the non-spastic subject data compared to the calculated values in the spastic subject data. A larger or steeper slope in the virtual trajectory with a shorter inflection point time, represents a virtual trajectory that more quickly tries to follow the actual trajectory. Since the motion of the leg during the pendulum knee test is toward the vertical gravitational zero, the virtual trajectory in non-spastic subjects follows a steep descent toward zero degrees. In contrast, the limb trajectory of subjects with spasticity is a slower, more gradual descent toward vertical zero degrees, as represented by the smaller value of the virtual trajectory slope, n and the higher value of the parameter k.

In the previous chapter it was postulated that in addition to aligning conceptually with the concept of the virtual trajectory described by the EPH (Latash, 1992), a model based on a sigmoid VT would provide an output of angular trajectory with comparable SSE, relative to the experimental data, to the SSE produced by the exponential VT model. Table 5.6 compares the SSE of both models for both the spastic and non-spastic populations. The results demonstrate that the SSE produced by the sigmoid VT model is comparable to the SSE produced by the exponential VT model.

Table 5.6 Model Accuracy Comparison.

Model	**Subject**					
	Spastic			**Non-Spastic**		
	BX	**CX**	**DX**	**AX**	**EX**	**FX**
	SSE	**SSE**	**SSE**	**SSE**	**SSE**	**SSE**
Exponential VT	0.2928	0.1504	0.0965	0.2192	0.7374	0.9814
Sigmoid VT	0.2449	0.2254	0.0951	0.2008	0.2359	0.5773

5.3 Cluster Analysis of Sigmoid VT Model Parameters

The goal of the cluster analysis algorithm described in the previous chapter was to determine if the output pendulum knee trajectory predicted by the forward model could be described by a smaller grouping of the five variables optimized by the gradient descent optimization routine: B_{rel}, K_{rel}, Tp , n, and k. It was hypothesized that the pendular trajectory could be described with just three variable classes: relative damping parameter, B_{rel}, relative stiffness parameter K_{rel}, and a virtual trajectory parameter, Θ_o , which would be a grouping of the variables describing the sigmoid VT function. Figure 5.8 shows the statistical clustering of parameters within the non-spastic data.

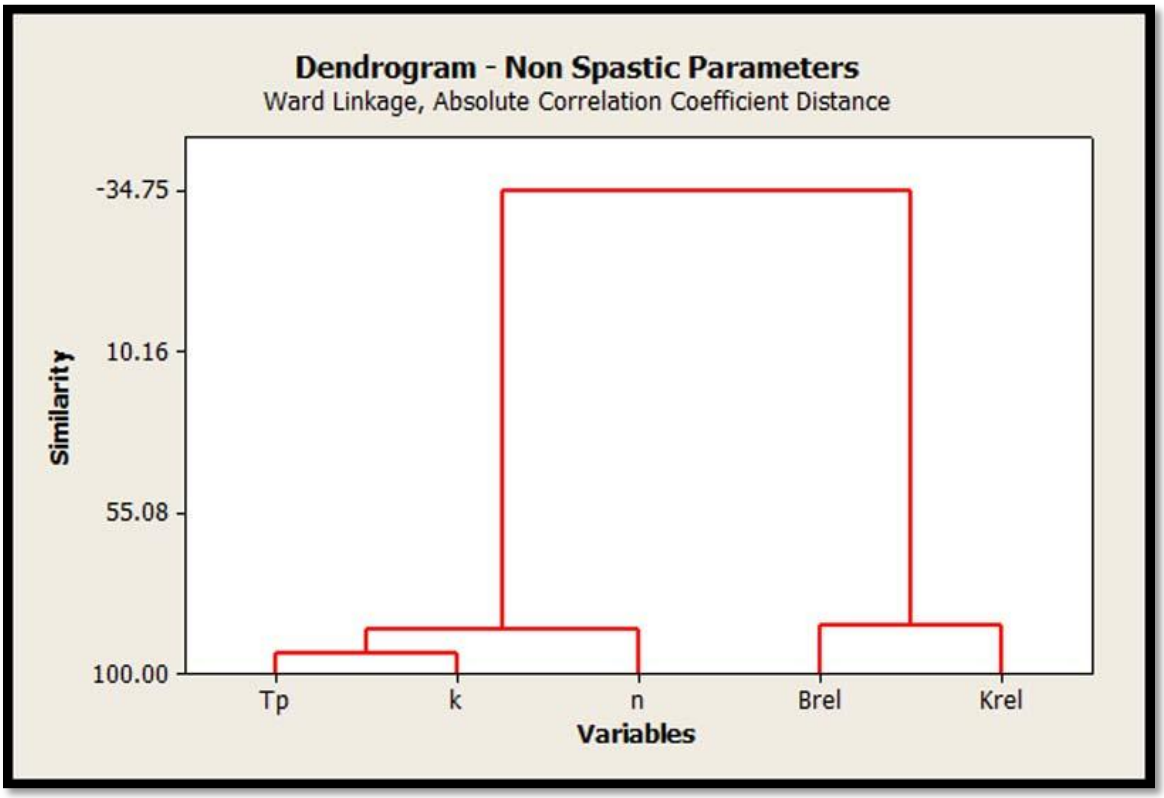

Figure 5.9 Dendrogram of optimized variables for non spastic subject data

The cluster of variables is shown on a tree diagram known as a dendrogram. A dendrogram is a visual representation of the variable correlation data. The individual variables are arranged along the bottom of the dendrogram and referred to as leaf nodes. Variable clusters are formed by joining individual variables or existing variable clusters with the join point referred to as a node (Nonlinear Dynamic, 2011). Since the goal of clustering is the reduction of variables by combing variables with similar characteristics, the dendrogram represents a visual representation of the similarity in the variances of the variables. The higher the similarity, shown on the y-axis, the greater the correlation. In the non-spastic data two distinct clusters appear to be formed.

The first cluster is a clustering all three variables which define the sigmoid VT, Tp, n and k. This first cluster combines the cluster of Tp-n, which has a similarity level of 94.45 out of 100, with a cluster of Tp-n-k, which has a similarity level of 87.66. The second cluster is formed between variables B_{rel} and K_{rel} respectively. Lin and Rymer (1991) theorize in their research that the impedance values of stiffness, K and damping, B, both increase with increasing muscle activity and that these increase are likely interrelated. This interrelation between stiffness and damping was also modeled by Flash (1987). The results of the cluster analysis suggest that it is possible to describe the dynamics of limb motion of non-spastic subjects during the pendulum knee test in terms of a grouped variable, Θ_o, encompassing the sigmoid VT parameters, and either B_{rel} and K_{rel} separately or another grouped variable combining the two. The importance of this conclusion is that it establishes that the VT along with the impedance values, B and K are capable of completely describing the limb motion dynamics.

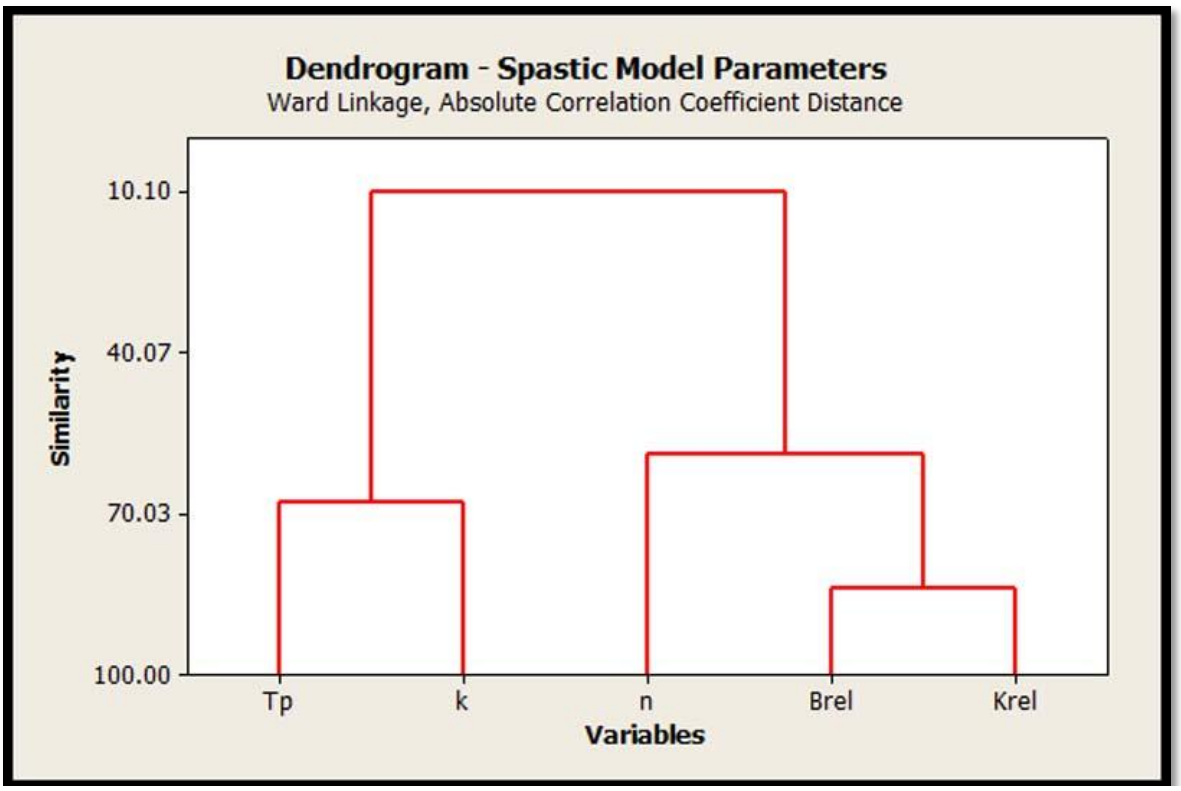

Figure 5.10 Dendrogram of optimized variables for spastic subject data.

Figure 5.8 illustrates the dendrogram for the same variables based on the spastic subject data. Examination of the dendrogram suggests that it might be possible to group variable Tp with variable n, with a similarity level of 68.14. Just as was seen in the cluster analysis of non-spastic data, there is a strong level of similarity in the variances of the variables B_{rel} and K_{rel} resulting in a cluster with a similarity level of 84.04. Overall, in the spastic data, while some correlations appear to exist, the level of similarity between the suggested clusters is not as high as the clusters formed from the analysis of the non-spastic data. Comparison of the cluster analysis in the spastic and non-spastic subject data reveals that in both data sets, clusters with high similarity are formed between two sets of parameters: Tp clustered with k and B_{rel} clustered with K_{rel}. The clustering of B_{rel} and K_{rel} reinforces the relationship between the impedance values of B and K found in previous

pendulum knee test models (Lin and Rymer, 1991; Flash, 1997). The results in both cases demonstrate that the limb dynamics in pendulum knee motion can be modeled with not just the impedance parameters but with the

5.4 Further Evidence of a Virtual Trajectory in the Relaxed Condition

The results presented in earlier sections have extended the concept of a virtual trajectory to the situation in which the subject is ideally relaxed. In active movements, the VT is described as a CNS produced template of a sequence of desired equilibrium points that represent the desired joint trajectory. In a subject-initiated movement, this virtual trajectory precedes the actual joint movement in time. The instantaneous VT angle is compared with the current actual angle to produce a net moment that attempts to reduce the error between the desired and actual angle, resulting in joint movement. In the simplest case, the net moments can be described as:

$$M_{net} = K(\Theta - \Theta_o) \tag{5.1}$$

Or more as shown in recent research describing active movements (de Lussanet et al., 2002; Chen et al., 2009):

$$M_{net} = K(\Theta - \Theta_o) + B(\dot{\Theta} - \dot{\Theta}_o) \tag{5.2}$$

An essential element of the PKD is that subjects are asked to relax and not to consciously intervene when the knee angle is changed from one position to the next. In the case in which the subject is ideally relaxed, theoretically one would presume that

there is no desired trajectory, and thus there is no VT. However, in that situation there is no muscle-generated net moment and Equations 5.1 and 5.2 only remain valid with M_{net} = 0, if $\Theta_o = \Theta$. Thus, the ideally relaxed case can be described as one in which the VT is released by the CNS to follow the actual trajectory with no lag in time, maintaining a constant $\Theta_o = \Theta$ over time. As such, the relaxed situation constitutes a special case of the EPH. As a consequence if would be expected that if relaxation were achieved, M_{net} would equal zero throughout the pendular movements.

As described earlier, it is well known that the classic ratcheting trajectory of the spastic PKD trajectory is the result of bursts of net knee moment that oppose the gravitational moment. This non-zero M_{net} is seen in the results of inverse dynamic computation of net moment in the spastic PKD as seen in Figure 5.11 where M_{net} has significant non-zero values. A similar inverse dynamic computation of the net moment of a subject without spasticity is shown in Figure 5.12. While the subject is supposedly relaxed, and is unimpaired by spasticity, the values of M_{net} also show large deviation from zero. In both the spastic and non-spastic cases, it is clear that neither subject is ideally relaxed. The results of the earlier modeling show that the inclusion of a virtual trajectory that does not ideally track the actual trajectory produces superior results. These results suggest that in the partially relaxed state, the joint has an initial actual angle, and initial virtual angle, and that once released and allowed to fall under the external influence of gravity, the CNS cannot perfectly allow the VT to track the actual angle, but produces a VT that cannot keep up with the changing joint angle. This produces a time varying error that results in non-zero M_{net}. Thus, in addition to differences in stiffness and damping between spastic and non-spastic PKD data, spasticity also modifies the VT.

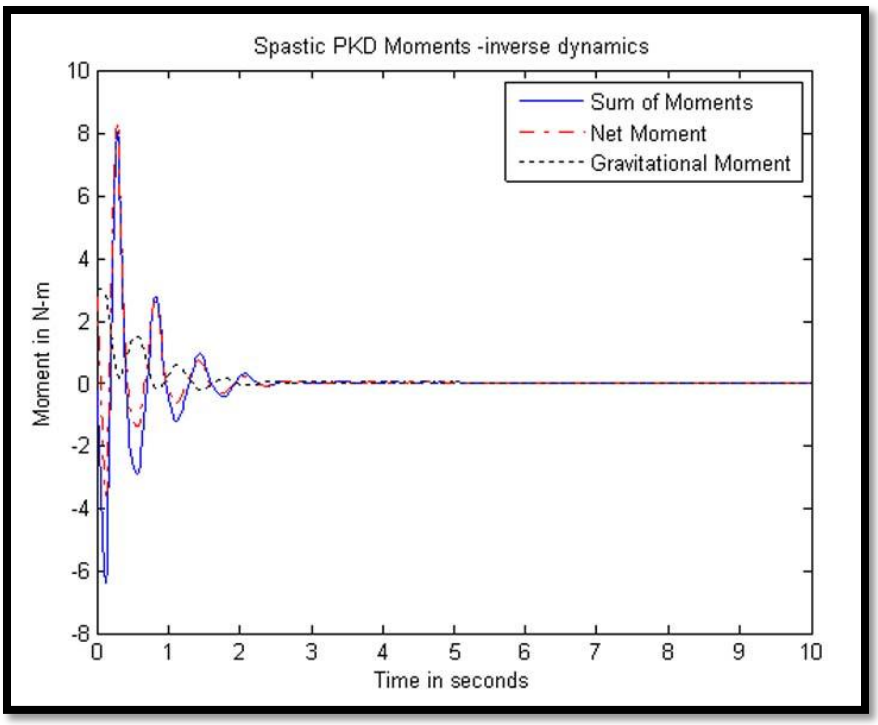

Figure 5.11 Inverse dynamic model output of spastic pkd moments.

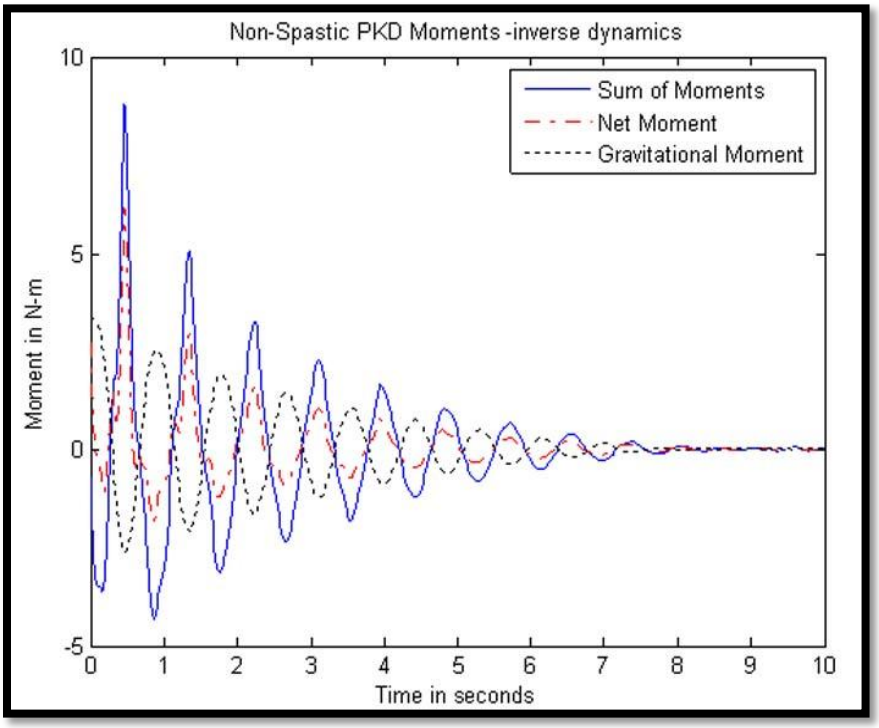

Figure 5.12 Inverse dynamic model output of non-spastic pkd moments.

Furthermore, in addition to altering the shape of the VT (see Figure 5.5 and 5.6), the modeling shows that the optimized starting angle of the VT of the non-disabled subjects is found to be equal to the starting angle of the actual trajectory while the optimized angle of the VT of the subjects with spasticity is found to be lower than the starting angle of the actual trajectory. This would indicate that when the knee raised to extension, the VT of the non-spastic subject may follow actual trajectory with a lag, but that given sufficient time, it will eventually achieve the same angle as the knee. When the leg is released, the VT may lag the actual trajectory, and eventually achieve the final resting angle as simulated in Figure 5.13. The VT optimized from the spastic data lags the actual angle, but also fails to achieve the angle from which the leg is released. This is represented in a stylized representation shown in Figure 5.14.

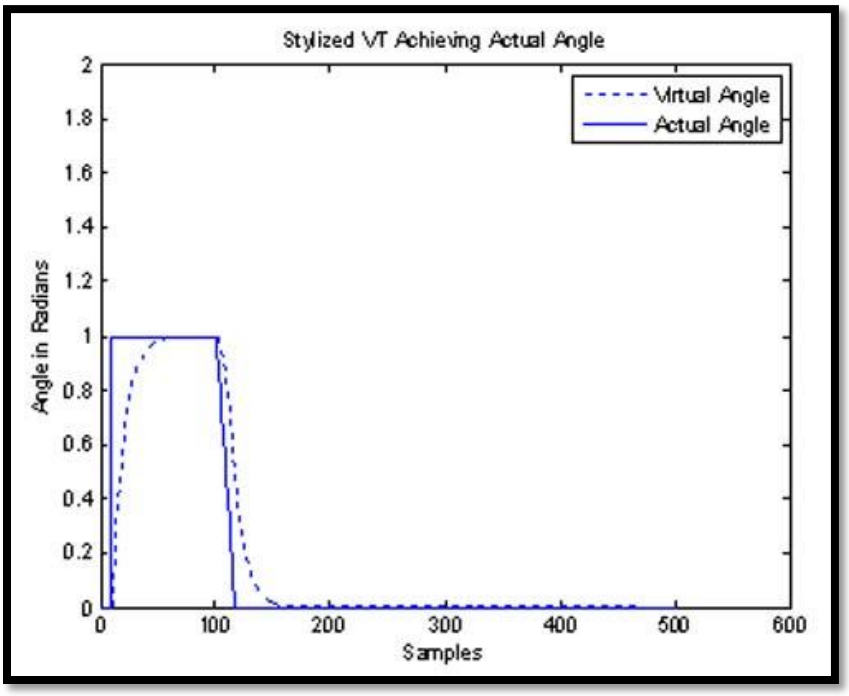

Figure 5.13 Stylized model of VT achieving actual angle.

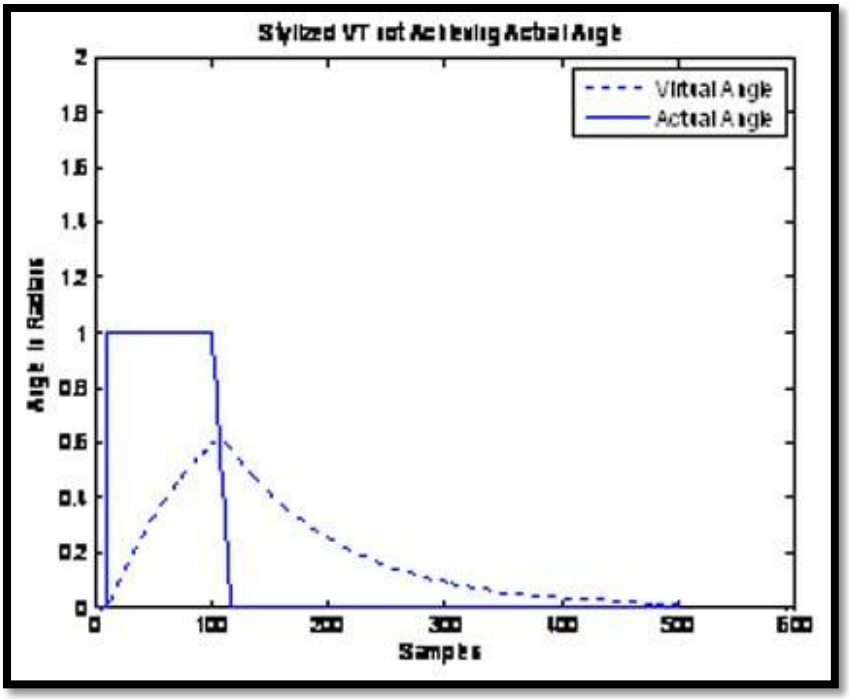

Figure 5.14 Stylized model of VT not achieving actual angle.

This outcome supports the research of Levin (2000) who argued that the ability to regulate the stretch reflex threshold, i.e. control the VT, throughout the entire physiological range of the joint is what separates the movements of subjects without clinical signs of spasticity from those of subjects with spasticity. Levin and Feldman (1994) had previously shown in their research that healthy subjects were able to relax at the initial elbow position due to an "increase in the threshold which precluded muscle activation in the whole physiological range of arm displacement". In contrast spastic patients were unable to increase the stretch reflex threshold to prevent muscle activation during even slow velocity stretching. Subjects with spasticity were shown to be unable to move the VT throughout the entire physiological range.

While the model output of the virtual trajectory suggests that there exist a lag between the actual trajectory of limb motion and the virtual trajectory, the virtual trajectory is calculated by a mathematical optimization of variables defined in Equation, 4.4. As such, the virtual trajectory formed is more theoretical in nature and it became important to determine if there was more physical evidence available to support this concept. Data were collected from the force transducer during the three phases of the pendulum knee drop. The force transducer was attached to the leg with a mounting that allowed the leg to be raised by a string, held at extension by the string, and then released by cutting the string. The force output from the transducer is positive when the leg is pulled in extension and negative when the leg is pushed in flexion. The force transducer output multiplied by the distance along the long axis from the lateral epicondyle to the attached position of the force transducer, allows for calculation of the moment exerted on the leg throughout the movement of the leg. This moment is called the holding moment, M_h.

Figure 5.15 shows the calculation of the holding moment for a spastic subject during the three phases of the pendulum knee drop. The three phases of the pendulum knee drop are clearly indentified in the figure. During the second phase of the leg motion, while the leg is being held, there is a steady decline in holding moment. The moment or torque applied to the leg can only change if the force applied to the leg changes. This would suggest that as the leg is being held in a stationary position (i.e. $\ddot{\Theta} = \dot{\Theta} = 0$), the measured force and by definition, the moment applied to the leg is decreasing.

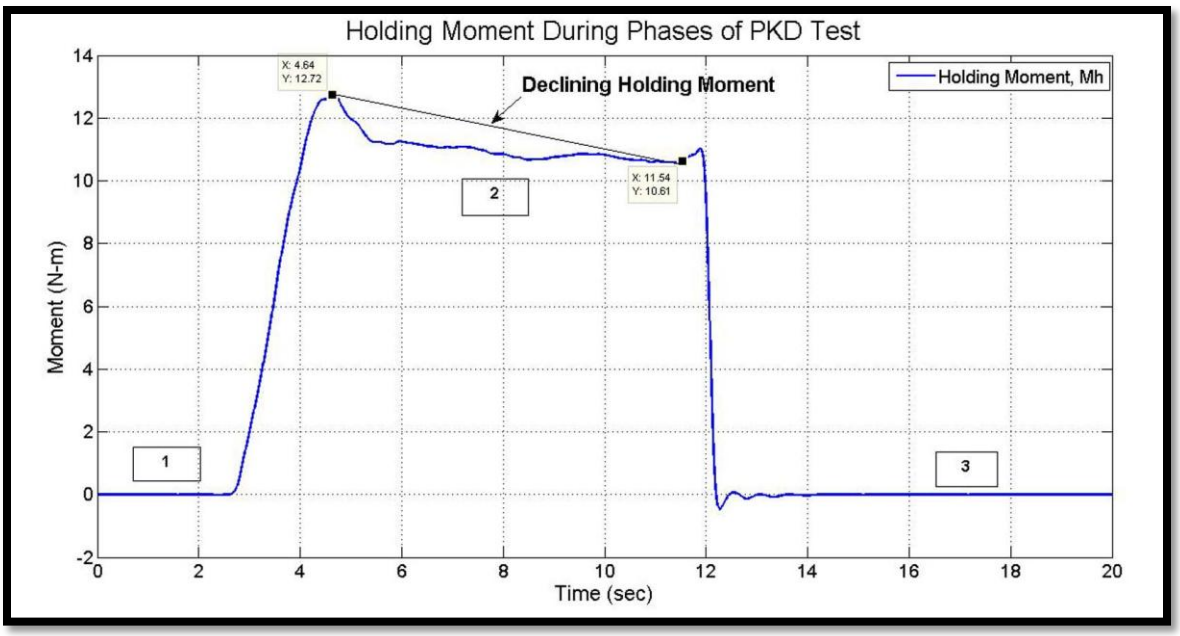

Figure 5.15 Holding moment of spastic subject

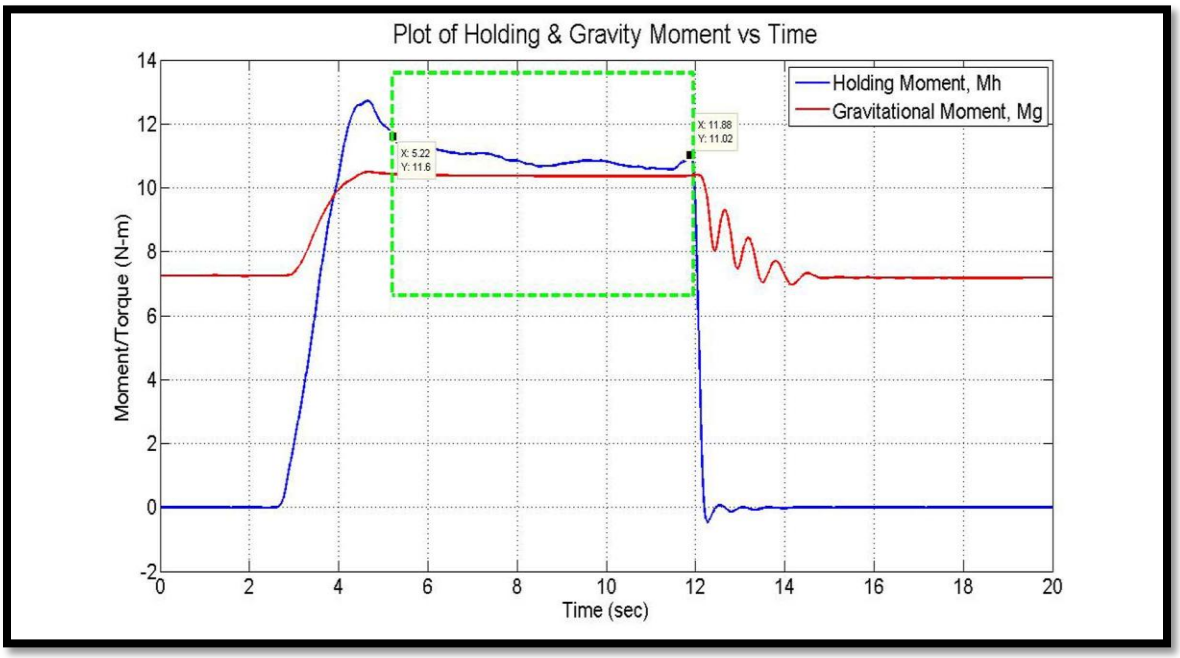

Figure 5.16 Comparison of holding moment, M_h and gravitational moment, M_g for spastic subject

A comparison of the holding moment during the phases of leg movement to the moment due to gravity, the gravitational moment, M_g, is shown in Figure 5.16. Looking at the green-highlighted holding phase of the PKD, as the holding moment decreases, the gravitational moment remains constant. The gravitational moment, M_g, was defined previously in Equation 4.1 as $mgl_c\sin\Theta$. In order for M_g to remain constant, the angle, Θ must remain constant. Figure 5.16 illustrates that although there no change in angle position of the leg during the holding phase of the test, the exits a decrease in the force applied. The value of the holding moment, M_h at the beginning of the constant angle reading in Figure 5.16 is 11.60 N-m and 11.02 N-m at the end of the region. This result was demonstrated consistently within the spastic data. If this result is interpreted within the context of the previous research in stretch reflex threshold, λ, regulation (Levin, 2000; Levin and Feldman, 1994) then it may be concluded that the slow decline of the force on the leg, when the leg is in essence at rest represents the virtual trajectory attempt to overcome its lag behind the actual trajectory. In light of these results and their potential implication a few additional research questions were formed:

1. Can the change in holding moment, in the absence of movement, be shown in subjects without spasticity?
2. Does the movement of Θ_o contribute to a form of active, neurally controlled stiffness that can be modeled?
3. Is it possible to separate this active stiffness from stiffness due solely to intrinsic muscle properties?

In order to facilitate answers to these questions, new experimental protocols was developed and examined with the analysis techniques described previously. These techniques are described in detail in Appendix A.

Consistent with the desire to show that one theory of motor control can explain both the non-spastic and spastic conditions, data from a similar use of the force transducer with non-spastic subjects shows that during period of constant angle after the leg has been pulled to a new angle, M_g remains constant and M_h gradually declines to the value of M_g. As in the spastic case, this change in M_h is attributed to a graduate change of VT to achieve the holding or actual angle.

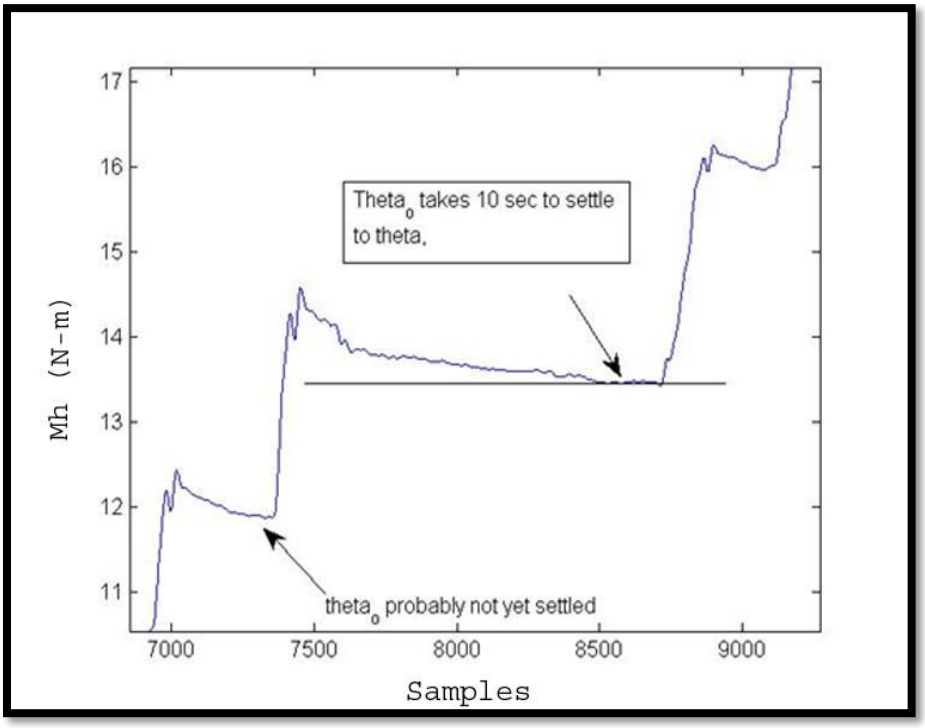

Figure 5.17 Isolated profile view of M_h during period of constant angle position.

CHAPTER 6

CONCLUSIONS

In the introduction of this dissertation a succinct objective was laid forth; to present a novel model and identification methodology of spastic and intrinsic properties of spastic knee joints using multiple pendulum tests for the intuitive assessment of spasticity. Pursuant to that goal three foundation research questions were posed:

1. Can we create experimental measures to develop a model of spasticity that can be interpreted within the framework of a general theory of motor control?
2. Can the underlying motor control framework provide a unique parameter capable of describing both normal and altered/abnormal movement?
3. Can the model be robust enough to explain active as well as passive movement?

The research method outlined in this dissertation takes the novel approach of incorporating the equilibrium point hypothesis into a trajectory-based analysis of pendulum knee motion. The novelty of this approach lies in the utilization of a mathematical sigmoid function in the representation of the virtual trajectory. The choice of a sigmoid function, though seeming to be a more complex curve, actually is composed of simple features which are more in line with the EPH: a delay, straight line VT, with the ability to adjust the starting and ending angles of the sigmoid. The incorporation of the equilibrium point hypothesis in forward model was not only recognition that examination of the entire trajectory of the limb, rather than just the first amplitude of swing, was necessary, but also by doing so, motion of the leg could be described by the simple extraction of three parameters: the relative damping coefficient B_{rel}, relative stiffness coefficient, K_{rel} and the virtual trajectory, Θ_o. The results demonstrate model's

ability to produces parameter values that not only differentiate subjects with spasticity from subjects with no clinical signs of spasticity but that can separate subjects based on severity of spastic condition.

6.1 Research Contributions

The major contribution of this research is the development of an unifying model of motor control that is robust enough to describe both active and passive movements. Previous research efforts utilizing the equilibrium point hypothesis focused on subject-initiated movement, in which the virtual trajectory, defined by the CNS precedes the actual joint movement in time. This research illustrates that in passive movements, the VT lags the actual angle and the degree of this lag is exacerbated in individuals with spasticity.

The novelty of this research is that the pendulum knee test was analyzed a three stage movement pattern of initial slow rise of limb, constant hold at near max extension and finally, release of the limb. While previous research efforts involving pendulum knee drop tests has described these sets of movements in a continuous context, there exist a dearth of research focused on measuring and analyzing the forces and torques acting on the limb through each stage of the test. Incorporation of a force transducer to measure the forces acting on the leg through each phase of movement was recognition of the coupling between the person performing the test, the test subject and its impact of this coupling on the motion of the limb. There exist little discussion of this interaction and its impact on the limb motion, in the literature.

Analysis of the change in force measurements on the limb as it is held in constant position is another novel feature of this research. The holding torque, calculated from measurements of force collected from the force transducer, decreased as the leg was held

at a constant angle. Evident in the data from both spastic and non-spastic subjects, this finding establishes a plausible physical representation of Latash's (1998) theoretical construct, within the equilibrium point hypothesis, of a virtual trajectory that lags the instantaneous actual trajectory. This finding provides validation of the use of a mathematical sigmoid function to represent the virtual trajectory, Θ_o. The ability the experiment protocol to demonstrate a slow exponential-like change in force output when the limb is held in constant position reinforces Levin's (2002) research which theorized that spasticity can be modeled as an inability to regulate the stretch reflex threshold, λ, throughout the entire physiological range.

The utilization of cluster analysis to discern relationships among optimized variables produced from the model is another innovative feature of the research. Cluster analysis aims to sort objects into groups such that there is a maximum degree of similarity between objects belonging to the same group and minimum association to objects in other groups. This research indicates that there is significant potential for cluster analysis based statistical methods applied to model parameters of produced from pendulum knee data to reduce the number of parameters needed to describe movement dynamics. In general, modeling of data tries to strike a balance between accurately reproducing the experimental data while minimizing the number of parameters or variables need to describe the dynamics of a system. The results of the statistical cluster analysis method confirm the hypothesis that pendulum knee data can be characterized with just three parameters: B, K and the grouped parameters described by Θ_o.

6.2 Future Research

This work was primarily two pilot studies. The most important consideration for future work is the expansion of the data sets employed in these analyses. While this research demonstrated the ability to produce significant results with the small sample size, it is hypothesized that with larger data sets, more significant results can be established.

The greatest area for future research lies in the development of experiment protocols and analyses that can produce measures of limb stiffness and damping that are solely due to the intrinsic properties of the muscle and joint. Appendix C details a graphical method of determining the intrinsic or neutral stiffness of the knee based on the knee pull-hold cycle experiment protocol described in appendix A. Further investigation is needed to determine if the intrinsic stiffness of the knee is dependent on its position relative to a neutral equilibrium position as described in Appendix C. The development of measures of intrinsic stiffness and damping allows for future research in the development of an expansive forward model capable of characterizing both active and passive limb motion. An example of this potential forward model is described in Appendix D.

The utilization of cluster analysis in examining the relationship between the parameters optimized by the forward model suggest that there may be a relationship between the stiffness parameter K_{rel}, damping parameter, B_{rel} and the variables defining the sigmoid mathematical equation of virtual trajectory, Θ_o. Cluster analysis would make it possible to develop a research design which seeks to compare, in spasticity treatment for example, model parameter relationships pre and post intervention. Having established a model that can consistently extract measures indicating the level of spasticity, cluster analysis can provide the mechanism to not only compare the unique changes that occur in

individual parameters but also compare the change in the variances among groups of variables. Comparison of the clusters formed by the extracted parameters pre and post intervention can provide insight into how the intervention changes the interaction among the modeled parameters.

APPENDIX A

STUDY TO DETERMINE NEURALLY-CONTROLLED STIFFNESS

Thus far in the research, the equilibrium point hypothesis has been incorporated in the development of a passive model of knee joint. The model is considered passive based largely on the requirement of the limb being relaxed, to achieve the aim of measuring the response to passive stretch of the muscle. Building on this framework of the EPH in describing active movement this final study accomplished two succinct goals. First, the study introduced an experiment protocol to measure the change in measured holding moment at constant held angle positions. Second, this study established an analysis protocol that supports the concept of a lagging virtual trajectory as theorized in the EPH.

This is a five subject pilot study on non-neurologically impaired subjects. The subjects range in age from 22 to 27. The setup for this study is exactly the same as the previous pendulum knee test studies as shown in Figure 4.5. The movement protocol for this test involves three stages: initial passive knee flexion and extension, passive gradual knee extension and hold, and finally, release into pendulum knee drop. The limb was first passively moved from its initial rest position to the "vertical-zero" position. Whereas the trakSTAR provides angle displacement relative to the transmitter, the position of the sensor does not necessary align with the axis for true gravitational zero. A vertical plumb line is used as the visual line of sight for the vertical zero position. Once the first position was reached and held, the knee was passively moved further into flexion incrementally and then incrementally back in extension until the vertical-zero position was again reached as shown in Figure A.1.

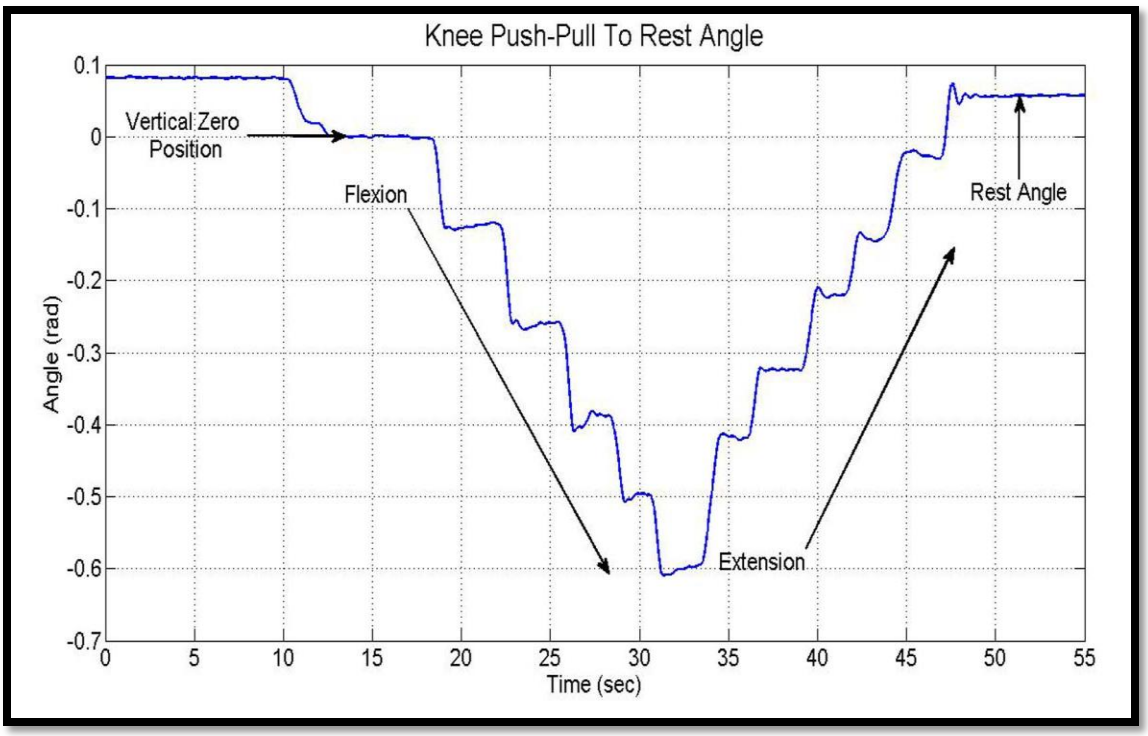

Figure A.1 Knee push-pull trajectory profile

The importance of this technique is that it established a method of determining the rest angle, which is the angle the leg is initially raised from during the pendulum knee test. The fact that the leg is flexed to the vertical zero position and then held approximately five seconds, allowed for identification of the trakStar position output to be acquired at that point of initial holding. The position data can then be adjusted by the value at the held position to produce the vertical zero position shown in the above figure. At the end of the extension move and hold cycle, near the vertical zero position the leg is released for several seconds and allowed to return to its initial position. It would normally be expected that the knee would return to the exact same initial angle before the beginning of the movements in flexion. However as shown in Figure 5.11, the “Rest Angle” position is slightly lower than the initial angle at the start of the movement, which can be explained as simply hysteresis within the muscle.

From the rest angle position after a few seconds of release, the leg is slowly lifted then held in position at 0.2 radians increments. At each increment the string used to raise the leg is clamped in position to a tripod. Once near max extension position is reached and after being held in that position for several seconds, the string is cut allowing the leg to oscillate freely. Once the leg stops oscillating, the leg is raised incrementally lower heights and released three more times. Position and force data are again collected from trakSTAR & Mini40 transducer respectively. The analysis of region one was aimed at graphically finding the rest angle, Θ_r, shown in Figure A.1. Analysis of region two of the data is used to ultimately graphically extract parameters that can be later applied to a new equation of motion capable of not only describing the pendulum knee data in region three of Figure, A.2, but all of the motion in general.

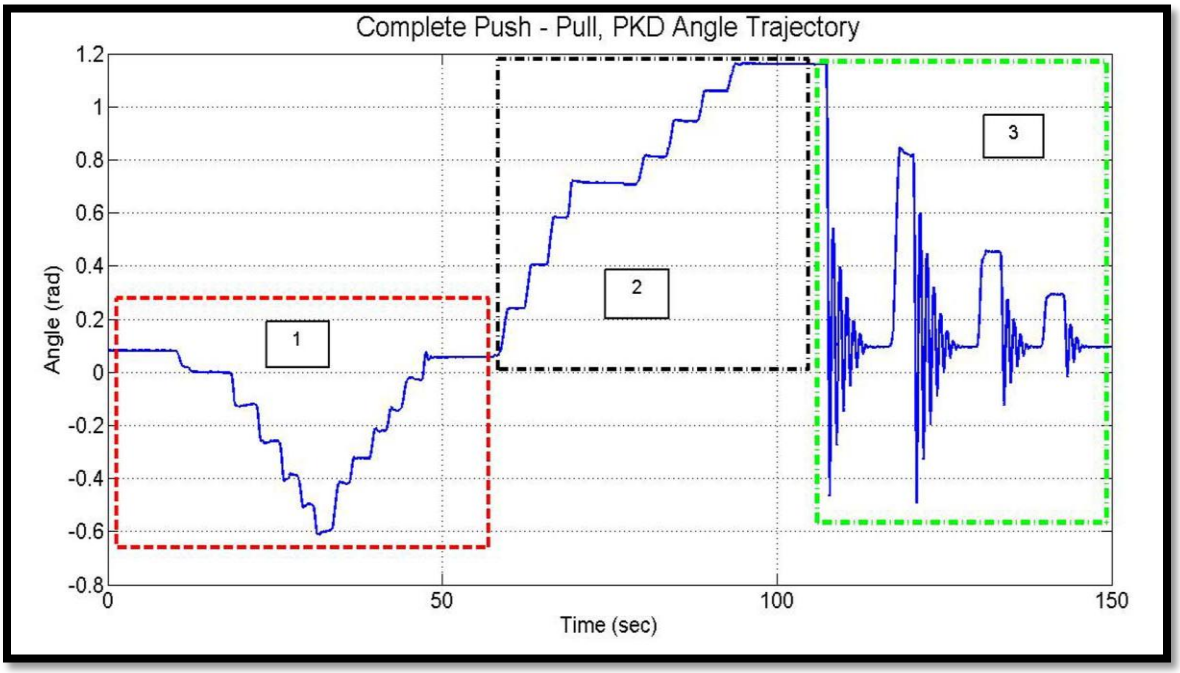

Figure A.2 Complete push-pull pkd angle displacement profile.

APPENDIX B

MODELING OF THREE STAGE DATA

Analysis of the data collected originates through the expansion of the equations of motion used previously in the pendulum knee test. The new equation becomes:

$$I\ddot{\Theta} + B\left(\dot{\Theta} - \dot{\Theta}_o\right) + K_a(\Theta - \Theta_o) + K_n(\Theta - \Theta_n) + M_h = mgl_c\sin\Theta \qquad (B.1)$$

Equation B.1 retains the same feature of previous equations in terms of the moment of inertia, I, damping coefficient, B, holding moment, M_h and the gravitational moment term, $mgl_c\sin\Theta$. Two new concepts are introduced by this equation. K_a, represents an active stiffness coefficient. This was previous modeled as just K in the previous equations and represents the proposition that the virtual trajectory, Θ_o represents a form of active neurally controlled stiffness.

K_n in Equation B.1 represents the component of stiffness that is due to intrinsic properties of the muscle and joint space. It is being called "neutral stiffness" because it being calculated using a muscle spring-model concept where changes the stiffness gain is due to the difference between the actual length or angle of the muscle and the muscle neutral position, Θ_n. Muscle neutral position is based on the concept of neutral body posture which is the been characterized in research by NASA as the body's preferred posture, similar to the free floating posture experienced when you totally relax in a swimming pool, or the posture typically associated with astronauts floating in space (G. Andreoni et al., 2000). In Appendix C, a graphical analysis procedure is introduced

describing the calculation of the neutral stiffness, K_n and neutral angle, Θ_n. Appendix D details the application of Equation B.1 to the pendulum knee data shown in region three in Figure A.2.

Figure B.1 shows a section of zoomed image showing one cycle of pulling to and then holding at that angle. While angle is not explicitly shown, we can assume that the angle is constant from B to C since $Mg=mgl_c\sin\Theta$ is constant between B and C. Applying Equation B.1 to the section of the plots of M_g and M_h between points B and C in the figure, after point B, since $\Theta$is held constant, $\ddot{\Theta}$ and $\dot{\Theta}$ = 0. Equation B.1 can then be rewritten to become:

$$M_h = M_g + M_n + M_a \tag{B.2}$$

where M_g is the gravitational moment, $mgl_c\sin\Theta$, M_n is the neutral stiffness moment defined in Equation B.1 as $K_n(\Theta - \Theta_n)$, and Ma is active stiffness moment, $K_a(\Theta - \Theta_a)$.

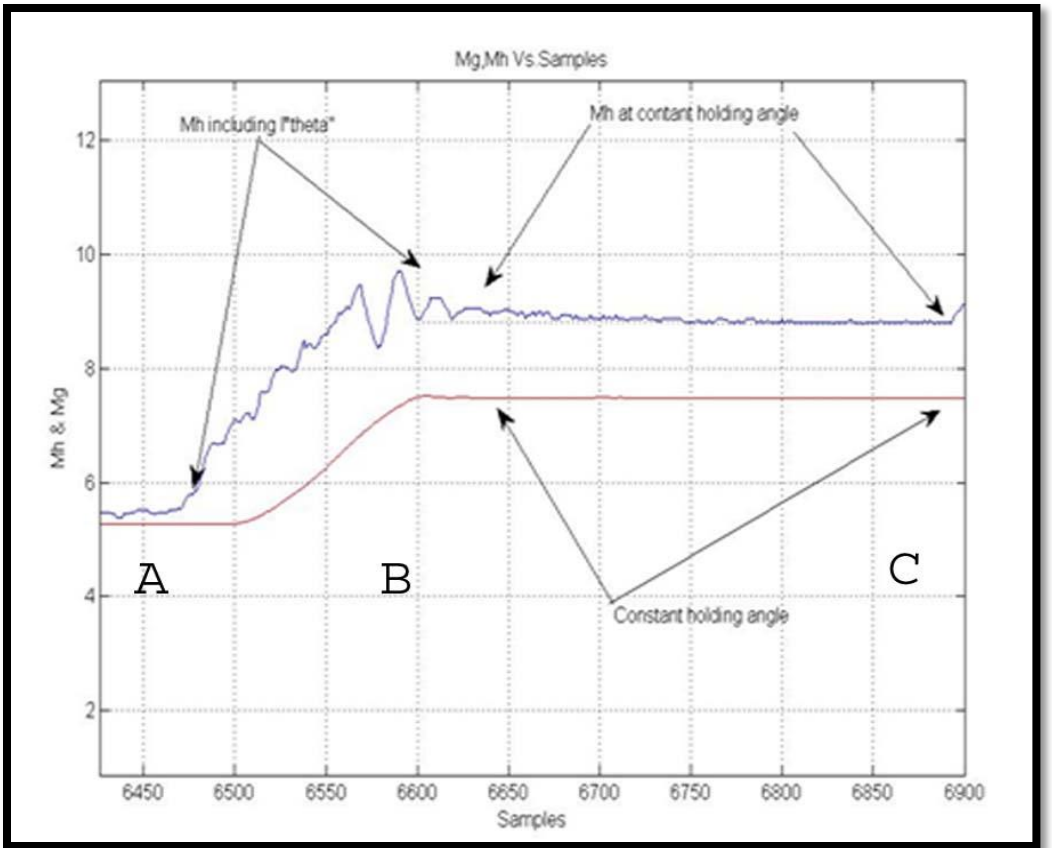

Figure B.1 Holding moment, M_h and gravitational moment M_g for a section of pull and hold.

During the period when the leg is being held, the subject is theoretically relaxed, as that is the primary condition needed for execution of the pendulum knee test. If the subject is relaxed and there is no movement of the limb, then no active stiffness, K_a, should be present because Θ_o, which represents the virtual trajectory, should be equal to Θ at this point. However, if we look carefully at the Figure B.1, we can see that between B and C, M_h slowly changes value, with an exponential-like drift toward a constant value. As M_h changes in this region, M_g is constant. This pattern is repeated at every pull to an angle then hold cycle as shown in Figures B.2 and earlier in chapter five, Figure 5.17.

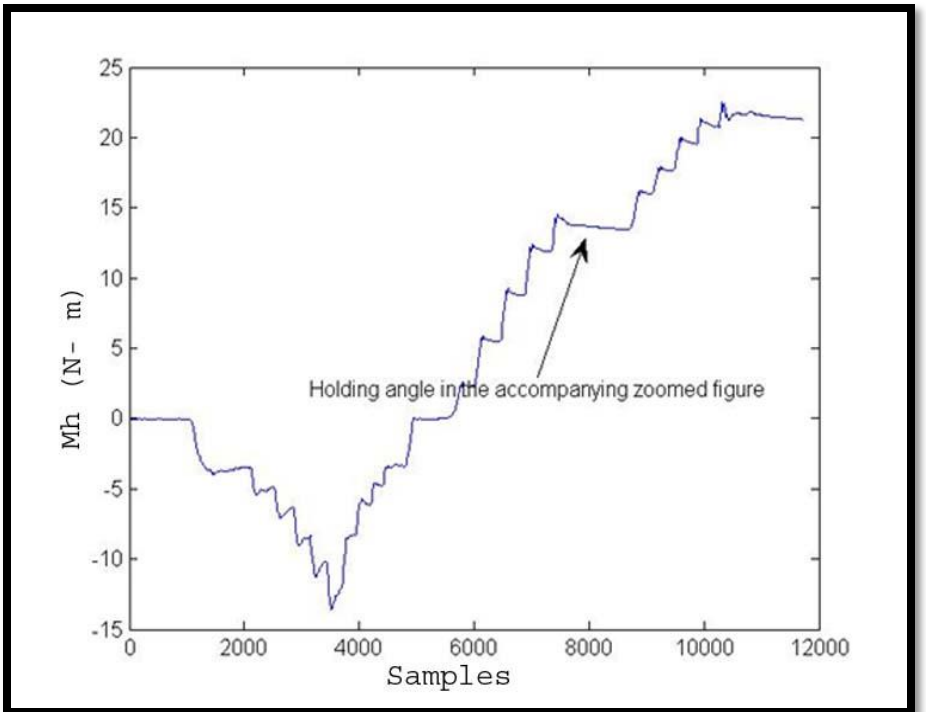

Figure B.2 Holding moment profile before pkd with one section profiled.

Since Θ is constant, $M_n = (\Theta - \Theta_o)$ must also be constant since Θ_n is the neutral angle of the knee, a constant value. The only way that M_h can change is if the virtual trajectory Θ_o changes since all the other terms in Equation B.2 depend on a constant Θ Therefore, in this state of relaxed non-movement of the leg, we have evidence that there is a slight lag in Θ_o as it follows Θ. This validates the theory originally proposed in the analysis spastic subject data, that when the leg drops in the PKD test, in both non-spastic and spastic subjects, Θ_o lags Θ to produce an active moment. This substantiates the use of the sigmoid for the trajectory of Θ.

APPENDIX C

COMPUTATION OF NEUTRAL ANGLE AND NEUTRAL STIFFNESS

Referring back to appendix B, Figure B.1, analyzing the data between points B and C, it has now been established that in terms of Equation B.1, $I\ddot{\Theta} = 0$, $B\dot{\Theta} = 0$, M_g is known, but M_n and M_a are combined. In the previous section, it was shown that when the leg is held constant, Θ_o exponentially declines towards Θ. This demonstrates that the active stiffness torque $Ma = Ka(\Theta - \Theta_o)$, declines towards zero because at point C, $\Theta_o = \Theta$. Therefore at point C:

$$M_n(C) = M_h - M_g \tag{C.1}$$

Figure C.1 shows a zoomed in section of plot of the holding moment, M_h, gravity moment, M_g and their difference (M_h-M_g) vs. angle, Θ. The key feature of this graph is the clusters of data points occurring at the holding angles. These clusters appear in M_h and (M_h-M_g). Given that while the leg is held at a constant angle, Θ_o approaches Θ, using Equation A.1, it can reasonably be assumed that the lowest value of these clusters in (M_h-M_g) is equal to M_n for that holding angle. Using this, we can graphically determine approximate values for K_n and Θ_n. Looking at a zoomed in image of Figure C.1, Referring two lines can be drawn, as shown in Figure C.2. The first line connects the values of M_h-M_g at points C. Having established that at point C, M_h-M_g=M_n, it can be concluded that this line connecting M_h-M_g interpolates M_n for all possible holding angles. From this, we can determine the angle at which M_n=0. This is Θ_n.

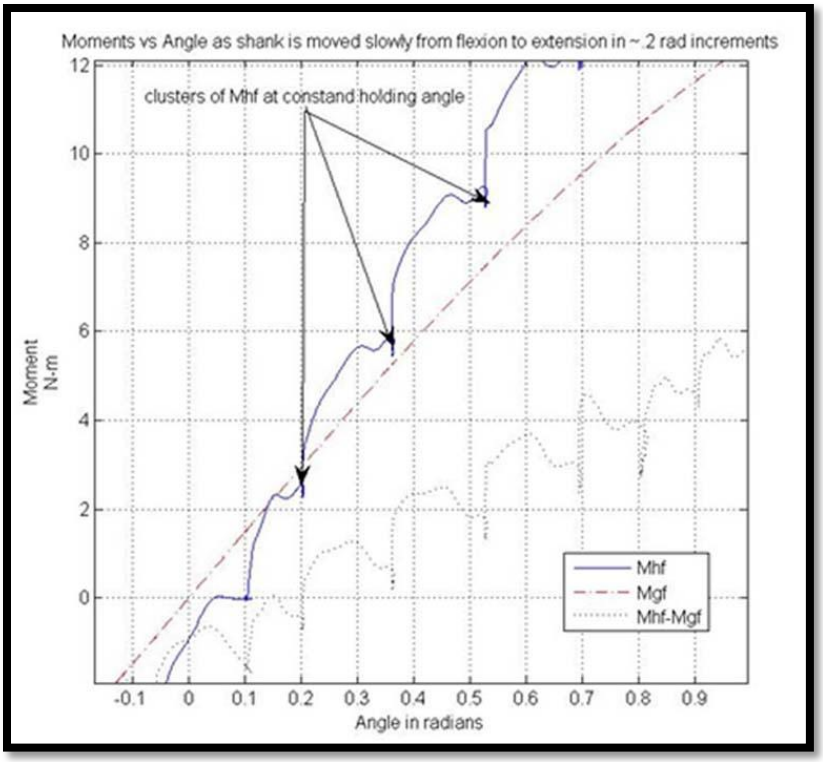

Figure C.1 Moments plotted vs. angle during pull and hold cycles.

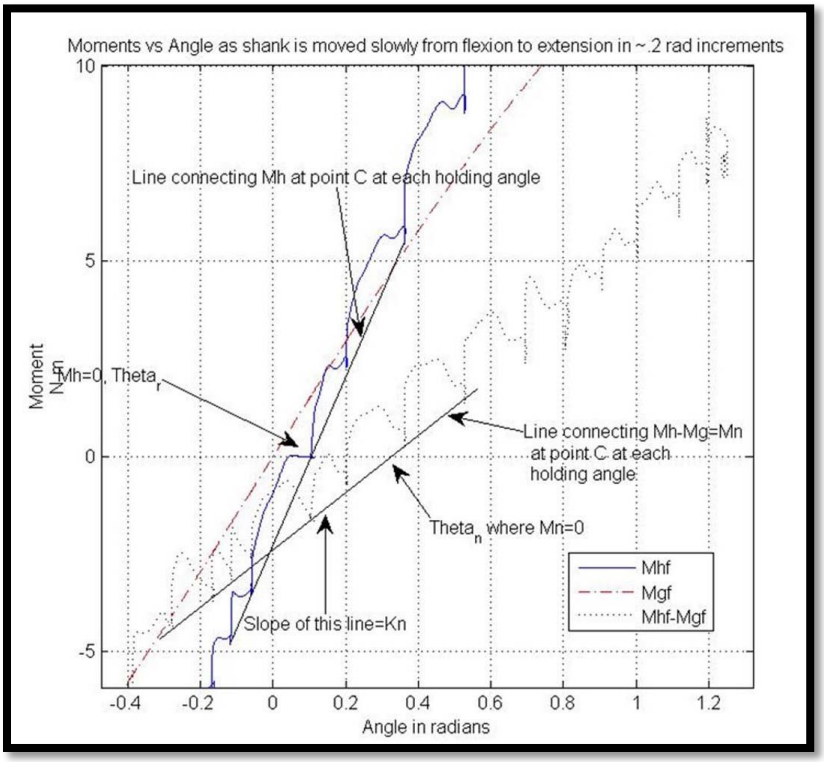

Figure C.2 Graphical calculations Θ_n, K_n and Θ_r

The slope of line connecting M_h-M_g = K_n. Similarly, the second line passes through M_h at all points C. It represents the interpolated M_h for all possible holding angles. The angle at which M_h=0 is Θ_r and this value should confirm the rest angle found in the analysis outlined in section 5.4.1. Table C.1 provides a breakdown of the values for neutral stiffness coefficient, K_n and neutral angle, Θ_n for the five subjects in this experiment protocol. Also calculated were the ratios of neutral stiffness to limb mass and moment of inertia, I respectively.

The determination of the rest angle, Θ_r, the knee neutral angle, Θ_n, and the knee neutral stiffness coefficient, K_n, can now be utilized in Equation B.1 to analyze the movement trajectory of the multiple pendulum knee drops originally shown in region three of Figure, A.2. Using the optimization techniques outlined in the previous chapter, the pendulum knee data can be modeled using Equation 5.1 to extract the parameters of active stiffness coefficient, K_a and the damping parameter, B.

Table C.1 Calculations of neutral stiffness, K_n and neutral angle, Θ_n.

Subject	**Limb Mass, m (kg)**	**Moment of Inertia, I**	**K_n (N-m)**	**K_n/m**	**K_n/I**	**□$_n$ (rad)**
1	3.93	0.38	4.67	1.19	12.29	0.21
2	2.71	0.21	2.11	0.78	10.05	0.22
3	6.10	0. 70	1.12	0.18	1.6	0.47
4	5.67	0.59	7.61	1.34	12.90	0.31
5	5.11	0.49	1.62	0.31	3.33	0.48

APPENDIX D

ACTIVE AND NEUTRAL STIFFNESS MODEL OF PENDULUM KNEE DATA

A new feedback model was created in Simulink utilizing the equations of motion outlined in Equation B.1. As shown active stiffness K_a, shown in green, replaces the lumped relative stiffness, K_{rel} from the previous model outlined in earlier chapters. The active damping parameter, B_a is equivalent to the relative damping parameter, B_{rel} modeled previously.

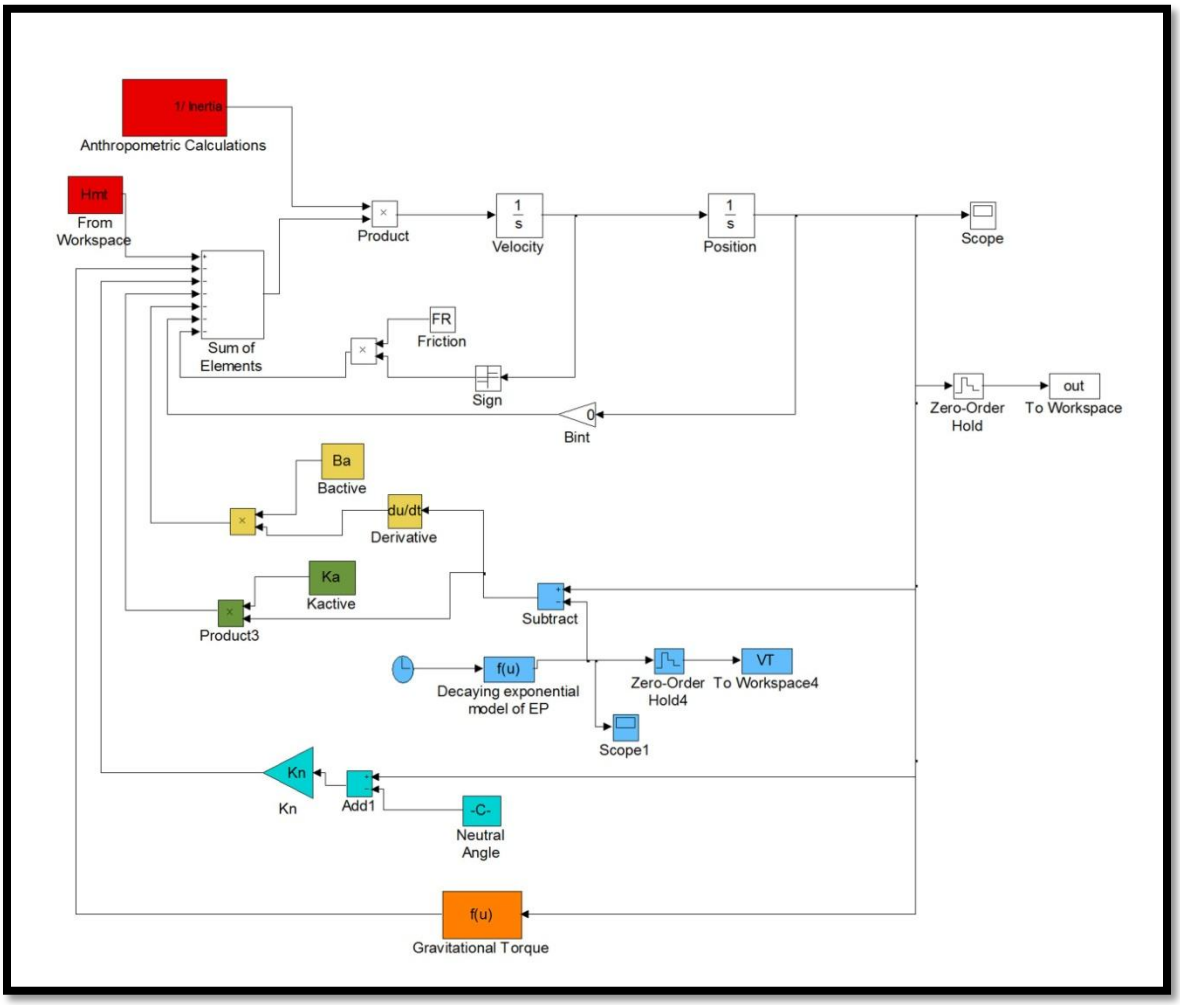

Figure D.1 Forward model to optimize parameters, K_a, B_a and virtual trajectory, Θ_o.

Utilizing the same Levenberg-Marquardt method based gradient-descent optimization program described in the previous chapter, the pendulum knee drop portion of data was modeled producing the optimized parameters, active stiffness, K_a, active damping, B_a and the parameters defining the virtual trajectory Θ_o as defined by Equation 4.4, in chapter 4 previously. During the third region of data, as shown in Figure A.2 from chapter five, each subject underwent between three and four pendulum knee drops. Each pendulum drop for each subject was molded separately. Figure D.2 shows a representative sample of the model output for subject 5.

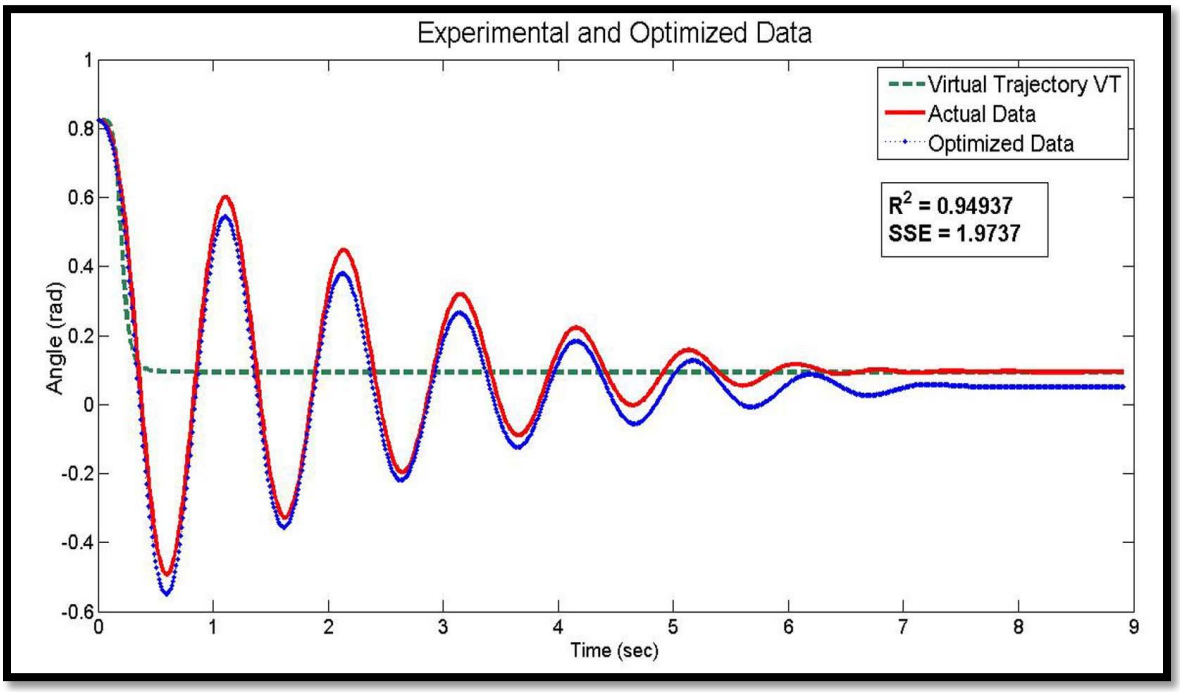

Figure D.2 Subject 5 forward model data compared with experimental data.

Table D.1 Model average output parameters of first PKD for all five subjects.

Subject	B_a	K_a	Θ_o Variables			R^2	SSE
			Tp	n	k		
1	0.4489	0.0053	1.2547	4.0309	0.2680	0.9364	4.5498
2	0.1843	0.0010	1.2953	4.7552	0.3517	0.8605	12.1782
3	0.9523	5.8594	1.2762	3.1648	0.1124	0.9265	3.8922
4	0.9915	2.6955	1.2507	2.8061	0.3197	0.8218	7.3772
5	0.7043	7.2700	1.2143	3.4291	0.3120	0.9094	3.5821

Table D.1 displays the optimized parameter values for all five subjects in their first pendulum knee drop. This data reflects the initial pendulum knee drop after the limb was held and suspended at near max extension for several seconds before being released. The data reveals several important results. First, there is a general consistency with subjects in the optimized parameters that define the sigmoid virtual trajectory, Θ_o. Having previously established the existence of a virtual trajectory that lags the actual trajectory in all movement, combined with the theory articulated by Levin (2008) that people without spasticity have the ability to move the stretch reflex threshold, λ, throughout the entire physiological range, this consistency in Θ_o among the subjects would be expected.

The distinguishing feature that separates the model created from Equation B.1 from the previous model created by Equation 4.3 used in the previous pendulum knee drop analysis is the torque due to stiffness. In Equation 4.3 the stiffness coefficient K, was modeled as a lumped stiffness that represented the stiffness of the system. As

outlined earlier this has been the standard modeling of the system that occurs during pendulum knee motion (Badj, Bowman and Vodovnik ,1984; Lin and Rymer, 1991). The accuracy of the model created from Equation 4.1 shows that all of the system stiffness is accounted for in this lumped K parameter. This then provides the framework for utilizing Equation 5.1 which sought to separate this lumped stiffness parameter into two stiffness parameters, active stiffness K_a and neutral stiffness K_n. The torque produced by the lumped stiffness parameter, K of Equation 4.1 is $K(\Theta - \Theta_o)$. Thus from a system perspective the Equation B.1 necessitates that:

$$K_a(\Theta - \Theta_o) + K_n(\Theta - \Theta_n) = K(\Theta - \Theta_o) \qquad (D.1)$$

The results suggest that the calculated sum of the active stiffness torque and the neutral stiffness torque is larger than the torque that would be calculated for the system under the lumped stiffness parameter, K. Given that the torque due to active stiffness, Ka replicates the relative stiffness torque $K(\Theta - \Theta_o)$ from the previous model of Equation 4.1, the increase in overall system stiffness calculated in this new model must be attributed to the neutral stiffness torque, $K_n(\Theta - \Theta_n)$. The neutral stiffness coefficient, K_n ranged from 1.12 N-m to 7.61 N-m. In the previous section, a method for graphically calculating K_n was introduced which was rooted in the application of Equation A.1 in each section of constant angular position. When the leg is held at a constant angle as shown in Figure B.1, the holding moment, M_h slowly changes value, with an exponential-like drift toward a constant value. The impact of this is that the values of the difference between the holding moment and gravitational moment (M_h - M_g), at all points C, as shown in Figures C.1 and C.2, may not actually be equal to the neutral stiffness moment,

M_n because the clusters in (M_h-M_g) have not yet reached their lowest values. There is still have a non-zero ($\Theta - \Theta_o$) as Θ_o may not have completely settled. This would have the effect of producing values of (M_h-M_g) that are slightly higher than they should be, resulting in a slightly higher K_n. This suggest that a closer examination of the time constant of the decline in the holding moment toward a constant value needs to be examined and incorporated into the calculation of the neutral stiffness coefficient, K_n.

The coefficient of determination, r^2 for the five subjects ranged from an average value of 0.82 to 0.94, demonstrating the model's ability to accurately reproduce pendulum trajectory data relative to the experimental data, even with higher than expected values for the neutral stiffness coefficient. The final model put forth in the section demonstrates the ability to expand beyond simply describing motion characterizing the pendulum knee test. The graphical techniques illustrated in this chapter introduce an approach to model all movements.

REFERENCES

Allison, S.C., Abraham L.D. & Petersen C.L. (1996). Reliability of the Modified Ashworth Scale in the assessment of plantarflexor muscle spasticity in patients with traumatic brain injury. *International Journal of Rehabilitation Research, 19(1)*, 67-78.

Ascension Technology Corporation Official Website (2009). *3D trakSTAR® Model for Short and Medium Range Applications.* Retrieved July 14, 2011, from http:// www.ascension-tech.com/medical/pdf/TrakStarSpecSheet.pdf.

Awaad, Y, Tayem H., Munoz S., Ham S. & Michon A.M. (2003). Functional Assessment Following Intrathecal Baclofen Therapy in Children With Spastic Cerebral Palsy. *Journal of Child Neurology, 18(1)*, 26-34.

Bajd, T. & Vodovnik, L. (1984). Pendulum testing of spasticity. *Journal of Biomedical Engineering, 6(1)*, 9-16.

Becher ,J.G., Harlaar, J., Lankhorst, G.J., & Vogelaar T.W. (1998). Measurement of impaired muscle function of the gastrocnemius, soleus, and tibialis anterior muscles in spastic hemiplegia: A preliminary study. *Journal of Rehabilitation Research and Developmemt, 35(3)*, 314-326.

Bizzi, E., Accornero, N., Chapple, W. & Hogan, N. (1984). Posture control and trajectory formation during arm movement. *Journal of Neuroscience, 4(11*), 2738-44.

Blackburn, M., van Vliet, P. & Mockett, S.P. (2002). Reliability of measurements obtained with the Modified Ashworth Scale in the lower extremities of people with stroke. *Physical Therapy, 82(1)*, 25-34.

Bellomo, A. & Inbar G. (1997). Examination of the λ equilibrium point hypothesis when applied to single degree of freedom movements performed with different inertial loads. *Biological Cybernetics,76(1)*, 63-72.

Bohannon, R.W. & Smith M.B. (1987). Interrater reliability of a Modified Ashworth Scale of Muscle Spasticity. *Physical Therapy, 67(2)*, 206-207.

Boyd, R.N., Barwood, S.A., Ballieu, C. & Graham, H.K. (1998). Validity of a clinical measure of spasticity in children with cerebral palsy in a randomized clinical trial. *Developmental Medicine & Child Neurology, 40(Suppl. 78)*, 7.

Boyd, R.N., Graham H.K. (1999). Objective measurement of clinical findings in the use of botulinum toxin type A for the management of children with CP. *European Journal of Neurology, 6(Suppl. 4)*, S23-S35.

Boyd , R.N. & Ada, L. (2001). Physiotherapy management of spasticity. In M.P. Barnes and G.R. Johnson (Eds.), *Upper Motor Neuron Syndrome and Spasticity: Clinical management and neurophysiology* (pp 96-121). Cambridge: Cambridge University Press.

Brown, R.A., Lawson, D.A., Leslie, G.C. & Part, N.J. (1988). Observations on the applicability of the Wartenberg pendulum test to healthy elderly subjects. *Journal of Neurology, Neurosurgery, and Psychiatry, 51(9),* 1171-1177.

Campbell, S.K., Almeida, G.L., Penn, R.D. & Corcos, D.M. (1995). The effects of intrathecally administered baclofen on function in patients with spasticity. *Physical Therapy, 75(5),* 352-362.

Chen, K., Foulds, R.A., Adamovich, S.V. & Swift, K. (2009). Experimental Study and Modeling of Equilibrium Point Trajectory Control in Single and Double Joint Arm Movement. Proceedingds from IMECE2009: *ASME International Mechanical Engineering Congress and Exposition*, 2, 355-359. doi:10.1115/IMECE2009-10251

Chen, K. & Foulds R.A. (2010). The Mechanics of Upper Limb Posture and Movement Control. *ASME International Mechanical Engineering Congress and Exposition*, November 12 - 18, 2010. Vancouver, British Columbia Canada. IMECE2010-37201.

Cheney, P.D. (1997). Pathophysiology of the corticospinal system and basal ganglia in cerebral palsy. *Mental Retardation and Developmental Disabilities Research Reviews, 3(2),* 153-167.

Chin, T.P., Duncan, J.A., Johnstone, B.R. & Graham, H.K. (2005). Management of the upper limb in cerebral palsy. *Journal of Pediatric Orthopaedics B, 14(6),* 389-404.

Coffey, R.J, Cahill, D, Steers, W, Park, T.S, Ordia, J., Meythaler, J., …Leibrock, L.G. (1993). Intrathecal baclofen for intractable spasticity of spinal origin: results of a long-term multicenter study. *Journal of Neurosurgery. 78(2),* 226-232.

Corry, I.S, Cosgrove, A.P., Walsh, E.G., McClean, D., & Graham, H.K. (1997). Botulinum toxin A in the hemiplegic upper limb: a double blind trial. *Developmental Medicine & Child Neurology 39(3),* 185-193.

de Lussanet, M.H.E., Smeets, J.B.J. & Brenner, E. (2002). Relative damping improves linear mass-spring models of goal-directed movements. *Human Movement Science, 21(1),* 85-100.

Dimitrijevic, M.R. (1995). Evaluation and Treatment of Spasticity. *Journal of Neurorehabilitation and Neural Repair. 9(2),* 97-110.

Elovic, E.P., Simone, L.K. & Zafonte, R. (2004). Outcome Assessment for Spasticity Management in the Patient with Traumatic Brain Injury. *Journal of Head Trauma Rehabilitation, 19(2),* 155-177.

Fee, J.W. & Samworth, K.T. (1995) Passive leg motion changes in cerebral palsied children after whole body vertical acceleration. *IEEE Transactions Rehabilitation Engineering, 3(2),* 228 -232.

Fee, J.W. & Miller, F. (2004). The Leg Drop Pendulum Test performed under general anesthesia in spastic cerebral palsy. *Developmental Medicine and Child Neurology, 46(4),* 273-281

Fee, J.W. & Foulds, R.A. (2004). Neuromuscular Modeling of Spasticity in Cerebral Palsy. *IEEE Transactions on Neural Systems and Rehabilitation, 12(1),* 55-64.

Feldman, A.G., Adamovich, S.V., Ostry, D.J. & Flanagan J.R. (1990). The origin of electromyograms - Explanations based on the equilibrium point hypothesis. In J.M. Winters & S.L.Y. Woo (Eds.), *Multiple Muscle Systems: Biomechanics and Movement Organization.* NewYork, NY: Spinger-Verlag.

Feldman, A.G., Adamovich, S.V. & Levin, M.F. (1995). The relationship between control, kinematic and electromyographic variables in fast single-joint movements in humans. *Experimental Brain Research, 103(3),* 440-450.

Feldman, A.G. & Latash, M. (2005). Testing hypotheses and the advancement of science: recent attempts to falsify the equilibrium point hypothesis. Experimental *Brain Research, 161(1),* 91-103.

Flanagan, J.R., Ostry, D.J. & Feldman, A.G. (1993). Control of Trajectory Modifications in Target-Directed Reaching. *Journal of Motor Behavior, 25(3),* 140-152.

Flash, T. (1987). The Control of Hand Equilibrium Trajectories in Multi-Joint Arm Movements. *Biological Cybernetics, 57(4-5),* 257-274

Fowler ,E.G., Nwigwe, A.I. & Ho, T.W. (2000). Sensitivity of the pendulum test for assessing spasticity in persons with cerebral palsy. *Developmental Medicine and Child Neurology, 42(3),* 182-189.

Fryer, G., Lamonte, R.J. & Simons, D.G. (1972). An electronically controlled automatic reflex hammer. *Medical and Biological Engineering, 10(1),* 125-129.

Gomi, H. & Kawato, M. (1996). Equilibrium-Point Control Hypothesis Examined by Measured Arm Stiffness During Multijoint *Movement. Science 272 (5258),* 117-120.

Good, D.C. Measurement of Spasticity. (2002). In D.A. Gelber & D.R. Jeffery (Eds.), *Clinical Evaluation and Management of Spasticity* (pp 27-44). Totowa, NJ: Humana Press.

Grace, A. (1990). *Optimization Toolbox for Use With MATLAB*. Natick, MA: Mathworks.

Gracies ,J.M., Marosszeky, J.E., Renton, R., Sandanam, J., Gandevia, S.C. & Burke, D. (2000). Short-term effects of dynamic Lycra splints on upper limb in hemiplegic patients. *Archives of Physical Medicine and Rehabilitation, 81(12),* 1547-55.

Graham, H.K. (2000). Pendulum test in cerebral palsy. *The Lancet, 355(9222),* 2184.

Graham, H.K. & Selber, P. (2003). Musculoskeletal aspects of cerebral palsy. *Journal of Bone and Joint Surgery-British, 85-B(2),* 157-66.

Grimm, R J. (1983). Program disorders of movement. *Advances in Neurology, 39,* 1-11.

Haas, B.M., Bergstrom, E., Jamous, A. & Bennie, A. (1996). The inter-rater reliability of the original and of the Modified Ashworth Scale for the assessment of spasticity with spinal cord injury. *Spinal Cord, 34,* 560-564.

He, J., Norling, W.R. &Wang, Y. (1997). A Dynamic Neuromuscular Model for Describing the Pendulum Test of Spasticity. *IEEE Transactions on Biomedical Engineering, 44(3),* 175-183.

He, J. (1998). Stretch reflex sensitivity: effects of postural and muscle length changes. *IEEE Transactions on Rehabilitation Engineering, 6(2),* 182-189.

Higashi, T., Funase, K., Kusano, K., Tabira, T., Harada, N., Sakakibara, A. & Yoshimura, T. (2001). Motorneuron pool excitability of hemiplegic patients: assessing recovery stages by using H-reflex and M responses. *Archives of Physical Medicine and Rehabilitation, 82(11),* 1604-1610.

Hogan, N. (1984). An organizing principle for a class of voluntary movements. *The Journal of Neuroscience, 4(11),* 2745-2754.

Hogan, N (1985). The mechanics of multi-joint posture and movement. *Biological Cybernetics, 52(5),* 315-331.

Howard ,J., Soo, B., Graham, H.K., Boyd, R.N., Reid, S., Lanigan, A., … Reddihough, D.S. (2005). Cerebral palsy in Victoria: motor types, topography and gross motor function. *Journal of Paediatrics and Child Health, 41(9-10),* 479-483.

Johnson, G.R. (2001). Measurement of Spasticity. In M..P. Barnes and G.R. Johnson (Eds.), *Upper Motor Neuron Syndrome and Spasticity: Clinical management and neurophysiology* (pp.79-95). Cambridge: University Press.

Johnson, G.R. (2002). Outcome measures of spasticity. *European Journal of Neurology, 9 (Suppl. 1),* 10-16

Kaeser, H.E., Gihring, H., Bergmann, R., Gfhring, I., Wachter, K.C. & Ettlin, T.M. (1998). Testing an antispasticity drug (Tetrazepam) with the pendulum test: a monocentric pilot study. *Journal of Neurorehabilitation and Neural Repair, 12(4),* 169-177.

Kellermayer, M.S.Z., Bianco, P., Mártonfalvi, Z., Nagy, A., Kengyel, A., Szatmári, D., … Lombardi, V. (2008). Muscle Thixotropy: More than Just Cross-Bridges? Response to Comment by Campbell and Lakie. *Biophysical Journal, 94(1),* 329-330.

Koman, L.A, Smith, B.P. & Shilt, J.S. (2004). Cerebral palsy. *Lancet, 363,* 1619-1631.

Krause, P., Edrich, T. & Straube, A. (2004). Lumbar repetitive magnetic stimulation reduces spastic tone increase of the lower limbs. *Spinal Cord 42,* 67-72.

Lance, J. (1980). Pathology of spasticity and clinical experience with Baclofen, In J. Lance, R. Feldman, R. Young, W. Koella (Eds.), *Spasticity:Disordered motor control* (pp. 185-204). Chicago: Yearbook.

Latash, M.L. & Gottlieb, G.L. (1991). Reconstruction of shifting elbow joint compliant characteristics during fast and slow movements. *Neuroscience, 43(2-3),* 697-712.

Latash, M.L. (1992). Virtual trajectories, joint stiffness, and changes in the limb natural frequency during single-joint oscillatory movements. *Neuroscience, 49(1),* 209-20.

Latash, M.L. (1998). *Neurophysiological Basis of Movement*. Champaign, IL: Human Kinetics.

Leonard, C.T. (1998). *The Neuroscience of Human Movement* (pp. 203-236). St. Louis, MO: Mosby.

Leslie, G.C., Muir, C., Part, N.J., Roberts, R.C. (1992). A comparison of the assessment of spasticity by the Wartenberg Pendulum test and the Ashworth grading scale in patients with multiple sclerosis. *Clinical Rehabilitation, 6(1),* 41-48.

Levin, M.F. (2000). Sensorimotor deficits in patients with central nervous system lesions: Explanations based on the λ model of motor control. *Human Movement Science, 19(1),* 107-137.

Levin M.F. (2005). On the nature and measurement of spasticity. *Clinical Neurophysiology, 116(8),* 1754-1755.

Levin M.F., Feldman, A.G., Milner, T.E., & Lamarre, Y. (1992). Reciprocal and coactivation commands for fast wrist movements. *Experimental Brain Research, 89(3),* 669-677.

Levin MF and Feldman AG. (1994). The role of stretch reflex threshold regulation in normal and impaired motor control. *Brain Research, 657(1-2),* 23-30.

Levin MF, Selles RW, Verheul MH & Meijer OG. (2000). Deficits in the coordination of agonist and antagonist muscles in stroke patients: implications for normal motor control. *Brain Research, 853(2),* 352-369.

Little, J.W. & Massagli, T.L. (1993). Spasticity and associated abnormalities of muscle tone. In: J.A. Delisa (Ed.). *Rehabilitation Medicine: Principles and Practice* (2nd ed., pp 666-680). Philadelphia, PA: JB Lippincott Company.

Martini, F., Ober, W.C., Garrison, C.W., Welch, K. & Hutchings, R.T. (2001). *Fundamentals of Anatomy and Physiology* (5th ed.). Prentice Hall College Div.

Mayer, N.H. (1997). Spasticity and Stretch Reflex. *Muscle and Nerve, 20(Suppl 6),* S1-S13.

McClelland III, S., Teng, Q., Benson, L.S. & Boulis ,N.M. (2007). Motor neuron inhibition–based gene therapy for spasticity. *American Journal of Physical Medicine & Rehabilitation, 86(5),* 412-421.

Murphy, N. & Such-Neibar, T. (2003). Cerebral palsy diagnosis and management: the state of the art. *Current Problems in Pediatric and Adolescent Health Care, 33(5),* 146-169.

Pandyan, A.D., Johnson, G.R., Price, C.I.M., Curless, R.H., Barnes, M.P. & Rodgers, H. (1999). A review of the properties and limitations of the Ashworth & modified Ashworth scales as measures of spasticity. *Clinical Rehabilitation, 13(5),* 373-383.

Powers ,R,K., Campbell, D.L. & Rymer, W.Z. (1989). Stretch reflex dynamics in spastic elbow flexor muscles. *Annals of Neurology, 25(1),* 32-42.

Rémy-Néris, O., Tiffreau, V., Bouilland, S. & Bussel, B. (2003). Intrathecal baclofen in subjects with spastic hemiplegia: assessment of the antispastic effect during gait. *Archives of Physical Medicine and Rehabilitation, 84(5),* 643-50.

Rosenbaum P. (2003). Cerebral palsy: what parents and doctors want to know. *British Medical Journal, 326,* 970-974.

Rothwell, J.C. (1994). *Control of Human Voluntary Movement* (2nd ed.). London: Chapman & Hall.

Schmit, B.D. & Gaebler-Spira, D. (2004). Mechanical measurements of the effects of intrathecal baclofen dosage adjustments in patients with cerebral palsy: A pilot study. *American Journal of Physical Medicine & Rehabilitation, 83(1),* 33-41.

Schweighofer, N., Arbib, M.A. & Kawato, M. (1998). Role of the cerebellum in reaching movements in humans. I. Distributed inverse dynamics control. *European Journal of Neuroscience, 10(1),* 86-94.

Sheean, G. (2002). The pathophysiology of spasticity. *European Journal of Neurology, 9(suppl 1),* 3-9.

Simons, D.G. & Mense, S. (1998). Understanding and measurement of muscle tone as related to clinical muscle pain. *Pain, 75(1),* 1-17.

Suzuki,M. & Yamazaki, Y. (2005). Velocity-based planning of rapid elbow movement expands the control scheme of equilibrium point hypothesis. *Journal of Computational Neuroscience, 18(2),* 131-149.

Vodovnik, L., Bowman, B.R., & Badj T. (1984). Dynamics of spastic knee joint. *Medical and Biological Engineering and Computing, 22(1),* 63-69.

Wallen, M.A., O'Flaherty, S.J. & Waugh, M.C.A. (2004). Functional outcomes of intramuscular botulinum toxin type A in the upper limbs of children with cerebral palsy: a phase II trial. *Archives of Physical Medicine and Rehabilitation, 85(2),* 192-200.

Walsh, E.G. (1993). Thixotropy: a time dependent stiffness. *Muscles, Masses and Motion* (pp. 78-102). London: MacKeith Press.

Wartenberg, R. (1951). Pendulousness of the legs as a diagnostic test. *Neurology, 1(1),* 18-24.

Winter, D.A. (2005). *Biomechanics and Motor Control of Human Movement* (3rd ed.). New York, NY: John Wiley & Sons.

Won, J., & Hogan, N., (1995). Stability properties of human reaching movements. *Experimental Brain Research, 107(1),* 125-136.